Dissertation

Formation and Stabilization of Vesicles in Mixed Surfactant Systems

Nina Vlachy

University of Regensburg
Natural Sciences Faculty IV
Chemistry & Pharmacy

Ph.D. Supervisor:	Prof. Dr. Werner Kunz
Adjudicators:	Prof. Dr. Werner Kunz
	Prof. Dr. Ksenija Kogej
	Prof. Dr. Jörg Heilmann
Chair:	Prof. em. Dr. Dr. Josef Barthel

July 2008

Promotionsgesucht eingereicht am: 20. April 2008
Promotionskolloquium am: 4. Juli 2008

For Katko: my sister, my toughest competitor, my biggest fan

Contents

Preface

Surfactants can self-assemble in dilute aqueous solutions into a variety of microstructures, including micelles, vesicles, and bilayers. In recent years, there has been an increasing interest in unilamellar vesicles, which are composed of a curved bilayer that separates an inner aqueous compartment from the outer aqueous environment. This interest is motivated by their potential to be applied as vehicles for active agents in cosmetics and pharmacy. Active molecules can be encapsulated in the bilayer membrane if they are lipophilic or in the core of the vesicle if they are hydrophilic. Furthermore catanionic systems can be used as models for biological membranes.

When oppositely charged surfactants are mixed, new properties appear due to the strong electrostatic interactions between the charged headgroups. These so-called catanionic mixtures exhibit low critical micelle concentration (cmc) values and a non-monotonic change in the surfactant packing parameter (P) as the mixing ratio is varied. One advantage of catanionic systems, as compared with more robust genuinely double chained surfactants, are their greater sensitivity to parameters such as temperature or the presence of salts. To optimize the applications it is important to have a general understanding of the interplay of interactions between the surfactants and of the factors influencing the phase diagram of a mixed system. In this thesis the formation and stabilization of catanionic vesicles was studied. The effect of alcohol and salt on the morphological transitions is described, and the potential of using such systems for cosmetical and pharmaceutical purposes was explored.

A short overview of the phase behavior of catanionic systems is given in the Introduction.

The morphological transitions occurring in mixed surfactant systems upon the in-

crease of the ionic strength are reported in Chapter 2. A micelle-to-vesicle transition is investigated and an intriguing new intermediate structure, named "blastulae vesicle", is described.

Many phenomena in colloid science that involve electrolytes show pronounced ion specificity. In order to elucidate the specific ion effects in catanionic surfactant systems with different surfactant headgroups were compared. Using various experimental techniques and MD simulations, and employing a general concept of 'matching water affinities', a detailed study of ion specificity in catanionic systems is described in Chapters 3 and 4. A Hofmeister like series for classifying surfactant headgroups is established.

Considering that controlling the precipitation phenomena is useful for a vast number of industrial applications, the effect of various additives on the stability of catanionic systems was probed and is reported in Chapter 5.

Chapter 6 introduces an important parameter that should be considered when formulating new encapsulating systems for either cosmetic or medical use: the toxicity of the participating surfactant molecules. We evaluated the cytotoxicity of a number of commonly used surfactants, as well as that of catanionic surfactant mixtures.

Seeing that the presence of only a small amount of a cationic surfactant in the mixture results in a large increase in its toxicity, we focused on a mixture of two anionic and in cosmetic formulation already commonly used surfactants. In Chapter 7 we present a way to form vesicles in such mixtures at room temperature and at physiological pH.

This thesis comprises different studies ranging from phase diagram determination to cytotoxicity studies. For this reason, the thesis was written so that each chapter layout follows the usual convention: Abstract, Introduction, Experimental Procedures, Results, Discussion and Conclusions. The bibliography is given at the end of the thesis in order to avoid repeating. The different studies led to several publications which are already published, accepted or submitted, summarized in the following table. A complete list of publications and a list of oral and poster presentations, which were presented at international congresses, are also given at the end.

Chapter	Publication
2	N. Vlachy, A. Renoncourt, M. Drechsler, J.-M. Verbavatz, D. Touraud, W. Kunz, Blastulae aggregates: New intermediate structures in the micelle-to-vesicle transition of catanionic systems. *J. Colloid Interf. Sci.* **2008** 320, 360-363.
3	A. Renoncourt, N. Vlachy, P. Bauduin, M. Drechsler, D. Touraud, J.-M. Verbavatz, M. Dubois, W. Kunz, B. W. Ninham, Specific alkali cation effects in the transition from micelles to vesicles through salt addition. *Langmuir* **2007** 23, 2376-2381.
3	N. Vlachy, M. Drechsler, J.-M. Verbavatz, D. Touraud, W. Kunz, Role of the surfactant headgroup on the counterion specificity in the micelle-to-vesicle transition through salt addition. *J. Colloid Interf. Sci.* **2008** 319, 542-548.
3	N. Vlachy, B. Jagoda-Cwiklik, R. Vácha, D. Touraud, P. Jungwirth, and W. Kunz, Hofmeister series of headgroups and specific interaction of charged headgroups with ions. *J. Phys. Chem. B* **2008** (Submitted).
4	N. Vlachy, M. Drechsler, D. Touraud, W. Kunz, Anion specificity influencing morphology in catanionic surfactant mixtures with an excess of cationic surfactant. *Comptes rendus Chimie Académie des sciences* **2008** (Submitted).
5	N. Vlachy, A. F. Arteaga, A. Klaus, D. Touraud, M. Drechsler, W. Kunz, Influence of additives and cation chain length on the kinetic stability of supersaturated catanionic systems. *Colloids Surf., A* **2008** (Accepted).
6	N. Vlachy, D. Touraud, J. Heilmann, W. Kunz, Determining the delayed cytotoxicity of catanionic surfactant mixtures on HeLa cells. *Colloids Surf., B* **2008** (Submitted).
7	N. Vlachy, C. Merle, D. Touraud, J. Schmidt, Y. Talmon, J. Heilmann, W. Kunz, Determining the delayed cytotoxicity of catanionic surfactant mixtures on HeLa cells. *Langmuir* **2008** (Submitted).

Chapter 1

Introduction

1.1 Surface Active Agents

1.1.1 General

Surface active agents (a.k.a. surfactants) are molecules with a chemical structure that makes them particularly favorable to reside at interfaces. All classical surfactant molecules consist of at least two parts, one which is soluble in water (the hydrophilic part) and the other which is insoluble in water (the hydrophobic part). The hydrophilic part (a polar or ionic group) is referred to as the head group and the hydrophobic part (a long hydrocarbon chain) as the tail (Figure 1.1). The hydrophobic part of a surfactant may be branched or linear. The degree of chain branching, the position of the polar head group and the length of the chain are parameters that affect the physico-chemical properties of the surfactant[1,2]. The primary classification of surfactants is made on the basis of the charge of the polar head group: anionics, cationics, non-ionics and zwitterionics.

Surfactant molecules adsorb at interfaces, thereby reducing the free energy of the system[3]. When surfactants are dissolved in water, the hydrophobic group disrupts the hydrogen-bonded structure of water and therefore increases the free energy of the system. Surfactant molecules therefore concentrate at interfaces, so that their hydrophobic groups are removed or directed away from the water and the free energy of the solution is minimized. The distortion of the water structure can also be de-

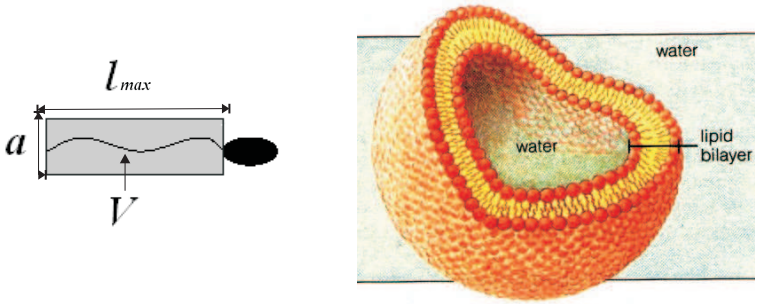

Figure 1.1: Schematic representation of a surfactant molecule (with all the parameters involved in the theory of the packing parameter) and a unilamellar vesicle.

creased (and the free energy reduced) by the aggregation of surface-active molecules into clusters (micelles) with their hydrophobic groups directed toward the interior of the cluster and their hydrophilic groups directed toward the water. The process of surfactant clustering or micellization is primarily an entropy-driven process[1,3]. However, the surfactant molecules transferred from the bulk solution to the micelle may experience some loss of freedom from being confined to the micelle. In addition, they may experience an electrostatic repulsion from other similarly charged surfactant molecules in the case of surfactants with ionic head groups. These forces increase the free energy of the system and oppose micellization. Hence, micelle formation depends on the force balance between the factors favoring micellization (van der Waals and hydrophobic forces) and those opposing it (kinetic energy of the molecules and electrostatic repulsion).

The concentration at which micelles first appear in solution is called the critical micellar concentration, abbreviated CMC, and can be determined from the discontinuity of the inflection point in the plot of a physical property of the solution as a function of the surfactant concentration[1,3]. Above this concentration, almost all of the added surfactant molecules are consumed in micelle formation and the monomer concentration does not increase appreciably, regardless of the amount of surfactant added to the solution. Since only the surfactant monomers adsorb at the interface, the surface tension remains essentially constant above the CMC. Thus, the surface tension can be directly related to the activity of monomers in the solution[3]. The CMC is strongly affected by the chemical structure of the surfactant[4,5], by the tem-

perature[6] and by the presence of cosolutes such as electrolytes[7] or alcohols[6]. Micelle formation, or micellization, can be viewed as an alternative mechanism to adsorption at interfaces. In both cases, the driving force of the process is the tendency of the surfactant to remove their hydrophobic groups from the contact with water[8].

1.1.2 Surfactant Self-Assembly: Vesicles

As was mentioned previously, surfactants can self-assemble in dilute aqueous solutions into a variety of microstructures, including micelles, vesicles, and bilayers. In recent years, there has been an increasing interest in unilamellar vesicles, which are composed of a curved bilayer that separates an inner aqueous compartment from the outer aqueous environment (Figure 1.1). This is mainly because of their wide application in biology and medicine as model cell membranes, as well as their strong potential as drug carriers and other encapsulating agents of industrial relevance[9]. Two major theoretical approaches have been pursued in the modeling of surfactant self-assembly: the curvature-elasticity approach and the molecular approach.

The curvature-elasticity approach describes the vesicle bilayer as a continuous membrane characterized by the spontaneous curvature and the elastic bending modulus[10,11]. In this approach, the formation of finite-sized vesicles thus depends on the interplay between these two quantities[12,13]. The theory provides an elegant, simple way to describe the formation of vesicles, however, because this approach is based on a curvature expansion of the free energy of a membrane, it breaks down for small vesicles, for which the curvature is quite pronounced.

The molecular approach was pioneered by Israelachvili, Mitchell, and Ninham[14–16] who developed a geometric packing argument that allows one to predict the shape of self-assembling microstructures, including spheroidal, cylindrical, or discoidal micelles, vesicles, and bilayers. Which aggregates form, is determined primarily by geometric packing of amphiphiles, hydrocarbon chain stiffness, and the hydrophilic-hydrophobic balance. For dilute solutions in which interactions between aggregates are not important, the necessary (geometric) conditions for formation of an aggregate can be described by a a surfactant packing parameter $P = v/(l_{max}a)$[14–16], where v is the volume per hydrocarbon chain, or the hydrophobic region of the surfactant,

a is the actual headgroup area in the film, and l_{max} is an optimal hydrocarbon chain length related to about 90% of the maximum extended length (see Figure 1.1). The optimal stability of the different aggregates occurs as follows: (1) spherical micelles $P \leq 1/3$; (2) globular or cylindrical micelles $1/3 < P \leq 1/2$ (3) vesicles or bilayers $1/2 < P \leq 1$.

Low packing parameters (around 1/3) are found for single chained surfactants with a strongly polar head group. An increase in the packing parameter can be obtained by adding a second chain, therefore doubling the hydrocarbon volume. To reach this value, double chain surfactants[17–22], two surfactants of opposite charge[23–26], or the association of a surfactant and a co-surfactant[27–33] can be used. In the latter two cases, a pseudo-double chain surfactant is obtained by either an ion-pair formation between the anionic and cationic surfactant or due to an association of the two different molecules via hydrogen bounds.

In many cases, the formation of vesicles requires the input of some form of energy, for example, sonication, injection or extrusion[34–39]. However, vesicles have been found to form spontaneously in some aqueous surfactant systems, including solutions containing (i) mixtures of lecithin and lysolecithin[40], (ii) mixtures of long- and short-chain lecithins[41], (iii) mixtures of AOT and choline chloride[42], (iv) dialkyldimethylammonium hydroxide surfactants[20,21,43–45], (v) cationic siloxane surfactants[46], and (vi) mixtures of cationic and anionic surfactants[24,47–50]. These spontaneously-forming vesicles offer advantages over the more traditional phospholipid vesicles in being easier to generate and more stable, thus making them more attractive as encapsulating agents in diverse practical applications, including the controlled delivery of drugs, active substances in cosmetics, and functional food ingredients such as enzymes[51,52].

1.1.3 Catanionic Surfactant Mixtures

The main thermodynamic driving force for the association of a cationic and an anionic surfactant mixture is the release of counterions from the aggregate surfaces. This results in a large entropy increase. Since the two surfactants are single-chained, the resulting catanionic surfactant can be considered as a pseudodouble-chained

surfactant, in the sense that the two chains are not covalently bound to the same headgroup. For these systems a non-monotonic change in P is observed, with a pronounced maximum as the mixing ratio is varied[1,3]. Due to the strong electrostatic interaction between the oppositely charged headgroups, catanionic mixtures exhibit CMC values much lower than those of the surfactants involved. The CMC is directly correlated to the cleaning efficiency of surfactants, pointing to yet another advantage of such systems.

Mixtures of anionic and cationic surfactants exhibit rich microstructure phase behavior in aqueous solutions. Aggregate structures such as spherical and rod-like micelles, vesicles, lamellar phases, and precipitates have all been observed depending on the concentration and the ratio of the surfactants in solutions[24,26,48,53–57]. Around equimolarity a zone of precipitation is observed. However, when one of the surfactants is present in a small excess, the cationic-anionic surfactant bilayers usually spontaneously form closed vesicles. The phase behavior of catanionic mixtures is represented in Figure1.2.

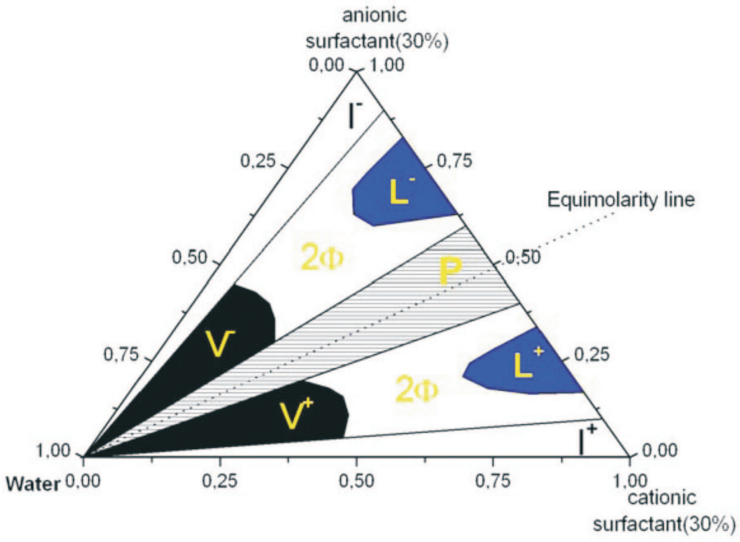

Figure 1.2: Schematic phase behavior encountered in catanionic surfactant systems. Phase notations: V^- and V^+: regions of negatively and positively charged vesicles; 2ϕ: two-phase regions, i.e. mostly demixing of phases between a vesicular and a lamellar phase or a vesicle and a micellar phase; L^- and L^+: lamellar phase with an excess of respectively anionic and cationic surfactants; P: precipitate region; I^- and I^+: mixed micellar solutions with an excess of respectively anionic and cationic surfactants (reproduced from Khan[58]).

Yuet and Blankschtein[59] presented a detailed molecular thermodynamic theory to describe the formation of catanionic vesicles. Their theory reveals that (i) the distribution of surfactant molecules between the two vesicle leaflets plays an essential role in minimizing the vesiculation free energies of finite-sized vesicles, (ii) the composition of mixed cationic/anionic vesicles is mainly determined by three factors: the transfer free energy of the surfactant tails, the electrostatic interactions between the charged surfactant heads, and the entropic penalty associated with the localization of the surfactant molecules upon aggregation, and (iii) the entropy associated with mixing finite-sized vesicles can be an important mechanism of stabilizing vesicles in solution. The present molecular-thermodynamic theory also has the ability to cover the entire range of vesicle sizes (or curvatures), thus enabling a description of small, energetically stabilized, vesicles.

The free energy of vesiculation, g_{ves}, can be viewed as composed of the following five contributions: (1) the transfer free energy, g_{tr}, (2) the packing free energy, g_{pack}, (3) the interfacial free energy, g_{σ}, (4) the steric free energy, g_{steric}, and (5) the electrostatic free energy, g_{elec}. These five free-energy contributions account for the essential features that differentiate a surfactant molecule in the vesicle and in the monomeric state. The transfer free energy, g_{tr}, reflects the so-called hydrophobic effect[60], which constitutes the major driving force for surfactant self-assembly in water. Indeed, the transfer free energy is the only favorable free-energy contribution to molecular aggregation, with the other four free-energy contributions working against this process. The hydrophobic region in a vesicle is different from bulk hydrocarbon. In a vesicle, the surfactant tails are anchored at one end on either the outer or inner interfaces, which restricts the number of conformations that each surfactant tail can adopt while still maintaining a uniform liquid hydrocarbon density in the vesicle hydrophobic region. This subtle difference between a bulk hydrocarbon phase and the hydrophobic region in a vesicle is captured by the packing free energy, g_{pack}. In addition, free-energy penalties are imposed, upon aggregation, by the creation of the outer and inner hydrocarbon/water interfaces, captured in g_{σ}, and by the steric repulsions and electrostatic interactions between the surfactant heads, captured in g_{steric} and g_{elec}, respectively.

A distinction is made in the literature between two types of catanionic systems: (1) In the 'simple mixtures' of cationic and anionic surfactants or catanionic surfactant systems with excess salt, both surfactants still behold their own counterions. (2) The 'true catanionics' (ion pair amphiphiles) consist of surfactant systems where the original counterions have been removed and replaced by hydroxide and hydronium ions. The combination of the counterions at equimolarity thus forms water molecules. Each surfactant stands as counterion for the surfactant of opposite charge. The present work will focus on the first type of catanionic systems (with counterions).

1.1.4 Application of Catanionic Vesicles in Cosmetic Formulation

Vesicles are commonly used in cosmetics and pharmacy as vehicles for active agents. Active molecules can thus be encapsulated in the bilayer membrane if they are lipophilic or in the core of the vesicle if they are hydrophilic. Encapsulation is useful to protect actives in preventing any undesired reaction. Vesicles can thus be used as vectors to deliver drugs to a specific place, without being destroyed. The pharmaceutical applications continuously increase and vesicles are used more and more in the dermatology for prevention, protection and therapy.

The first encapsulation experiments on catanionic systems were performed by Hargreaves and Deamer[61] on the cetyltrimethylammonium bromide / sodium dodecylsulfate system. They successfully entrapped glucose, however, the system was limited to high temperatures ($> 47°C$). Ten years later, Kaler at al.[24] proceeded with similar experiments using vesicles formed from cetyltrimethylammonium tosylate and sodium dodecylbenzenesulfonate (CTAT/SDBS) mixtures. A more comprehensive study of the entrapment ability was made by Tondre et al.[62] on the CTAT/SDBS and by Kondo et al.[50] on the didodecyltrimethylammonium bromide / sodium dodecylsulfate (DDAB / SDS) system. The surfactant concentration as well as the ratio of the two participating surfactant have proved to have a big effect on the entrapment efficiency.

Another problem is the release of the entrapped active ingredient. In most cases a non-ionic surfactant is used (i. e. Triton X-100)[50]. A more elegant solution for targeted drug delivery is designing vesicles that become unstable at an easily tuned pH value. It is known that, for example, tumors and inflamed tissues exhibit a decreased extracellular pH[63–67]. For this reason a large number of groups have focused their attention on the preparation of pH-sensitive liposomes[68–78] as possible drug carrier systems. Furthermore, improving the biocompatibility of products used in cosmetic formulation even further is always sought after. For this reason it is important to identify the skin irritating properties of commercially used surfactants. In addition to their entrapment abilities, vesicles serve also as models for membranes of biological cells[79–81] and as templates[82–85] for the synthesis of nanoparticles, extraction of rare earth metal ions[86], and as gene delivery systems[87].

1.2 Ion Effects

1.2.1 Ions in Water

It has long been known that the dissolution of ions brings about changes in solvent structure[88]. The region of modified solvent surrounding an ion has been denoted as a cosphere of the ion[89]. The degree and manner in which cospheres overlap in the close-range encounter of two ions depends specifically on the nature of both ions and the primary forces between them. Ion hydration has been studied extensively experimentally[88,90–93] as well as theoretically[94–98]. Terms such as 'contact' pairs and 'solvent-separated' pairs have come into use to distinguish the results of complete and partial elimination of solvent molecules from between two interacting ions (see Section 1.2.3.). The basic features responsible for ion-specific short-range interactions are, in the case of monoatomic ions, their charge, their size, their polarizability, and availability of electrons and/or orbitals for covalent contributions. Additional features of polyatomic ions are the charge density distribution, and, in some cases, the presence of hydrophobic groups[99]. The ease with which hydration effects accompanying association-dissociation processes can be observed, depends

on the number of ion pairs existent at any instant. Thus the effects are observable more readily with weak electrolytes and with pairs of multivalent ions, than with strong 1-1 electrolytes.

Ions have long been classified as being either kosmotropes (structure makers) or chaotropes (structure breakers) according to their relative abilities to induce the structuring of water. The degree of water structuring is determined mainly by two quantities: the increase or decrease of viscosity in water due to added salt, and entropies of ion solvation. For example, the viscosity η of an aqueous salt solution typically has the following dependence on ion concentration c[91]:

$$\eta/\eta_\circ = 1 + Ac^{1/2} + Bc + \cdots \tag{1.1}$$

where $\eta_\circ$ is the viscosity of pure water at the same temperature. A is a constant independent of c; its corresponding term can be explained by Debye-Hückel theory as being due to counterion screening at low ion concentrations. The constant B, which is called the Jones-Dole B coefficient, is the quantity that describes the degree of water structuring. B is positive for kosmotropic ions and negative for chaotropic ions. (One issue in interpreting experiments is how to separate the contributions of the anion from the cation. The standard assumption is that K^+ has the same B coefficient as Cl^-, because K^+ and Cl^- have approximately the same ionic conductance[100] and because the value of B for KCl is approximately zero.)

Water structuring is also reflected in entropies of ion solvation. Again, the effects of the anion from the cation need to be separated (it is assumed that the solvation entropies are additive[90]). Furthermore, the ion solvation entropy needs to be divided into ion and hydration water contributions. Subtracting the former, ΔS_{II} is obtained, which describes the change in entropy of hydration water due to the presence of an ion[90]. Ions which are kosmotropic in viscosity experiments tend to have a negative hydration component to their solvation entropy, implying that they order the nearby waters, while chaotropic ions have a positive ΔS_{II}. Figure 1.3 plots the entropy of water near monovalent ions as calculated from the entropy of hydration of the ion (from dissolving the ion in water) versus the ionic radius of the ion[92]. A negative ΔS_{II} (upper portion of Figure 1.3) indicates tightly bound

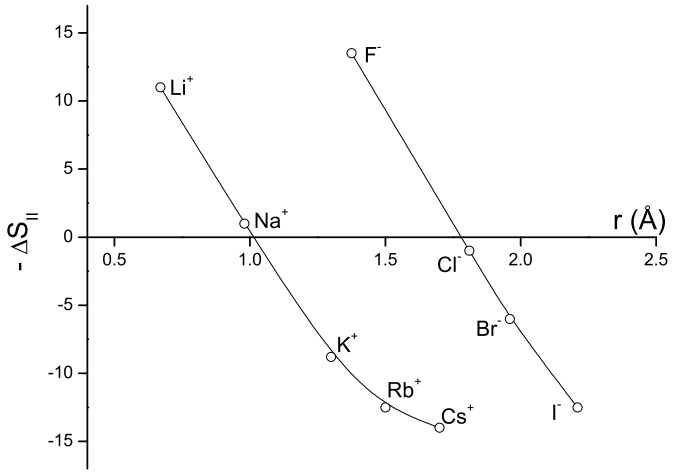

Figure 1.3: The entropy of pure water minus the entropy of water near an ion in $calK^{-1}\ mol^{-1}$. The crystal radii of the ions in angstroms are plotted along the abscissa. Positive values of ΔS_{II} (lower portion of figure) indicate water that is more mobile than bulk water. Negative values of ΔS_{II} (upper portion of figure) indicate water that is less mobile than bulk water. Kosmotropes are in the upper portion of the figure; chaotropes are in the lower portion of the figure (Figure reproduced from Collins[101]).

water that is less mobile than bulk water, whereas a positive ΔS_{II} (lower portion of Figure 1.3) indicates loosely held water that is more mobile than bulk water. Increasing ion size (decreasing ion charge density) is associated with increasing mobility of nearby water molecules. If this mobile, loosely held water is immediately adjacent to the ion, as suggested by x-ray and neutron diffraction data[102], then the horizontal line in Figure 1.3 indicating $\Delta S_{II} = 0$, separates strongly hydrated ions (above the line) from weakly hydrated ions (below the line). Since this transition from weak to strong hydration occurs at a larger size for anions than for cations, the anions must be more strongly hydrated than the cations, since anions begin to immobilize adjacent water molecules at a lower charge density than do cations. The experiments show that water is ordered by small or multivalent ions and disordered by large monovalent ions. Therefore, water ordering has generally been interpreted in terms of ion charge densities[90,103]. Charge densities are high on ions that have a small radius and/or a large charge.

The water-ordering effect of ions is also theoretically extensively studied. Contin-

uum electrostatics models such as that of Debye and Hückel[104] utilize a macroscopic dielectric constant and assume that all interactions involving ions are strictly electrostatic, implying the existence of long range electric fields strong relative to the strength of water-water interactions. In these models, ions are often thought of as point charges and water as a dipole which orients in the long-range electric field. Such models are unable to accurately describe such simple ion-specific behaviors as their tendency to form contact ion pairs, which is a major determinate of the solubility of specific salts and of the role of specific ions in biological systems. For example, models employing a macroscopic dielectric constant predict that all ions are strongly hydrated and will be repelled from nonpolar surfaces by image forces. In fact, weakly hydrated ions (e.g., ammonium, chloride, potassium, and the positively charged amino acid side chains) actually adsorb to nonpolar surfaces[105–107] and interfaces[108,109]. The driving force for this adsorption has been to be the release of weakly bound water to become strongly interacting bulk[110], a process not included in the calculations utilizing the macroscopic dielectric constant. Sophisticated microscopic calculations have indicated a role for the polarizability[111,112] of weakly hydrated ions (as opposed to their dehydration energy) and dispersion forces[113] in driving them to neutral interfaces.

1.2.2 Hofmeister Effect

A related property is the Hofmeister effect[114,115]. In 1888, Franz Hofmeister completed the first systematic study on specific-ion effects. He reported that salts affect the solubility of proteins in water. Certain ions precipitate proteins in water ('salting out') while others help solubilize them ('salting in'). This behavior has been interpreted as a modulation of the hydrophobic effect by salts due to the changes in the water structure brought about by ions. Such salt effects correlate with charge densities of the salts. Small ions tend to cause 'salting out', that is, to reduce hydrophobic solubilities in water, whereas large ions tend to cause 'salting-in', increasing nonpolar solubilities. In Hofmeister's papers an ordering of salts, and later an ordering of ions, usually denoted as 'The Hofmeister series' was developed. 'The Hofmeister series' orders ions as a monotonic function of their surface charge den-

sity and thus water affinity, with the strength of water-water interactions separating strongly hydrated from weakly hydrated species. It is most convenient to generate a separate series for anions and for cations (c. f. Figure 1.4).

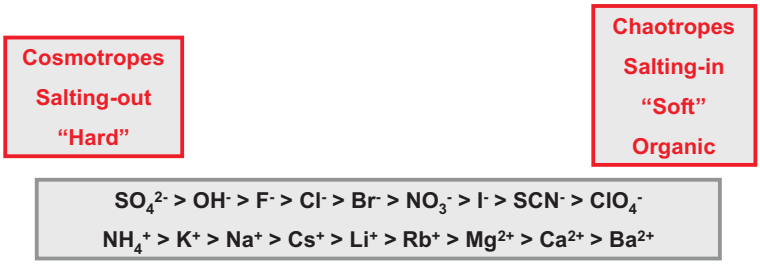

Figure 1.4: A typical Hofmeister series.

1.2.3 Ion Pairing in Water

Ion pairing describes the (partial) association of oppositely charged ions in electrolyte solutions to form distinct chemical species called ion pairs. If the ion association is reasonably strong (the value depends on the charges of the ions and the relative permittivity of the solvent), there is usually little difficulty in separating the properties of the ion pair from the long-range nonspecific ion-ion interactions that exist in all electrolyte solutions. However, when the ion association is weak, there is a strong correlation between these nonspecific ion-ion interactions (characterized in terms of activity coefficients) and ion pair formation (characterized in terms of an association constant). Species are generally described as ion pairs if two oppositely charged ions in solution stay together at a separation r, which is smaller than some specified cutoff distance R. Ions further apart than R are considered 'free'. Various theories have been proposed for choosing the value of R and for describing the properties of the ion pairs and free ions that together produce the observed behavior of electrolyte solutions. It is generally accepted that ions can not approach each other more closely than some 'distance of closest approach' a due to the strong repulsive forces of the electron shells of the ions, even if polarizable. The distance a is understood to bear some relation to the sum of the (crystal ionic) radii of the oppositely charged ions, generally $a \geq r^+ + r^-$. In summary, two ions of opposite sign are considered to form an ion pair if their distance apart is between a and R for

a time longer than the time needed to diffuse over such a distance[116]. Once ions are paired, they are thought to have no tendency to associate with other ions in dilute solutions, although, at higher electrolyte concentrations, ion triplets, quadruplets, or larger aggregates may form. A major role in the association of ions in solution into pairs is thought to be played by long-range electrostatic forces between the ions, usually modeled as a Coulomb's law attraction, attenuated by the solvent permittivity. Very short-range interactions (hard or nearly-hard sphere repulsions) involve the mutual exclusion of ions at $r < a$. However, at distances $a < r < R$, solvation of the constituent ions must be considered. On this basis an ion pair may be classified as a (double) solvent-separated ion pair (2SIP), when the primary solvation shells of both ions remain essentially intact, as a solvent-shared ion pair (SIP), if a single solvent layer exists in the space between the ion partners of the pair, or as a contact ion pair (CIP), if no solvent exists between the partners and the ions are in direct contact (Figure 1.5).

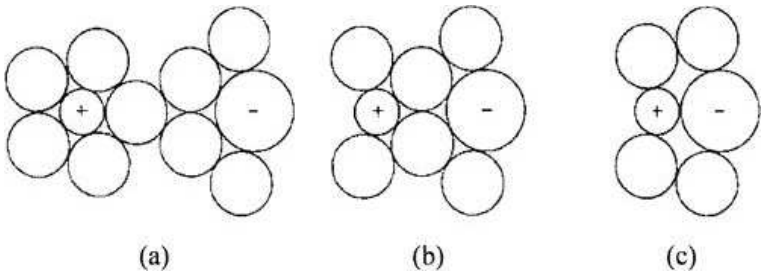

Figure 1.5: Schematic representation of ion-pair types: (*a*) solvent separated (2SIP), (*b*) solvent shared (SIP), and (*c*) contact (CIP). The complete solvation shell around the ion pair is not displayed. (Reproduced from Marcus and Hefter[117])

1.2.4 Collins' Theory of Matching Water Affinities

Taking into account experimental findings a simple model for the ion-induced structuring and disordering of water has been proposed[103]. Collins[103] proposed that ion effects on water structure could be explained by a competition between ion-water interactions, which are dominated by charge density effects, and water-water interactions, which are dominated by hydrogen bonding. For example, lithium is a small ion with high charge density, so it interacts strongly with the water dipole to strongly

orient the water molecules in the ion's first solvation shell. Larger ions having lower charge density have a lower tendency to orient water in the ion's first solvation shell (chaotropes). Accordingly, ions with high charge density have a high propensity to order water (kosmotropes). He suggested that anions are stronger than cations at water ordering because of the asymmetry of charge in a water molecule: the negative end of water's dipole is nearer to the center of the water molecule than the positive end. Therefore, anions feel a larger electrostatic potential at the surface of a water molecule than cations. The calculations of Kalyuzhnyi et al.[118] indicate that the solvation model of Collins yields qualitative agreement with the experimental data.

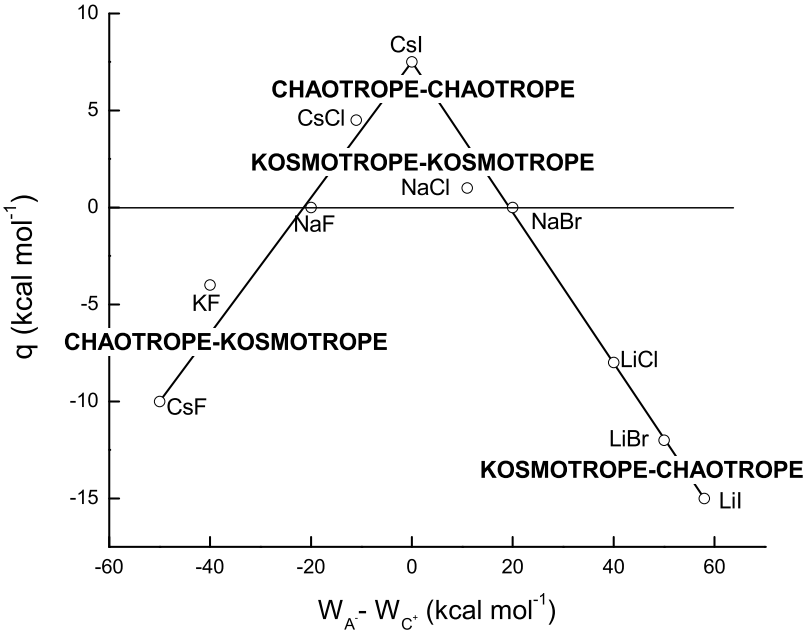

Figure 1.6: Relationship between the standard heat of solution of a crystalline alkali halide (at infinite dilution) in $kcal \cdot mol^{-1}$ and the difference between the absolute heats of hydration of the corresponding gaseous anion and cation, also in $kcal \cdot mol^{-1}$. The ions are cassified as chaotropes (weakly hydrated) or kosmotropes (strongly hydrated). The enthalpy of solution of chaotrope-chaotrope and kosmotrope-kosmotrope salts is positive (takes up heat), whereas the enthalpy of solution of chaotrope-kosmotrope and kosmotrope-chaotrope salts is either negative (gives off heat) or positive (takes up heat). Figures reproduced from Collins[101].

Collins' law of matching water affinities states that oppositely charged ions in

free solution form inner sphere ion pairs spontaneously only when they have equal water affinities[103]. Experimental observations of the systematic dependence of the heats of solution of simple alkali halides on the water affinity of the individual ions (absolute free energies of hydration) and the dependence of the solubilities of the alkali halides on ion size contributed to the realization that a simple law controlled the tendency of ions of opposite charge to form inner sphere ion pairs. In Figure 1.6, the enthalpy of solution is plotted on the vertical axis: those salts clearly above the line at 0 produce cold solutions upon dissolution; those salts clearly below the line at 0 produce hot solutions upon dissolution. Plotted on the horizontal axis is the difference in absolute free energies of hydration (water affinity) of the constituent ions of the salt. We see that when the constituent ions of a salt are matched in water affinity (kosmotrope-kosmotrope and chaotrope-chaotrope salts), cold solutions are produced, suggesting that no strong interactions with water have occurred (which would release heat) and that the oppositely charged ions of the dissolved salt tend to stay together. This is to be expected: the point charge at the center of a (small) kosmotropic ion can get closer to the point charge at the center of an oppositely charged (small) kosmotropic ion than it can to the point charge at the center of the oppositely charged portion of a medium size zwitterion (water molecule); and, the point charges at the centers of the two charges on the medium size zwitterions can get closer to the charges on other water molecules than it can to the point charge at the center of a (large) chaotrope. In contrast, when the constituent ions are mismatched in water affinity (kosmotrope-chaotrope and chaotrope-kosmotrope salts), hot solutions are often produced, suggesting that a strong interaction of the small ion with water has occurred and that the oppositely charged ions of the dissolved salt have separated. This is also to be expected, since the point charge at the center of a (small) kosmotropic ion can get closer to the point charge at the center of the oppositely charged portion of a medium size zwitterion than to the point charge at the center of the oppositely charged (large) chaotrope. The requirement of a chaotrope-kosmotrope or kosmotrope-chaotrope salt for an exothermic heat of solution is a necessary but not sufficient condition since when such a salt is dissolved the kosmotropic ion will generate heat as it goes from a (large) chaotropic partner

to a (medium size zwitterionic) water molecule, and the chaotropic ion will take up heat as it goes from a (small) kosmotropic partner to a medium size zwitterionic) water molecule. The net effect can be exothermic or endothermic.

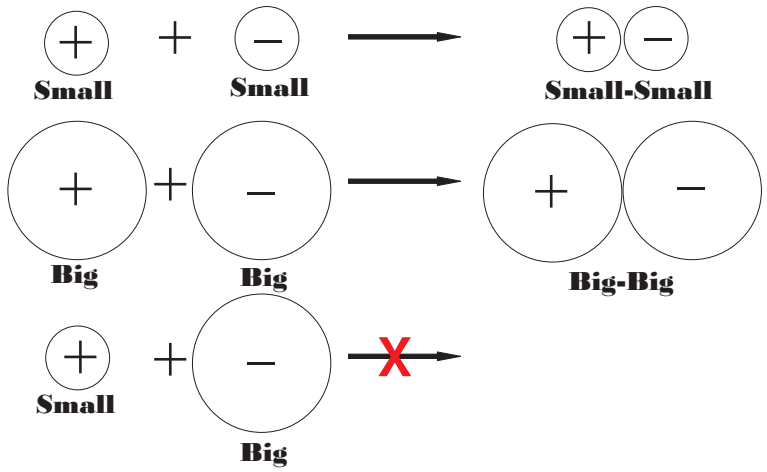

Figure 1.7: Ion size controls the tendency of oppositely charged ions to form inner sphere ion pairs. Small ions of opposite sign spontaneously form inner sphere ion pairs in aqueous solution; large ions of opposite charge spontaneously form inner sphere ion pairs in aqueous solution; and mismatched ions of opposite charge do not spontaneously form inner sphere ion pairs in aqueous solution.

This is schematically represented in Figure 1.7. Small ions of opposite charge will tend to come together because the point charges at their centers can get closer to each other than with the point charges at the centers of the medium size water molecules. Large ions of opposite charge will come together because the released water molecules can form stronger medium - medium interactions. And (small) kosmotropic ions will not spontaneously dehydrate to form an inner sphere ion pair with an oppositely charged (large) chaotropic ion because the point charge at the center of the kosmotropic ion can get closer to the point charge at the center of the oppositely charged portion of a medium size zwitterions than to the point charge at the center of an oppositely charged (large) chaotrope. Thus, it can be concluded that oppositely charged ions in free solution spontaneously form inner sphere ion pairs only when they have equal water affinities.

1.2.5 Ion-Specific Effects in Colloidal Systems

Ion-water interactions are important throughout biology and chemistry. Ions affect the conformations and activities of proteins and nucleic acids[119–123]. Ion complexation in cells is crucial for the activities of biomolecules such as enzymes and drugs[124,125]. Ions regulate the electrostatic potentials, conductances, and permeabilities of cell membranes[126,127], the structures of micelles, and the hydrophobic effect, which drives partitioning, permeation, and folding as well as binding processes[107,128]. In chemistry, ions affect the rates of chemical reactions[129,130], rates of gelation[131] (widely used in food applications), ion-exchange mechanisms[132] (widely used for chemical separations), and the expansion and contraction of clays, responsible for environmental processes such as mudslides[133,134].

It has been observed that in association colloids, the changes in the balance of forces controlling the aggregate structure are reflected in the changes in interfacial concentrations of water and other components[135]. In surfactant systems, this change is reflected in the different self-aggregation morphologies. This is especially true for catanionic mixtures, due to their enhanced sensitivity to outside parameters. For this reason, catanionic surfactant systems have been chosen to elucidate the ion-specific behavior and role of the surfactant headgroups in colloidal chemistry.

Part I

Salt-Induced Morphological Transitions in Non-Equimolar Catanionic Systems

Chapter 2

Blastulae Aggregates: Spontaneous Formation of New Catanionic Superstructures

2.1 Abstract

The transition of ionic micelles to vesicles upon the addition of salt was explored. The catanionic surfactant solution was comprised of sodium dodecylsulfate (SDS) and dodecyltrimethylammonium bromide (DTAB) with an excess of SDS. The change in aggregate size can be accommodated by the increase of counterion binding and consequent dehydration of the surfactant headgroups. A new type of intermediate structure was found: a symmetrically shaped spherical super-structure, which we named blastulae vesicle. In contrast to known raspberry-like or egg-carton structures, we believe that charge fluctuations within the bilayers are responsible for this spontaneous super-aggregation to occur in the presence of only a small amount of sodium chloride. A possible mechanism for the observed pattern formation is proposed.

2.2 Introduction

It is known for a long time that double chain surfactants can spontaneously form vesicles[43]. A similar phenomenon can be observed with mixtures of cationic and anionic surfactants (here called catanionics). These systems display a wide variety of phase behavior and structures such as micelles, vesicles, discs and folded bilayers can be observed[24,136,137]. Recently, new self-assembled structures, such as onion phases and icosahedra were found in 'true' catanionic solutions with no other ions than the surfactant molecules[138,139]. Spontaneously formed vesicles are of applicational interest, especially in catanionic systems, since they can be tailored at will by varying the anionic / cationic surfactant ratio, the size of the chain length or the nature of the polar heads[26].

For dilute systems, local aggregate curvature determined by geometrical constraints embodied in a surfactant packing parameter $P = v/(l_{max}a)$, where v and l_{max} are the volume and length of the hydrophobic part, respectively, and a the area per molecule at the interface (headgroup) is a convenient variable that characterizes phase diagrams[15]. A necessary condition for the formation of vesicles from either single or mixed surfactants can be shown to be that the packing parameter is $1/2 < P < 1$. For a single surfactant that condition can be satisfied by choosing a double chained surfactant, e.g. didodecyldimethylammonium bromide (DDAB); for mixed surfactant systems a pseudo-double chain surfactant is obtained by ion-pair formation between an anionic and a cationic surfactant[18,45].

However, this condition is not sufficient. While the type of aggregate that forms with ionic surfactants can be broadly understood in terms of a balance between forces due to the packing properties of surfactant tails and those due to double-layer electrostatic interactions, conditions for the formation of single or few walled vesicles are very subtle[16,140,141]. For effects of global packing constraints and inter-aggregate interactions, see André et al.[142]. As the surfactant parameter (intrinsic local curvature) varies in the range $1/2 < \mathrm{P} < 1$ by e.g. varying head group area via salt addition or temperature or mixing chain lengths, then, if the surfactant chains are flexible, the system forms vesicles that grow as P increases to form a lamellar phase

at $P = 1$.

If the chains are not flexible, the system at first forms multiwalled vesicles, then vesicles, then lamellar phases again. At $P = 1$ this curious phenomenon is due to packing constraints that emerge because the interior and exterior surfactants of a curved bilayer experience very different constraints. Depending on those chain and headgroup constraints the system forms cubic phases at P $\approx$ 1. These are phases of zero average curvature but varying Gaussian curvature. Again, with increase in surfactant concentration equivalent to increased repulsion between aggregates, the system can form equilibrium states of supra aggregation. In these the interior can be micelles or cubic phases protected by few walled vesicles.

The appearance of so many different structures is known for a very long time[20,45,143–149]. But apart from the system of double chained didodecyldimethylammonium salts with different counterions studied by Ninham and Evans, they have been little explored.

Vesicles from catanionic systems are easily prepared. There is an expectation that they might also be used as vehicles for controlled delivery of drugs[62,150,151] or as templates for the synthesis of hollow particles[150–152]. One advantage of catanionic vesicles as compared with more robust genuinely double chained surfactants is their greater sensitivity to parameters such as temperature[153] or the presence of salts[47] used to induce transitions from vesicles to micelles or to precipitation. Of particular interest is the direct transition from micelles to vesicles. Such a phenomenon offers in principle an easy way of encapsulating active agents by dissolving them in the micellar phase prior to vesicle formation. Micelle-to-vesicle transition was already observed when diluting a micellar solution with water[26,154,155], changing the anionic / cationic surfactant ratio[156–158], increasing temperature[159], or upon the addition of organic additives[160] and salt[161–163].

The effect of ionic strength on catanionic systems was previously studied experimentally by Brasher et al.[47]. Their results show that the addition of monovalent salt changes the phase behavior and aggregate properties of mixed surfactant solutions. Theoretically the effect of salt on the catanionics was described by Yuet et al.[59], however, due to the constrictions of the model (smeared surface charges and

point-sized ions), they could not reveal the specificity of different ions.

In the present chapter, we explore salt-mediated transition of micelles to vesicles in a well-studied system[47,48,164]. We are concerned with the influence of salts on a catanionic system composed of sodium dodecylsulfate (SDS) and dodecyltrimethylammonium bromide (DTAB) in aqueous solution, with an excess of anionic surfactant. Increasing amounts of sodium chloride was successively added to a solution of mixed SDS / DTAB micelles. The micellar system was first characterized by rheometric measurements and cryo-TEM. We report on the particular morphologies that arise during the salt-induced micelle to vesicle transition. The formation of irregular convex-concave patterns and a secondary self-assembly of vesicle-like structures upon the addition of sodium chloride is presented. In order to study this transition in detail, the concentration of salt in the system was increased in small increments and the effect was studied using dynamic light scattering, cryo- and freeze-fracture transmission electron microscopy. Two different microscopy techniques were used in order to exclude the artifacts that might arise during the preparation of samples. FF-TEM provides a direct visualization of the three-dimensional structure of particles. The fracture follows the path of least resistance, and in colloidal dispersions, the fracture surface propagates along the interface of two phases. This makes FF-TEM ideal to study membrane surfaces. To observe whether the vesicles are closed and if the membranes are intact cryo-TEM was employed. Furthermore, cryo-TEM is very appropriate to study micellar solutions.

2.3 Experimental Procedures

Materials Sodium dodecyl sulphate (SDS) (purity: 99%) and sodium chloride were purchased from Merck, Germany. The cationic surfactant used was 99% dodecyltrimethylammonium bromide (DTAB) purchased from Aldrich, Germany. All chemicals mentioned above were used as received without further purification. Millipore water was used as solvent in all cases.

Sample Preparation Surfactant stock solutions were prepared by dissolving weighed amounts of dried substances in Millipore water. The solutions were then left for 24 hours to equilibrate at 25°C. The catanionic solutions were prepared by mixing the surfactant stock solutions to obtain a fixed anionic / cationic surfactant mass ratio of 70/30 (this corresponds to a molar ratio of about 2.5/1). The total surfactant concentration was kept at 1 wt.% at all times. Salts were added to the micellar solution at increasing concentrations. The solutions were then stirred and left to equilibrate for a week at 25°C before making measurements.

Dynamic Light Scattering (DLS) Measurements Particle size analysis was performed using a Zetasizer 3000 PCS (Malvern Instruments Ltd., England), equipped with a 5 mW helium neon laser with a wavelength output of 633 nm. The scattering angle was 90° and the intensity autocorrelation functions were analyzed using the CONTIN software. All measurements were performed at 25°C.

Rheology Rheological experiments were performed on a Brookfield DV - III+ rate controlled rheometer. A cone-and-plate geometry of 48 mm diameter and with a 0.8 deg cone angle was used (spindle model CP - 40).

Cryo-Transmission Electron Microscopy (cryo-TEM) Specimens for cryo-TEM were prepared by placing a small drop (ca. 4μl) of the sample on a holey carbon grid. Immediately after blotting with filter film to obtain a thin liquid film over the grid, the sample is plunged into liquid ethane (at its melting temperature). The vitrified film is then transferred under liquid nitrogen to the electron microscope. The grid was examined with a Zeiss EM922 EF Transmission Electron Microscope (Zeiss NTS mbH, Oberkochen, Germany). Examinations were carried out at temperatures around 90 K. The TEM was operated at an acceleration voltage of 200 kV. Zero-loss filtered images (DE = 0 eV) were taken under reduced dose conditions (100 - 1000 e/nm^2). Images were registered digitally by a bottom mounted CCD camera system (Ultrascan 1000, Gatan, Munich, Germany) combined and processed with a digital imaging processing system (Digital Micrograph 3.9 for GMS 1.4, Gatan, Munich, Germany).

Freeze-Fracture Electron Microscopy Samples used for cryo-fracture were cryoprotected by 30% glycerol and frozen in liquid N_2. Freeze-fracture was performed in a Balzers (Balzers, Switzerland) apparatus at $-150°C$ under a vacuum of 10^{-6} Torrs. Metallic replicas were obtained by Pt and carbon shadowing of fracture surfaces. The replica were examined and photographed with a Philips CM 12 transmission electron microscope.

2.4 Results

2.4.1 Characterization of SDS / DTAB Micellar Solution

The system under study is a well-known mixture of cationic and anionic single-chain surfactants. The total surfactant concentration (1 wt.%; ≈ 33 mM) and the anionic / cationic molar ratio (2.5 / 1) remained constant throughout all the experiments. The initial sample was colorless and isotropic, corresponding to the micellar region of the phase diagram (Figure 2.1).

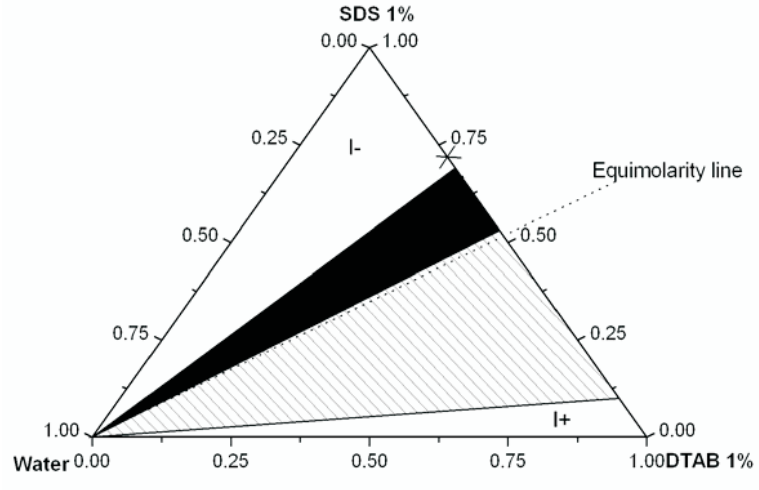

Figure 2.1: Schematic ternary phase diagram of the SDS / DTAB system at 25°C (the black cross shows the starting point (reference sample), to which sodium chloride was added)

DLS measurements confirm a micellar solution indicating a hydrodynamic radius (R_H) of 10 nm and a relatively high polydispersity index (0.27). Figure 2.2 (left) shows a cryo-TEM image of our reference solution (without added salt), exhibiting very long rod- or ribbon-like micelles, in equilibrium with spherical micelles (hence

explaining the high polydispersity). Long rod-like micelles have already been observed by SANS measurements in systems similar to ours[165]. Results from rheometry experiments show that the viscosity decreases with applied strain rate (Figure 2.2 (right)) therefore exhibiting properties of non-Newtonian shear-thinning fluids. This kind of behavior is common for solutions containing large non-spherical molecules in a solvent with smaller molecules. It is generally supposed that the large molecular chains tumble at random and affect large volumes of fluid under low shear, but that they gradually align themselves in the direction of increasing shear and produce less resistance. This behavior confirms the presence of rod-like micelles. No enthalpy change could be detected by differential scanning calorimetry so that no information could be deduced about possible phase transitions occurring in the system between 10 and 80°C[166–168]. Probably, the amount of surfactant was too low for such a detection with our equipment.

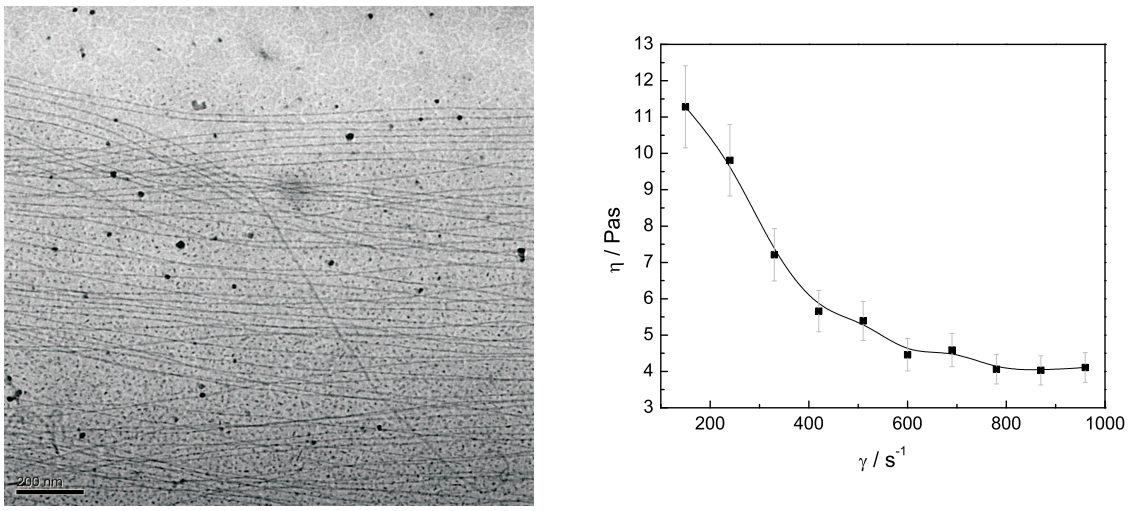

Figure 2.2: Left: Cryo-TEM image of a SDS/DTAB aqueous solution at the molar ratio of 2.5/1 and a total surfactant concentration of 1 wt.% (reproduced from ref.[169]); right: viscosity of the same sample as a function of shear rate.

2.4.2 Salt-Induced Micelle-to-Vesicle Transition

Upon the addition of sodium chloride, the solutions exhibited a transition from a colorless to a blue solution, the blue color being typical of the presence of large objects. Samples with different salt concentrations were analyzed by dynamic light

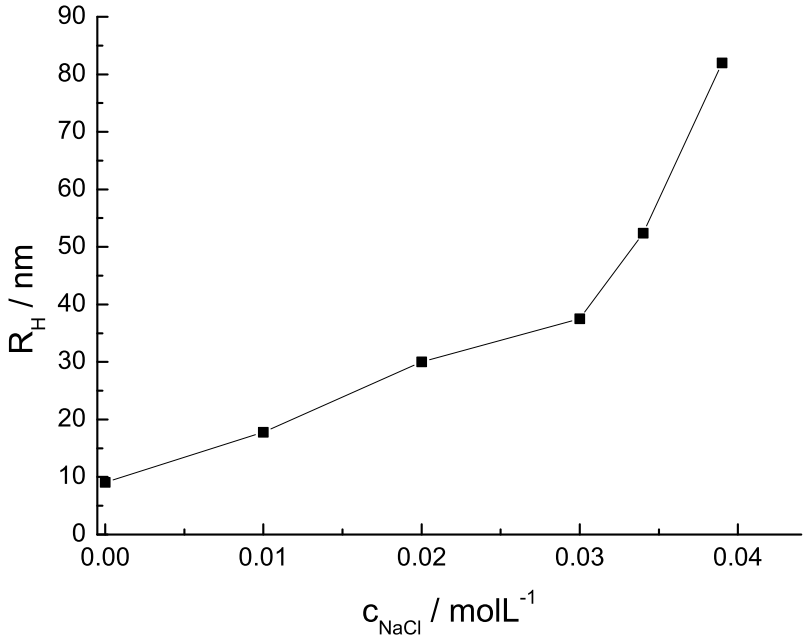

Figure 2.3: Increase in the mean hydrodynamic radius of catanionic aggregates upon the addition of sodium chloride.

scattering. The addition of chloride salts causes an increase in average particle size and a certain turbidity of the solution (Figure 2.3). DLS indicated a significant increase in the mean hydrodynamic radius (R_H) of the micelles from 10 to ca. 70 nm. It can be expected that the salt screens the electrostatic interactions, which leads to smaller headgroups and therefore a higher packing parameter.

Freeze-fracture and cryo-TEM confirm the formation of lamellar sheets in the sample (Figure 2.4). However, by carefully observing the cryo-TEM images one can see that at lowest concentration of added salt (10 mM) the long rod-like micelles present in the starting solution start to break-up and cluster together, see Figure 2.5 (left). Other images from the same solution show that these clusters seem to form small pieces of lamellae, which eventually close to form round vesicles. The curving of membranes is represented by the presence of darker, stiff-looking edges, due to the higher electron density in these points. Figure 2.5 (right) shows some curved pieces of lamellar sheets as well as some complete vesicles. The vesicles represented in cryo-TEM appear to be perforated; such perforated vesicles have previously been

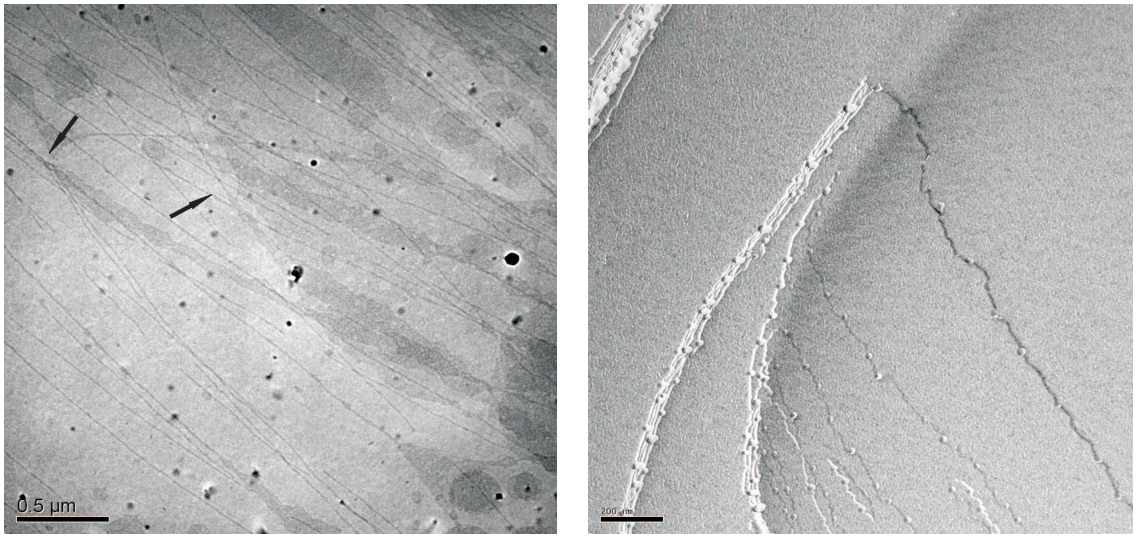

Figure 2.4: Cryo-TEM (left) and FF-TEM (right) photographs representing the formation of multi-lamellar sheets upon the addition of 10mM NaCl. The arrows show regions where we can observe the unraveling of ribbon-like micelles into lamellar sheets. The molarity in the case of FF-TEM experiments corresponds to the concentration of the solutions prior to cryo-protecting.

observed in various surfactant systems[170–174]. Surprisingly, FF-TEM images do not confirm such perforations.

The addition of salt produces dramatic effects detected by freeze-fracture. At 20 mM of NaCl large spherical, highly undulated aggregates are observed. As mentioned previously, FF-TEM exploits the property that surfaces fracture along the area of least resistance. In the case of vesicles this is within the bilayer. Therefore, only 3-dimensional objects can be observed. The size range of the particles is from 150 to 500 nm, see Figure 2.6 (left). This apparent polydispersity is most likely due to the characterization technique used; the measured size of the object depends on the region where the samples are fractured. Some of the aggregates are fractured close to the middle; Figure 2.6 (right) shows a ring of vesicles. Since the aggregates pictured in Figure 2.6 are observed in high amounts, they most likely represent the same object, fractured in different places (close to the 'poles' of the blastulae vesicles, as opposed to the middle of the vesicle). The images suggest that the inside of these particles are hollow and filled with the same solvent as the surrounding (water). Due to the similarities in appearance we named the observed structure blastulae, taking the name from biological origin; the blastulae are an early

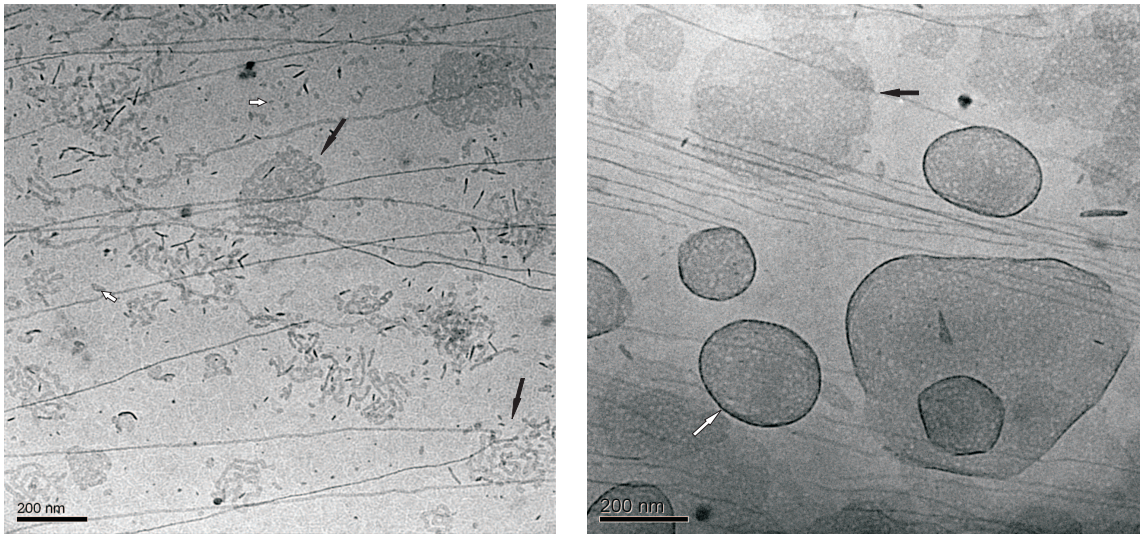

Figure 2.5: Cryo-TEM photographs representing the breaking-up of ribbon-like micelles and consequent clustering of the pieces. Clusters of elongated aggregates are indicated by black (left), whereas individual aggregates are designated by white arrows. The image on the right shows clusters of smaller aggregates (black arrows) and vesicles with perforated surfaces (white arrows).

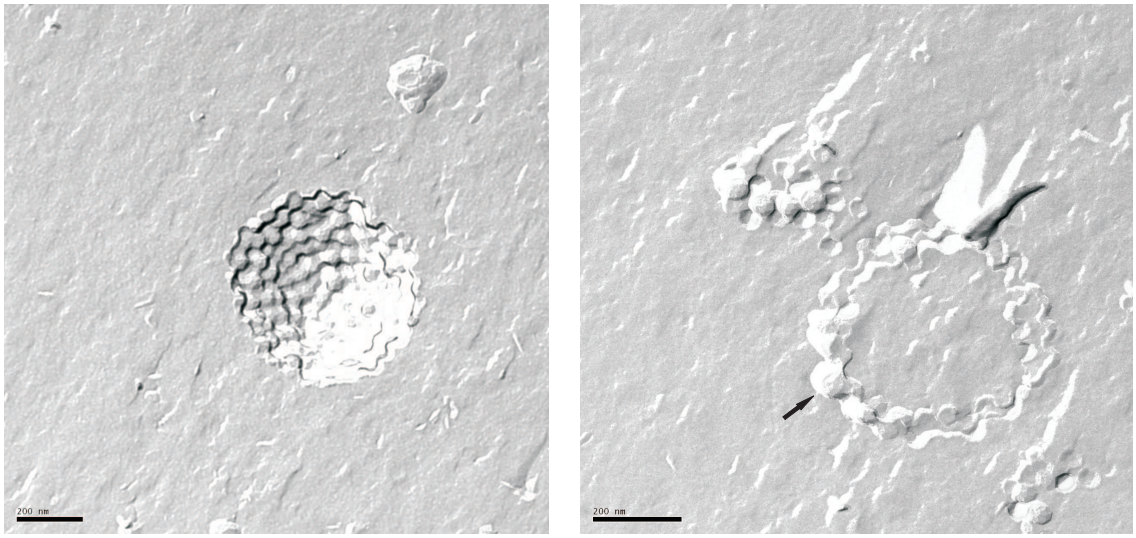

Figure 2.6: FF-TEM photographs representing the formation of blastulae-like clusters upon the addition of 20mM NaCl cut near the surface (left); cut through the middle (right), clearly representing the solvent filled cavity. The arrow shows an individual vesicle with its own membrane.

stage of embryonic development consisting of a spherical layer of cells surrounding a fluid-filled cavity. On the basis of the present pictures we cannot say, whether the blastula vesicle is an aggregate consisting of one individual membrane or a cluster of elongated micelles as observed in cryo-TEM. Both possibilities will be explored

further in the text. However, it is interesting to note that some unilamellar individual vesicles are also present. Interestingly, the average diameter of the vesicles (ca. 60 nm) is of the same size as the bulges forming the blastulae structure. This might speak for the possibility that the blastula is actually a cluster of individual small vesicles. These, however, are not deformed in a way that it is usually observed in aggregates. A mechanism for this type of clustering will be discussed later on, pointing to the similarity with specific-site (or ligand-receptor) binding. It should be noted that similar aggregates have been observed in another context[175,176] and will also be discussed later.

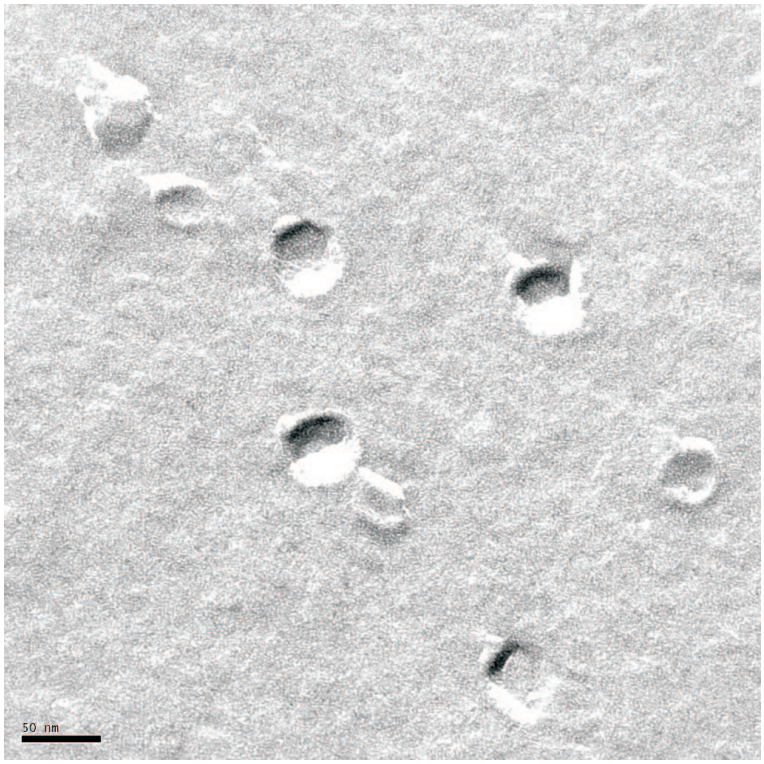

Figure 2.7: FF-TEM image of individual unilamellar vesicles upon the addition of 30 mM NaCl. The bar represents 100 nm.

As more salt is added to the system the clusters begin to disaggregate. At sodium chloride concentrations of 30 mM only individual unilamellar vesicles are observed as can be seen in Figure 2.7.

Finally, at NaCl concentrations of 40 - 45 mM, a loose and unstructured, randomly packed aggregation of vesicles is observed, see Figure 2.8. These aggregates are not spherically symmetrical and the individual vesicles forming the aggregates are

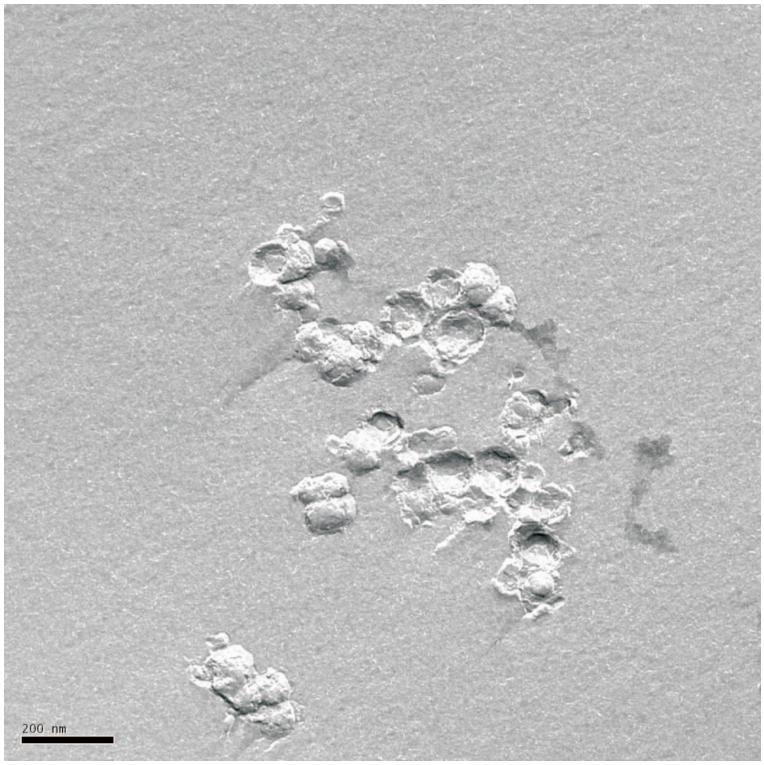

Figure 2.8: FF-TEM photograph representing the aggregation of vesicles upon the addition of 45 mM NaCl to the reference SDS/DTAB micellar solution. The bar represents 200 nm.

deformed.

In summary, two features are new in this system: i) the appearance of blastulae structures, and ii) the series of different structures that are induced by salt addition only, without any further additives.

2.5 Discussion

2.5.1 Models of the Micelle-to-Vesicle Transition

In the following we propose a possible mechanism for the observed pattern formation. The different steps are represented in Figure 2.9.

'Lamellar Model' It is well known that, as an electrolyte is added to a mixed micellar solution, the effective surface area of the surfactant headgroups becomes smaller. This effect is mainly due to counterion concentration and screening as well as consequent dehydration of the neutralized heads. This effect favors a lamellar

packing (step $a \rightarrow b'$). The formation of large multi-lamellar sheets is energetically unfavorable, so these start curving and consequently forming large spherical objects. A theoretical model has been suggested by Safran et al.[13], showing that in cases of mixed surfactants vesicles are more stable than lamellar structures. This is due to the formation of surfactant bilayers, where the two monolayers consist of different surfactant concentrations, which results in equal and opposite monolayer spontaneous curvatures. This model is in accordance with our result, where the large spherical aggregates are shown to form from micelles via lamellar sheets. The main factor governing the packing arrangement in these phases is the degree of hydration of the polar headgroup.

As the polar headgroups are dehydrated even more by the addition of salt, the packing parameter increases and the formation of individual vesicles is favored. In the present catanionic system the outer layer of the vesicles is composed of positively and negatively charged groups with the latter being in excess. A redistribution of charges may then take place in the highly flexible vesicle membranes leading to local patches of positive and negative charges. The locally positive charges of one vesicle can interact favorably with the negative charges of another vesicle and vice versa (Figure 2.9, stage f). In other words, the vesicles can attract each other due to the $+,-$ interactions among the headgroups of surfactants belonging to different vesicles. This is somewhat similar to charge fluctuations in polarizable objects leading to van der Waals interactions. But the difference is that here the ion charge distribution of the headgroups fluctuates, and not the electron distribution. The local Coulomb attraction may be strong enough to overcome the overall repulsive force of equally charged vesicles acting at larger distances. Since vesicles are spontaneously formed from lamellar sheets, they are, at this starting point, in close enough contact for this to happen. In this case only localized parts of the membrane (patches) are interacting, similarly to specific site binding.

As the ion strength in the solution is increased the blastulae vesicles disaggregate. We suppose this is due to the fact that the interactions between the oppositely charged headgroups of neighboring vesicles are weaker than those within a vesicle (one must consider the additional strong van der Waals forces between the hydropho-

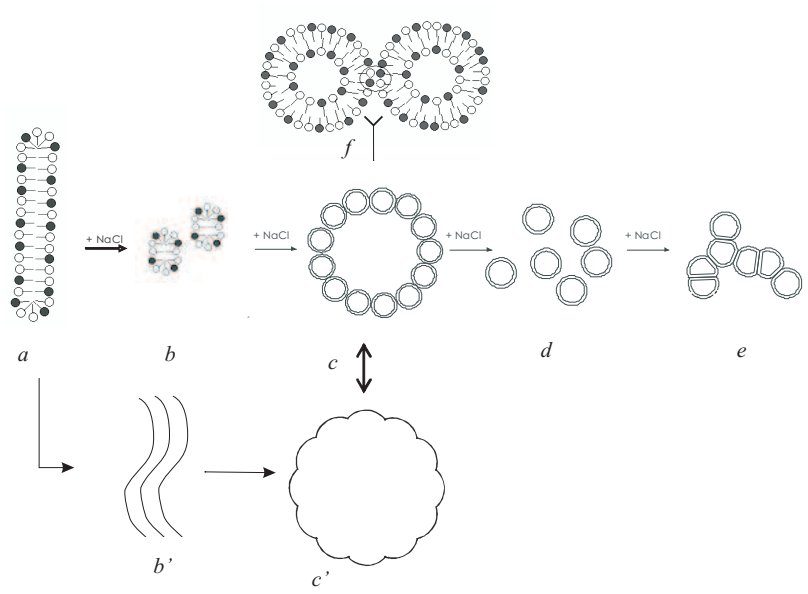

Figure 2.9: Schematical representation of the observed structures that form through increasing salt concentration: From the starting micellar solution, which exhibits rod-like micelles (a) two possibilities are presented: In the 'clustering model', the rod-like micelles (a) start breaking-up into smaller pieces (b), which start clustering together to form spherical aggregates. In the 'lamellar model', multi-lamellar sheets are formed upon addition of salt (b'). These start closing to form undulated giant vesicles(c'). At higher ionic strength, the formation of blastulae clusters (c) is observed, where the outer layer is composed of individual vesicles, which enclose a fluid-filled cavity. The vesicles interact through oppositely charged headgroups of surfactants belonging to different vesicles (f; the open and filled circles represent headgroups of opposite charges). As salt concentration is further increased, the attraction is screened and the vesicles segregate (d). Still higher concentrations of salt in the system produce a non-specific interaction, where van der Waals forces dominate, causing the vesicles to loosely aggregate while deforming (e).

bic surfactant tails). Therefore, as more salt is added and the charges on the vesicles are screened, the 'bonds' between the vesicles are broken. The cluster begins to disaggregate due to the net negative charge of the individual vesicles, resulting in the formation of individual unilamellar vesicles.
At still higher ionic strength the electrostatic repulsions are screened and the effect of van der Waals forces becomes significant. A loose and unstructured, randomly packed aggregation of vesicles is observed. A similar behavior (flocculation of vesicles) was observed upon the addition of NaCl to the micellar solution of dodecylbenzene sulfonic acid[177].

'Clustering Model' In this model, the ribbon-like micelles start breaking up into smaller cylindrical aggregates (corresponding to step $a \rightarrow b$). These could be small vesicles, which grow until retaining a radius at which they are most stable (small vesicles are thermodynamically unfavorable due to high curvature). Again these aggregates start clustering together despite an overall net negative charge. Steps $c \rightarrow e$ remain the same as in the 'lamellar model'.

2.5.2 Blastulae Vesicles

Microscopy images clearly show that the blastulae clusters are spherical and hollow. Figure 2.6 (right) pictures the fluid-filled cavity and the astounding symmetry of the aggregate. The interesting phenomenon is that in this cluster the vesicles are not deformed in a way that is usually observed in aggregates. Aggregation of vesicles without accompanying deformation of membrane had until now been observed only in systems to which specific ligands and receptors were added. In such case no deformations occur when vesicles are brought together by a specific site-binding (ligand-receptor) interaction. This is because not the whole vesicle surface is involved in the interaction, but only a discrete number of contact points on each surface. This kind of self-assembly of vesicles driven by ligand-receptor coupling was reported by Chiruvolu et al. and Walker et al.[178–180].
It is interesting to translate this concept to blastulae formation by proposing a fluctuation of the electron density in the membrane as was described above. Such

a formation of localized partitions of opposite charge has been previously reported by Aranda-Espinoza et al.[181]. A spontaneous partitioning of positively charged mixed bilayer vesicles in the presence of negatively charged particles resulting in an electrostatic repulsion between oppositely charged particles was observed. In our case the effect is reversed, electrostatic attraction of vesicles of equal net charge are found. Recently, the asymmetry of charge in lipid bilayers induced by monovalent salts was reported. According to Gurtovenko[182], the difference in the headgroup orientation on both sides of the bilayer, coupled with salt-induced orientation of water dipoles, leads to an asymmetry in the charge-density profiles and electrostatic potentials of the bilayer. In this report lipid vesicles with only one type of molecules are present. In our case, where two oppositely charged surfactants are present, the salt-induced asymmetry may be the reason for the patches of the single charged surfactants of opposite sign. Finally, the overall shape of the blastulae formed by the 'attached' vesicles can be explained by the preferential local aggregate curvature determined by geometrical constraints, obeying the same rules as the formation of vesicles from surfactants. It should be noted that the attraction of overall equally charged objects is discussed from time to time in literature[183]. The present findings and the model proposed here may help to understand such phenomena.

As far as coexistence of vesicles and micelles are concerned, intermediate structures have been reported in the literature: open vesicles, mesh phases, or even patches and discs[56,170,184]. However, to our knowledge such symmetrically shaped hollow structures as the blastulae vesicles have never been observed before in catanionic systems. One of the possible explanations is that blastulae are the diluted counterpart of the 'oyster phase' which has been observed for other charged bilayers in the absence of salt[185].

The rationale in the sequence of observed shapes (as schematically represented in Figure 2.9), when spontaneous curvature is varied via composition, is given by a general mechanism: a co-crystallization occurs, followed by a segregation of excess material. The amount of non-stoichiometric component distributes between the lattice and the edges and thus controls the shape of the crystallized colloids[186].

2.5.3 The Occurrence of Convex-Concave Patterns in Biological Systems

Experimentally, the occurrence of convex-concave deformations of high regularity, similar to our blastulae, was first observed in a study of lipid extracts from bacterial membranes[187,188]. The egg carton pattern is mostly found in complex lipid mixtures of biological origin such as Streptomyces hygroscopicus and brain sphingomyelin[189]. Later on, this kind of curved patterns has also been observed in a few examples with a more simple composition such as in vesicles of DMPC mixed with a polymerized amphiphile with butadiene groups[190], N-nervonoyl sphingosylphosphorylcholine[191] both in their gel state and in systems containing the lipid complex soybean lecithin and poly(diallyldimethylammonium chloride)[192]. However, the repeating convex-concave patterns in these so-called 'egg carton' structures are found on flat sheets and the objects are multilamellar vesicles with diameters largely exceeding the diameters of the bulges. By contrast, FF-TEM images of the present catanionic system show that the building blocks forming the blastulae aggregate are of the same average diameter as the individual vesicles present (ca. 60 nm) in solution. The origin of convex-concave bilayer deformation is believed to result from constraints imposed by limiting hydration of the headgroup and a frustration arising from the spontaneous curvature of the bilayers[193]. This effect had already been discussed by Gebhardt et al.[194]. Undulation and the formation of so-called egg carton structure had been extensively studied theoretically. A 'hat and saddle' model was proposed by Helfrich[195] to explain the existence of corrugated membranes of biological origin. Fournier has shown that anisotropic inclusions can induce spontaneous bending in flat lipid membranes, which attract each other to form an egg carton structure[196,197]. A model calculation based on bilayer bending elasticity yielding disordered egg carton textures was proposed by Goetz and Helfrich[198]. However, all these calculations are not appropriate to explain the peculiar vesicle patterns experimentally observed in present work.

2.5.4 Raspberry Vesicles

For the same reason the blastulae are different from the so-called raspberry vesicles. The term 'raspberry vesicles' was used previously to describe convex-concave vesicles obtained after the induction of osmotic shock on giant unilamellar vesicles in different phospholipid systems[175]. The 'raspberry effect' is related to the deflating of the liposome due to the volume reduction, the consequence being the existence of an excess membrane. This excess membrane induces the formation of inverted 'daughter vesicles'. Similar observations have been reported by Ménager and Cabuil[176] for the osmotic shrinkage of liposomes filled with a ferrofluid and in the case of liposomes subjected to a gradient of glucose[194]. However, the evolution of these vesicles is different from the one observed in our case. The initial membrane undulation of giant vesicles seems to be a common step in all cases. In the aforementioned cases, the osmotic shrinkage of vesicles was shown to be reversible which is proof of a persistent membrane neck connection between the mother and daughter vesicles. At high enough osmotic strength the membrane ruptured. No vesicles with individual membranes were observed. This is not the case in our system, where the increase of ionic strength promotes the formation of individual membranes, resulting in a spherically symmetrical cluster of unilamellar vesicles, the blastulae. Higher ionic strength results in a separation of the vesicles.

2.5.5 Blastulae Vesicles: A General Trend in Catanionic Systems?

Finally, we would like to report that similar images have been found also in samples containing cesium chloride and in a system composed of sodium dodecylcarboxylate and DTAB in the presence of sodium chloride (c. f. Figure 2.10). Further experiments and theoretical insights are necessary in order to clarify the exact mechanism of formation of such structures and the reason for this intermediate structure to be found only in catanionic systems containing salt.

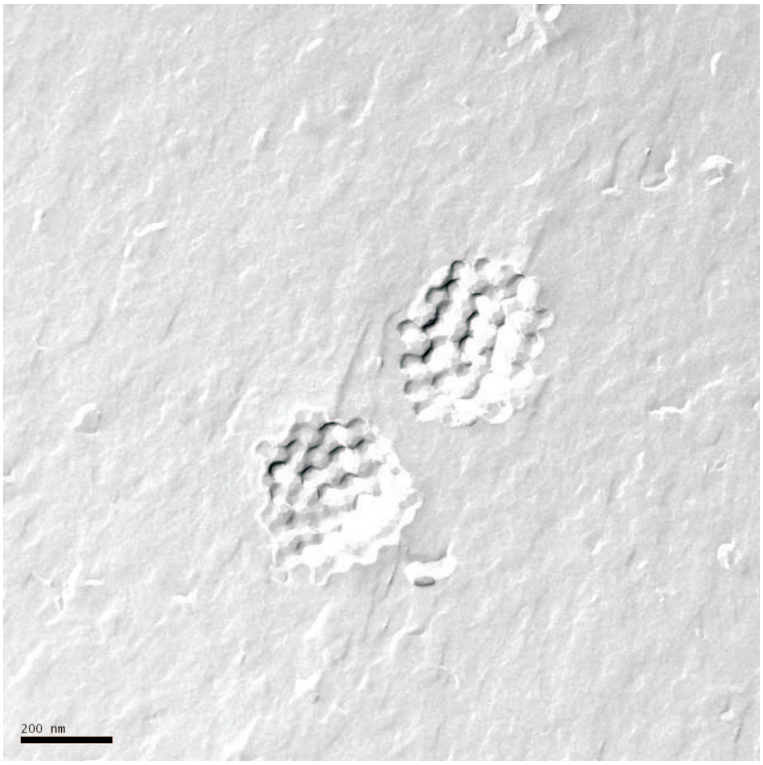

Figure 2.10: Blastulae vesicles in an SDS / DTAB system with the addition of 20 mM CsCl.

2.6 Conclusions

We have presented a way to make hollow regularly shaped structures by spontaneous secondary self-assembly of vesicles without additives except salt. These spherical, symmetrical aggregates of individual vesicles were never observed previously, even in systems with ligand-receptor binding. A mechanism of formation for this type of super-structures was proposed, showing the importance of charge fluctuation. Finally, such blastulae aggregates could be considered as an intermediate step in the formation of unilamellar vesicles from bilayers in non-equimolar catanionic systems.

Chapter 3

Specific Alkali Cation Effects in the Transition from Micelles to Vesicles Through Salt Addition

3.1 Abstract

A transition from micelles to vesicles is reported when salts are added to catanionic micellar solutions composed of sodium dodecanoate (SL) / dodecyltrimethylammonium bromide (DTAB) and sodium dodecylsulfate (SDS) / DTAB, with an excess of the anionic component. The counterion binding and increase in aggregate size was monitored by mass spectrometry, rheology and dynamic light scattering measurements, whereas the vesicles were characterized by freeze-fraction and cryo-transmission microscopy experiments. The effect of counterions on the formation of vesicles in both systems was studied and compared to evaluate the role of the surfactant headgroups on the counterion specificity. The change in aggregate size can be accommodated by the increase of counterion binding and consequent dehydration of the surfactant headgroups. A classification of the cations could be made according to their ability to increase the measured hydrodynamic radii. It was observed that, if the sulfate headgroup of the anionic surfactant is replaced by a carboxylic group, the order of the ions was reversed.

3.2 Introduction

The investigation of specific ion effects has engaged researchers for decades. Despite that, ion properties and their interactions with other molecules are still not understood in detail, and we are far away from being able to predict their behavior. A major difficulty in the study of salts presents the fact that many phenomena involve the action of cations and anions of the electrolyte.

Molecular self-assembly in surfactant systems is largely dependent on the number of water molecules surrounding the headgroups. When ions are added to a solution, they dehydrate the surfactant headgroups[3,59]. This causes a decrease in the value a (effective area per molecule at the interface) and consequently an increase of the structural packing parameter P, which may result in the formation of vesicles. The effect of salts on a charged system can differ much depending on their kosmotropic or chaotropic character. It is well known that small ions of high charge density (e.g. sulfate, carboxylate, sodium) are strongly hydrated (kosmotropes), whereas large monovalent ions of low charge density (e.g. iodide, potassium) are weakly hydrated (chaotropes)[101,199]. Each salt is therefore expected to have an individual influence on vesicle formation, whether it tends to adsorb at the interface between micelle and water or remains strongly hydrated in the bulk.

Collins' concept of 'matching water affinities'[101] provides us with a simple model of specific ion-ion interactions. From various experimental results (for an extensive review see ref.[200]) Collins concluded that the dominant specific forces on ions of the same valency in water are short-range forces of chemical nature and that "the long range electrostatic forces generated by simple ions in water are weak relative to the strength of water-water interactions"[200]. Therefore, contact ion-pair formation is actually dominated by hydration-dehydration. A good agreement was also found with recent calculations of water pairing, where explicit water molecules were modeled[201]. It is challenging to see if this simple concept holds also for specific ion-headgroup interactions.

A salt induced micelle-to-vesicle transition was studied in two catanionic systems: sodium dodecanoate (SL) / dodecyltrimethylammonium bromide (DTAB) and sodium

dodecylsulfate (SDS) / DTAB. An excess of the anionic surfactant was present in both systems. The two systems differed only in the headgroup of the anionic surfactant in order to elucidate the fact that not the types of the ion alone, but rather the specific cation-surfactant interactions shape the surface behavior. Large cation specificity was found, however the series experienced a reversal when the carboxylate ion was exchanged for a sulphate one. SDS / DTAB is a well-known throughly studied system[47,48], whereas, by using a fatty acid based surfactant, the system resembled more to a biological membrane than a system containing SDS; it had been determined that cellular membranes consist of roughly 2 to 5 % of free long-chain carboxylic acids. The catanionic surfactant trimethylammonium headgroup, in comparison, resembles the choline group that is often present in membranes[202,203]. The effect of different anions and cations on the micellar solutions was studied by phase diagrams, rheology, dynamic light scattering and mass spectrometry, whereas the vesicles were characterized by freeze-fracture and cryo-TEM imaging. The mechanism of micelle-to-vesicle transition was investigated and compared.

3.3 Experimental Procedures

Materials The surfactants, sodium dodecyl sulfate (SDS; Merck, Germany; assay $> 99\%$), sodium dodecanoate (SL; Sigma, Germany; grade: 99-100%) and dodecyltrimethylammonium bromide (DTAB; Merck, Germany; assay $> 99\%$) were used as received. All sodium and chloride salts used in the experiments were supplied by Merck, Germany. Millipore water was used as solvent in all cases.

Sample Preparation Surfactant stock solutions were prepared by dissolving weighed amounts of dried substances in Millipore water. The solutions were then left for 24 hours to equilibrate at 25°C. The anionic-rich region of the phase diagrams was used in both cases. The catanionic solutions were prepared by mixing the surfactant stock solutions to obtain a fixed anionic / cationic surfactant mass ratio: 60/40 (this corresponds to a molar ratio of about 2/1) and 70/30 (molar ratio 2.5/1) was used for SL / DTAB and SDS / DTAB mixtures, respectively. The starting ratio

was determined from phase diagrams (see Figures 2.1 and 3.1). The total surfactant concentration was kept at 1 wt.% at all times. Salts were added to the micellar solution at increasing concentrations up to 50 mM. The solutions were then stirred and left to equilibrate for a day at 25°C before making measurements.

Electrospray Mass Spectrometry (ES-MS) Cation affinities for the vesicular interface/carboxylate group were determined by electrospray mass spectrometry. ES-MS was carried out using a Thermoquest Finnigan TSQ 7000 (San Jose, CA, USA) with a triple stage quadrupole mass spectrometer. The solutions were sprayed through a stainless steel capillary held at 4 kV, generating multiple charged ions. Data were collected using the Xcalibur software.

Other Methods Cryo- and freeze-fracture transmission electron microscopy, dynamic light scattering and rheology were performed as described in Chapter 2.

3.4 Results

3.4.1 Phase Diagrams

The addition of salts to the catanionic mixtures at a certain ratio of the surfactants induced an easily observable aggregation, due to a formation of a bluish color or turbidity. Salts were added to samples from all parts of the phase diagrams, however homogeneous vesicular systems upon salt addition were observed only at a certain anionic / cationic surfactant ratio (see Phase Diagrams, Figures 2.1 and 3.1). For this reason, the starting solution was taken from the micellar region of the phase diagram, a little way from the equimolarity line, with an excess of the anionic species (with a mass ratio of 60/40 and 70/30 for SL / DTAB and SDS / DTAB mixtures, respectively).

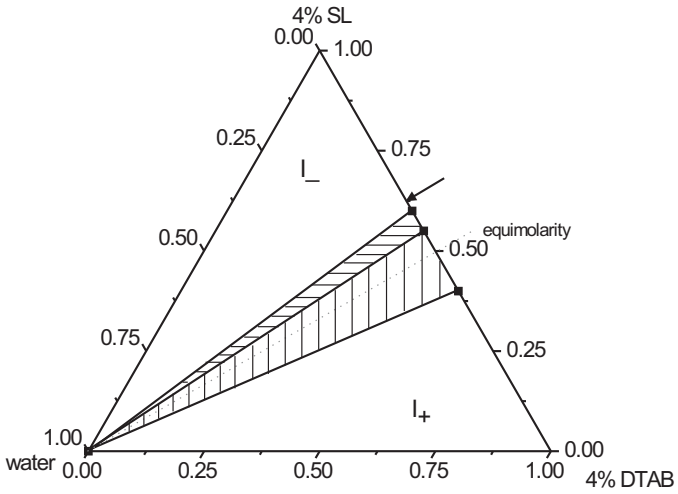

Figure 3.1: Schematic ternary phase diagram of the SL / DTAB system (right) at 25°C (the black arrow shows the starting point (reference sample), to which different salts were added). Figure reproduced with permission from the doctoral dissertation of A. Renoncourt.

3.4.2 Counterion Effects

The effect of various cations was studied by varying the concentration of different alkali chloride salts (LiCl, NaCl, KCl, CsCl). As the concentration of salt in the system was increased, the solutions exhibited a transition from a colorless to a blue solution, the blue color being typical of the presence of large objects. This transition could be observed for all salts, however, the concentration at which vesicles appeared was strongly dependent on the nature of the cation. Further increase of added salt concentration finally led to a phase separation, with one of the two phases being blue and isotropic and the other turbid.

Samples with different salt concentrations were first analyzed by dynamic light scattering. The addition of chloride salts causes an increase in average particle size and a certain turbidity of the solution (Figure 3.2). DLS indicated a significant increase in the mean hydrodynamic radius (R_H) of the micelles from 10 up to ca.170 nm. In agreement with our visual observations the rate of increase of the measured hydrodynamic radius was different for each chloride salt. This highlights strong cation specificity.

For instance, in the SL / DTAB system (Figure 3.2, left) a small amount of LiCl ($<$ 10 mM) was sufficient to dramatically increase the hydrodynamic radius (over 100 nm), whereas with CsCl, concentrations higher than 60 mM were needed to obtain particles of that size. A classification of the cations can be made according to their ability to increase the measured hydrodynamic radius of the aggregates forming in the SL / DTAB surfactant mixture: $Cs^+ < K^+ < Na^+ < Li^+$.

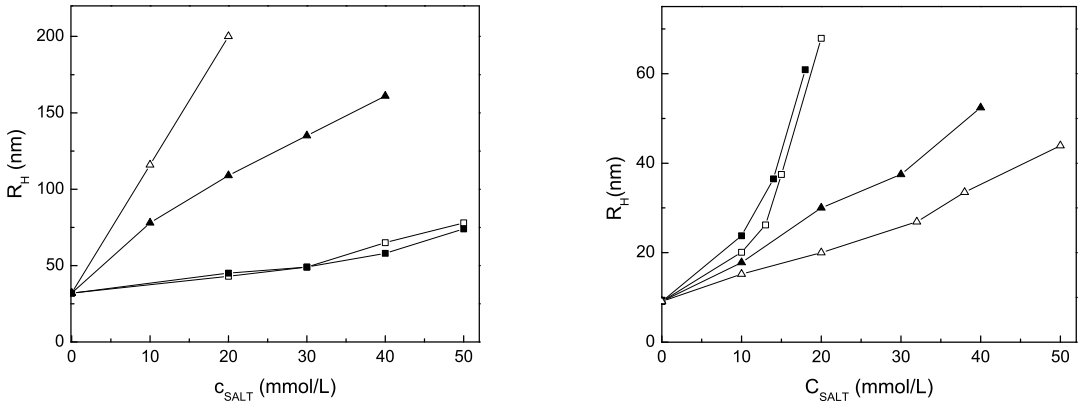

Figure 3.2: The effect of various cations on the growth of the hydrodynamic radii R_H of the catanionic aggregates in SL / DTAB (left) and SDS / DTAB (right) systems with an excess of anionic surfactant in both systems: LiCl (△), NaCl (▲), KCl (□), CsCl (■).

However, if the carboxylic headgroup of the anionic surfactant was replaced by a sulfate group, the order in which the ions assist the formation of vesicles was reversed (compare with Figure 3.2, right). Salts containing big cations having a smaller charge density (for instance CsCl) more efficiently induced vesicle/aggregate formation than small highly charged and highly hydrated cations (such as LiCl). A reversed Hofmeister series was therefore observed: $Cs^+ > K^+ > Na^+ > Li^+$.

Cation affinities for the vesicular interface / sulphate (or carboxylate) group were determined by electrospray ionization mass spectrometry. Although in this method the ionization process takes place in the gas phase, the chemical nature of surfactant monomers and simple ions is the same in the liquid and in the gas phase. Therefore, the preferential ion-surfactant interactions can easily be noted[204,205]. Re-

sults show that most of the mass signals (peaks) remain unchanged independently of the nature of the added salts. A typical ES-MS spectrum of the complete m/z region (m and z are the mass and charge of an ion, respectively) is shown in Figure 3.3.

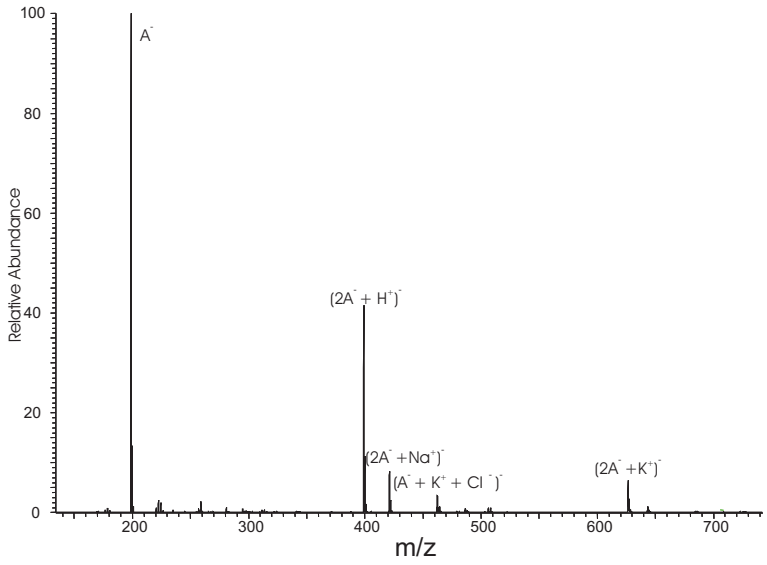

Figure 3.3: ES-MS spectrum of 1 wt.% SL / DTAB micellar solution with 15mM NaCl; A^- : dodecylcarboxylate anion (199 Da); C^+ : dodecyltrimethylammonium cation (228 Da).

Figure 3.4 represents the anion fragmentation patterns of the SL / DTAB catanionic mixture upon the addition of various salts: for better visibility only a part of the m/z region is presented. A closer look reveals that the position of the peak representing the binding of sodium ions to the carboxylate $(2A^- + Na^+)^-$ remained unchanged. Also the size of the peak was comparable in all spectra with the exception of spectrum (A). When LiCl was added, two same-sized peaks appeared, one representing the binding of sodium, the other of lithium ions to the carboxylate anion. This suggests that Li^+ was able to come closer to the vesicular surface, replacing a part of the sodium ions at the interface. The exactly opposite was observed in the case of CsCl (Figure 3.4D). The latter suggests a very small occurrence of cesium ions at the vesicle interface (very small $(2A^- + Cs^+)^-$ peak). A general ordering of the cations could be determined from the ES-MS spectra, with lithium showing the greatest affinity for the anionic group and the other cations following: $Li^+ > Na^+ > K^+ > Cs^+$. As observed previously, this order exhibited a reversal if the

surfactant mixture contained a sulphate headgroup (SDS).

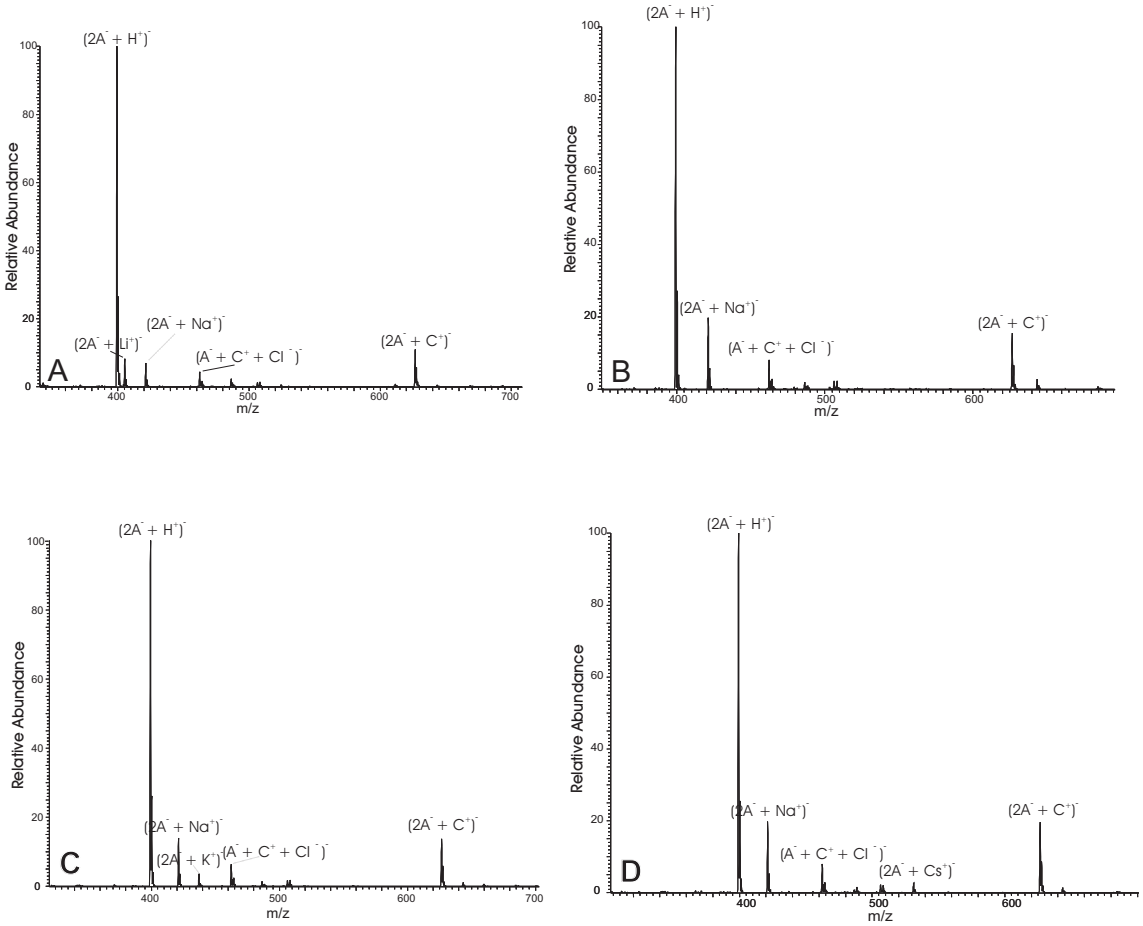

Figure 3.4: Ion binding as determined by ES-MS: addition of 15mM of (A) LiCl, (B) NaCl, (C) KCl and (D) CsCl to a SL / DTAB micellar solution; A^- : dodecylcarboxylate anion (199 Da); C^+ : dodecyltrimethylammonium cation (228 Da).

Results from rheology experiments performed on catanionic solutions with various salts showed that the viscosity decreases with applied strain rate (c. f. Figure 3.5). This behavior is common for solutions containing large non-spherical molecules, which tumble at random under low shear, but align themselves in the direction of increasing shear and produce less resistance as the shear rate is increased[3]. This behavior pointed to the presence of rod-like micelles in the solutions, which was confirmed also by microscopy (see ahead). No change in the rheological behavior of the samples was observed however as the nature of the salt is varied. Probably, the change in the overall concentration of elongated micelles present in the solution was

too low for such detection to be possible with our equipment.

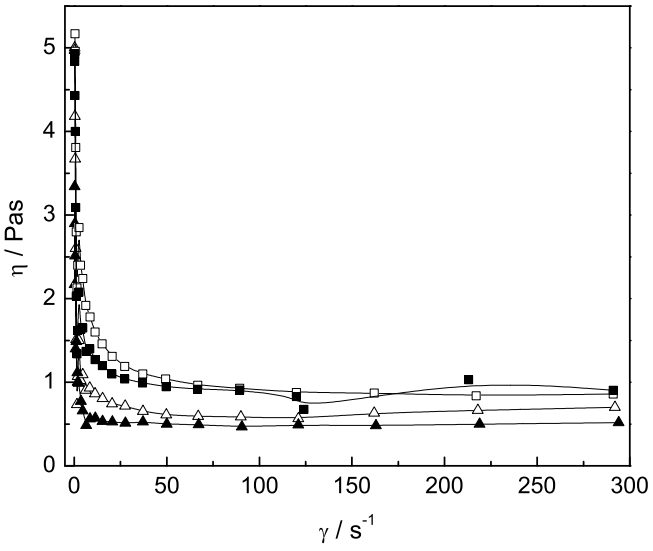

Figure 3.5: Viscosity of 1 wt.% SL / DTAB micellar solution upon the addition of 15 mM LiCl (△), NaCl (▲), KCl (□), CsCl (■) as a function of shear rate.

Homogeneous samples exhibiting a bluish color typical for solutions containing vesicles were further investigated by cryo- and FF-TEM. The images confirmed an increase in the size of the aggregates and high polydispersity (common to non-equimolar catanionic systems). Figure 3.6(A) shows a picture similar to what we have reported in the previous chapter. Not only the SDS / DTAB system, but also the SL / DTAB system confirmed the presence of long ribbon-like micelles unraveling and forming sheets. It seems that the addition of salts produced a similar effect in both systems, hinting at a general mechanism of micelle-to-vesicle transitions in catanionic systems. Figure 3.6(B) shows many half-closed and some already fully-closed vesicles.

Cryo-TEM images of the SDS / DTAB system confirm the high polydispersity in such mixtures. Vesicles of various sizes were seen to exist in equilibrium with ribbon-like micelles.The increase in measured R_H was therefore most likely due to

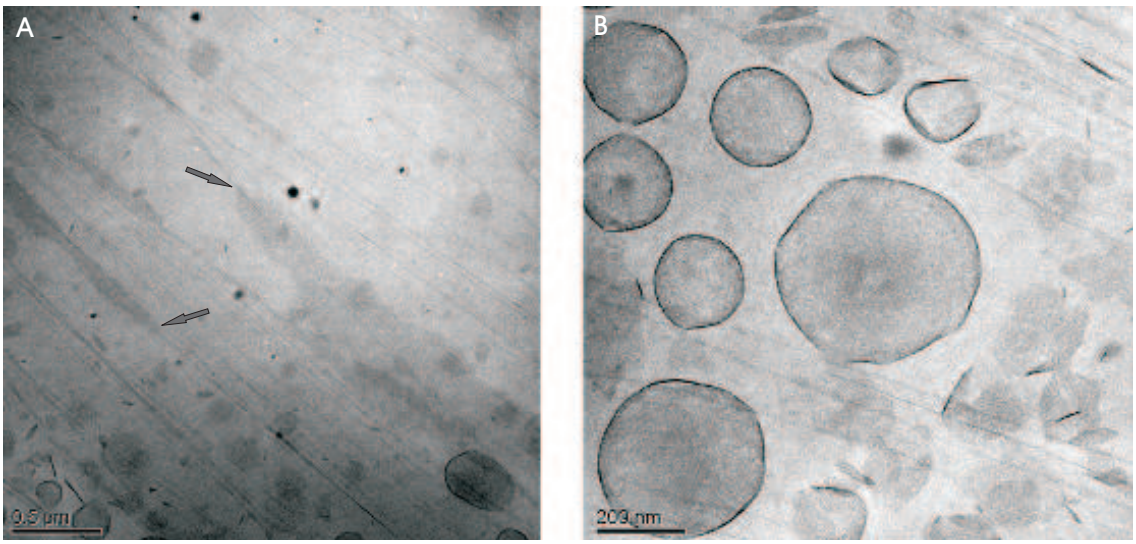

Figure 3.6: Cryo-TEM photographs of a SL/DTAB aqueous solution at the molar ratio of approximately 2/1 and a total surfactant concentration of 1wt.% upon the addition of 20 mM of NaCl. The arrows in (A) show the presence of long ribbon-like micelles unravelling and forming sheets. These sheets then curve and form spherical aggregates (B).

the combined effects: formation of vesicles as well as the elongation of rods. The latter effect is well known in literature[206,207].

FF-TEM, because of the advantageous fracture course within hydrophobic zones, provides us with the information regarding the membrane surface of the vesicles. A peculiar difference could be observed. The addition of sodium ions to the two systems assisted in the formation of very different vesicles. While the sulfate group containing surfactant mixture formed polyhedral (faceted) vesicles with very stiff looking membranes, the carbooxylate system exhibited the presence of individual unilamellar vesicles with completely smooth membranes (Figure 3.7). Faceted vesicles are present when the tails of the surfactants are rather stiff due to crystallization. This is commonly seen in catanionic systems. This stiffness may also describe the hydration of the surfactant molecule.

Similar behavior could be found within one system, when the effect of various cations on the membrane stiffness was compared. The stronger preferential binding of ions could also be observed by the distortion of the SDS / DTAB vesicle membrane as it became dehydrated when Cs^+ and Li^+ ions were compared (see Figure 3.8).

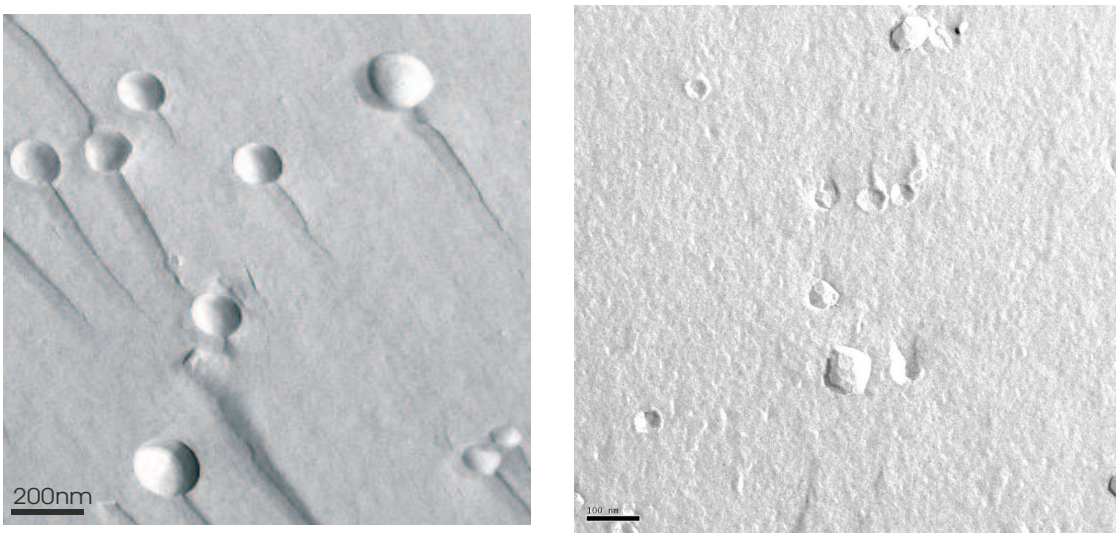

Figure 3.7: FF-TEM photographs representing the effect of 30 mM NaCl on the SL / DTAB (left) and the SDS / DTAB (right) micellar solution. The left image presents vesicles with completely smooth membranes. When the carbooxylate group is exchanged for a sulphate group, the vesicles become stiff-looking and faceted.

3.4.3 Co-ion Effects

The binding of counterions to a mixed catanionic micelle/solution interface depends on the surfactant molar ratio[1], i.e. the charge of the aggregates. Zeta potential measurements of the catanionic solutions with and without salt confirmed the presence of negatively charged aggregates. Therefore, no anion specificity was to be expected. Samples were nevertheless checked also in the presence of various sodium salts (NaCl, NaBr, Na_2CO_3, NaSCN, NaOAc, $NaNO_3$). All salts proved to have a significant influence on the growth of the micelles, however, no significant specificity could be found for the different anions (the curves overlap - c. f. Figure 3.9).

3.4.4 Nonionic Effects

Two non ionic additives, glucose and urea, having respectively salting-out and salting-in effects, were also added to the same mixed micelles solutions. No effect whatsoever on the growth of the measured hydrodynamic radius could be noticed. Even though glucose and urea were added at a concentration as high as 1 mol/L, no increase in the hydrodynamic radius of the aggregates was found.

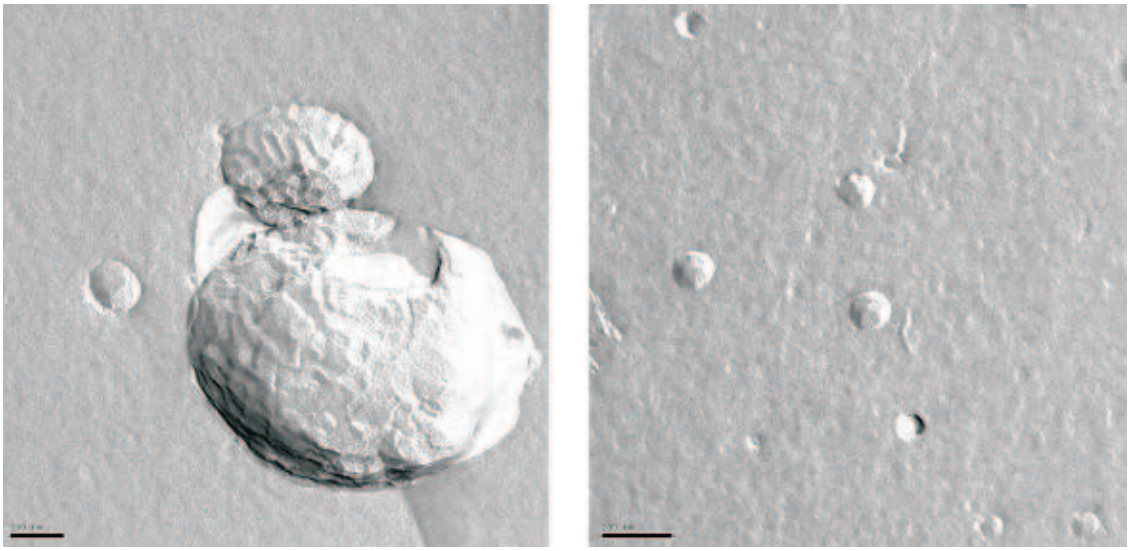

Figure 3.8: FF-TEM images the effect of 45 mM CsCl (left) and LiCl (right) on the reference SDS / DTAB micellar solution. The bars represent 100 nm in both cases.

3.4.5 Effects of 'Hydrophobic Ions'

Above observations on alkali salts have shown that all alkali cations caused an increase in the measured hydrodynamic radii. At high electrolyte concentrations the electrostatic repulsions are screened and the vesicles aggregate. This effect has not been observed when so called 'hydrophobic' ions are present. Tetramethylammonium chloride (TMAC) and choline chloride (ChCl) were added to mixed micellar solutions of SDS / DTAB and SL / DTAB. Results obtained by DLS show only a slight increase of the hydrodynamic radius upon the addition of TMAC to a micellar solutions (from 20 to 30 nm).

A larger difference in the cation affinity for the aggregate surface could be determined by ES-MS. Figure 3.10 shows anion fragmentation patterns upon the addition of salt, tetramethylammonium chloride (for better visibility only a part of the m/z region is presented). ES-MS spectra hint that TMA^+ was able to come closer to the vesicular surface, replacing a part of the sodium ions at the interface (Figure 3.10(A)). The exact opposite was observed in the case of carboxylates (Figure

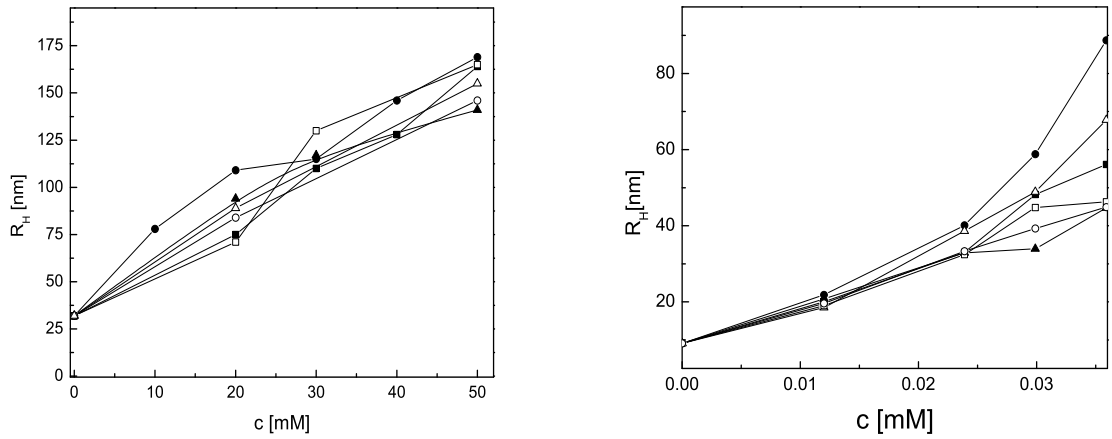

Figure 3.9: The effect of various anions / sodium salts on the growth of the hydrodynamic radii R_H of the catanionic aggregates in SL / DTAB (left) and SDS / DTAB (right) systems: NaCl ((•), NaSCN (□), NaBr (■), Na_2CO_3 (△), NaOAc (○) and $NaNO_3$ (▲)

3.10(B)). The results obtained for choline chloride salts were comparable.

FF-TEM images of the SDS / DTAB solution showed the presence of vesicles at low TMAC concentrations (c.f. Figure 3.11, left), similarly to the case of alkali salts. However, the membranes of the vesicles were more flexible and are therefore more likely to fuse. Surprisingly, at higher concentration only small discs and mi-

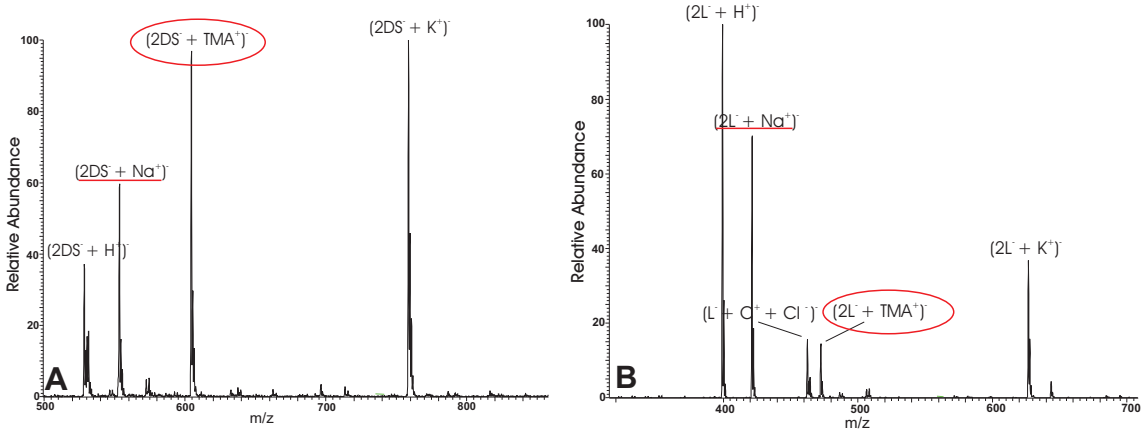

Figure 3.10: Ion binding as determined by ES-MS: addition of 40 mM of TMAC and to a (A) SDS / DTAB and (B) SL / DTAB micellar solution. DS- : dodecylsulfate anion (265 Da); L- : dodecylcarboxylate anion (199 Da); K+ : dodecyltrimethylammonium cation (228 Da).

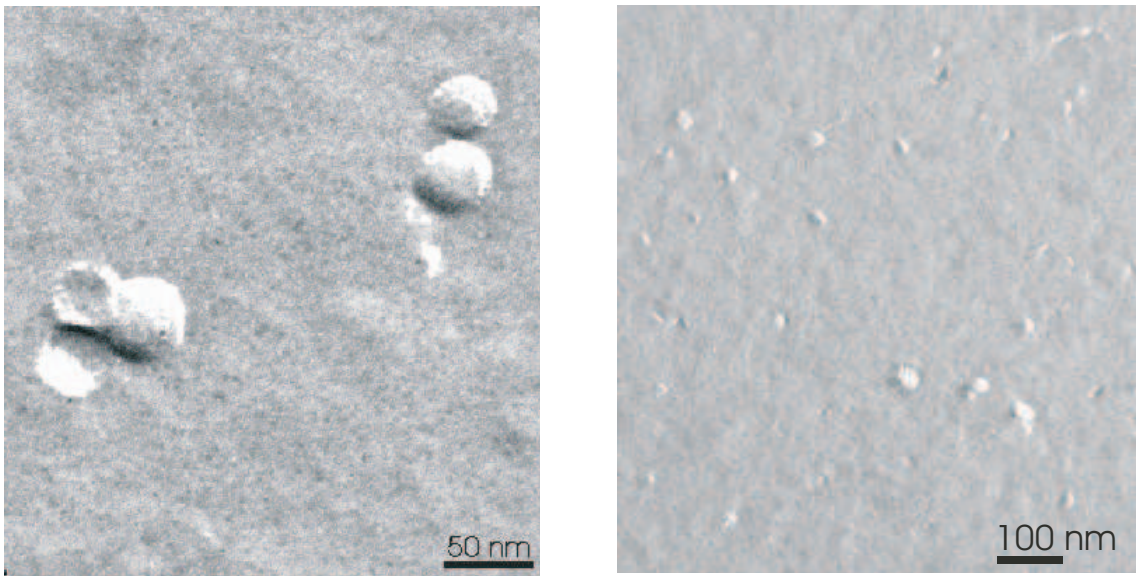

Figure 3.11: FF-TEM photographs representing the effect of 20 mM (left) and 40 mM (right) TMAC on the reference SDS/DTAB micellar solution.

celles could be observed (Figure 3.11, right). In the case of SL / DTAB, however, no vesicles were observed. Small discs and micelles were present over the whole concentration region. The same picture could be found when 50 mM of ChCl was added to SDS/DTAB and SL/DTAB.

3.5 Discussion

3.5.1 Aggregation Behavior of Catanionic Systems

The main thermodynamic driving force for the association of a cationic and an anionic surfactant mixture is the release of counterions from the aggregate surfaces. This results in a large entropy increase. For these systems a non-monotonic change in P is observed, with a pronounced maximum as the mixing ratio is varied[1,3]. In the system presented here vesicles could only be formed when the anionic surfactant is in molar excess compared to the cationic surfactant. Therefore, only this ratio was considered here.

The geometry of aggregates in colloidal systems is attributed to the packing of the amphiphilic molecules. The packing parameter is dependent on the length and vol-

ume of the hydrophobic tail and the size of the hydrophobic head of the surfactant molecule. These factors are often expressed in a packing parameter $P = v/(l_{max}a)$, where v and l_{max} are the volume and length of the hydrophobic part, respectively, and a the area per molecule at the interface. If the hydrocarbon part of the surfactant is kept constant and only the headgroup is varied, then the difference in the aggregation behavior can be attributed solely to the properties of the polar headgroup. Because a describes the effective headgroup size, which in the case of ionic surfactants is largely determined by repulsive electrostatic forces, and not the ionic radius, the change of morphology in surfactant systems is largely dependent on the number of water molecules surrounding the headgroups. It has been observed by chemical trapping method[135] that in association colloids, the changes in the balance of forces controlling the aggregate structure are reflected in the changes in interfacial concentrations of water and other components. The ions, when added to a micellar solution, can dehydrate the surfactant headgroups. This causes a decrease in the value a and consequently an increase of the structural packing parameter P. As a consequence, the critical micellar concentration is reduced[60,208] and the aggregate morphology changed[209]. The effects are caused by destruction of the hydration layer of the surfactant, decreased electrostatic repulsions, and an increased counterion binding[60]. Consequently, the surfactant monomers can be packed closer together leading to a bilayer formation.

3.5.2 Counterion Properties

The effect of salts on a charged system can differ much depending on the salting-in or salting-out properties of their ions[107,115,210]. Salting-out ions are usually small, with relatively small polarizabilities. They have high electric fields at short distances and have tightly bound hydration water. NMR evidence[211] suggests that small ions do not show specific binding to micelles and retain their mobility and their water of hydration right up to the micellar 'surface'[212] although this result depend on the type of surfactants. Salting-in ions are usually large, with significant polarizabilities. They have weak electric fields and a loose hydration sheath, which can be easily removed. NMR proves that they perturb phospholipid (surfactant) headgroups in a

significant way, probably through ion pairing[213]. Each salt is therefore expected to have an individual influence on vesicle formation, whether it tends to adsorb at the interface between micelle and water or remains strongly hydrated in the solution.

3.5.3 Collins' 'Law of Matching Water Affinities'

Recently, a simple 'law of matching water affinities' has been proposed[101]. It is based on the tendency of oppositely charged ions to spontaneously associate in aqueous solution. Only oppositely charged ions with matching absolute free energies of hydration should spontaneously form inner sphere ion pairs. This is supposed to be due to the fact that the strength of interaction between the ions and the water molecules is correlated to the strength with which the ion interacts with other ions[200]. Small cosmotropic ions can come close together forming inner sphere ion pairs without intermediate water molecules. The same is supposed to be true for big chaotropic ions, whereas when a cosmotropic ion approaches a chaotropic counterion, the ions should remain separated by at least one water molecule. With this model an impressive number of phenomena and properties can be described.

3.5.4 Counterion Selectivity of Alkyl Sulfates

In the present case the headgroups in excess are alkylsulfates. In contrast to double-charged sulfate ions, such headgroups have a more chaotropic behavior. With this assumption and according to Collins' concept, alkylsulfates should come in close contact with chaotropic ions like cesium, whereas lithium ions remain further away. Therefore it is expected that Cs^+ screen more efficiently the negative charge excess on the aggregates than Li^+, and this is precisely what is observed, c.f. Figure 3.2 (right). The same ordering of cations was found in systems containing pure SDS micelles[214] and in the case of another anionic surfactant with a sulfate group, sodium dodecylbenzenesulfonate[177]. To make a more quantitative analysis we compare the salt concentrations to the excess concentration of SDS (compared to DTAB), which is approximately 0.015 mol/L. From Figure 3.2 (right) it can be inferred that this concentration roughly corresponds to the asymptotic limit for micelle to vesicle

transition in the case of K^+ and Cs^+ chlorides. Therefore it may be concluded that these cations have a strong propensity to the sulfate groups and that sulfate headgroup-cation pairs are formed; in this case the excess negative charge of the vesicles is neutralized. This finding is in agreement with the association constants found for a similar surfactant n-octylbenzenesulfonate[154].

3.5.5 Counterion Selectivity of Alkyl Carboxylates

We have seen that with the sulfate group the binding increases with the decreasing size of the hydrated alkali metal ions. The order is reversed when the headgroup is exchanged for a carboxylate. The carboxylate headgroup exhibits water-ordering properties and the addition of an alkyl chain should not change the kosmotropic behavior of the headgroup. According to Collins' concept, alkylcarboxylates should then come in close contact with kosmotropic ions like lithium, making it more possible to form inner-sphere ion pairs, whereas cesium ions remain further away. Therefore, it is expected that Li^+ screens more efficiently the negative charge excess on the aggregates than Cs^+, and this is precisely what is observed in Figure 3.2 (left). The same order of counterion-binding to carboxylate headgroups that was found in our catanionic surfactant system are found in polyelectrolyte solutions[215–218], when measuring the cation affinity to ion-exchange resins[219,220], in studies of membrane potentials[220], of electrophoretic mobility of colloids[221], and of ion-transport phenomena[222]. Our results are also in agreement with measurements of counterion binding to soap micelles[81,212,223,224] and long-chain fatty acids[222,223,225]. Recent MD simulations have shown that the carboxylate groups dominate the counterion behavior even in complex systems such as proteins[210].

3.5.6 Alkyl Sulfates vs. Alkyl Carboxylates

Similar counterion specificity was observed in the case of polyelectrolytes. As in the case of surfactants, the specific-ion effects do not depend only on the individual properties of the participating ionic group and its counterion (charge, size, charge distribution and polarizability), but also on the overall charge of the polyion, as well

as on the possible cooperating binding sites which might influence the binding site. Furthermore, even at high dilution a substantial number of counterions is forced into close proximity to the polyion by the long-range electrostatic forces[226,227], so that there always exist a large number of ion pairs for which solvation effects should be observable. Strauss[217,218] used the dilatometric method to measure the volume changes that occurr when polyelectrolyte solutions are mixed with solutions containing different specifically interacting counterions. Polyelectrolytes containing sulfate and carboxylate headgroups exhibit opposite series of counterion binding, similar to the series observed in our experiments on surfactant micelles. Dilatometric results clearly show specificities depending on both the polyion and on the metal ion which would not be expected on the basis of long-range electrostatic density of the polyion. The effects of the latter are governed predominantly by the linear charge density of the polyion and the linear charge densities of the studied sulfonates and acrylates are the same. It follows that the interactions giving rise to the observed volume changes involves specific sites on the polyions. Similar results of alkali cations to polyacrylates and polysulfonates have been discussed also by other authors[215,216,228–230]. The reversal of the cation series in the presence of polyacrylates was attributed to a competition between water of hydration and the anion for a given cation, which is related to the charge distributions, polarizabilities, and the effective field strengths of the ions[221,222]. The concept was however not studied thoroughly.

The reversion of series was observed also when measuring the cation affinity to ion-exchange resins[219,220,231], ion-transport phenomena[222], swelling of hydrogels[232] and counter-ion binding to long-chain fatty acids[212,215,223,224,233,234].

3.5.7 Molecular Dynamics Simulations

Also MD simulations show similar results. Chialvo and Simonson[235] modeled a short-chain polystyrenesulfonate and found the interaction with Li^+ too weak to cause desolvation. Similarly, Lipar et al.[230] reported the binding to polyanetholesulfonic acid to be strongest for Cs^+. Recently, an extended computational study of pairing of sodium and potassium with a broad set of biologically relevant anions was described[201,236]. The monovalent sulfate and the carboxylate groups and their

pairing with sodium vs. potassium were examined. The structures of the four investigated contact ion pairs, together with the cation - anion oxygen distances are shown in Figure 3.12.

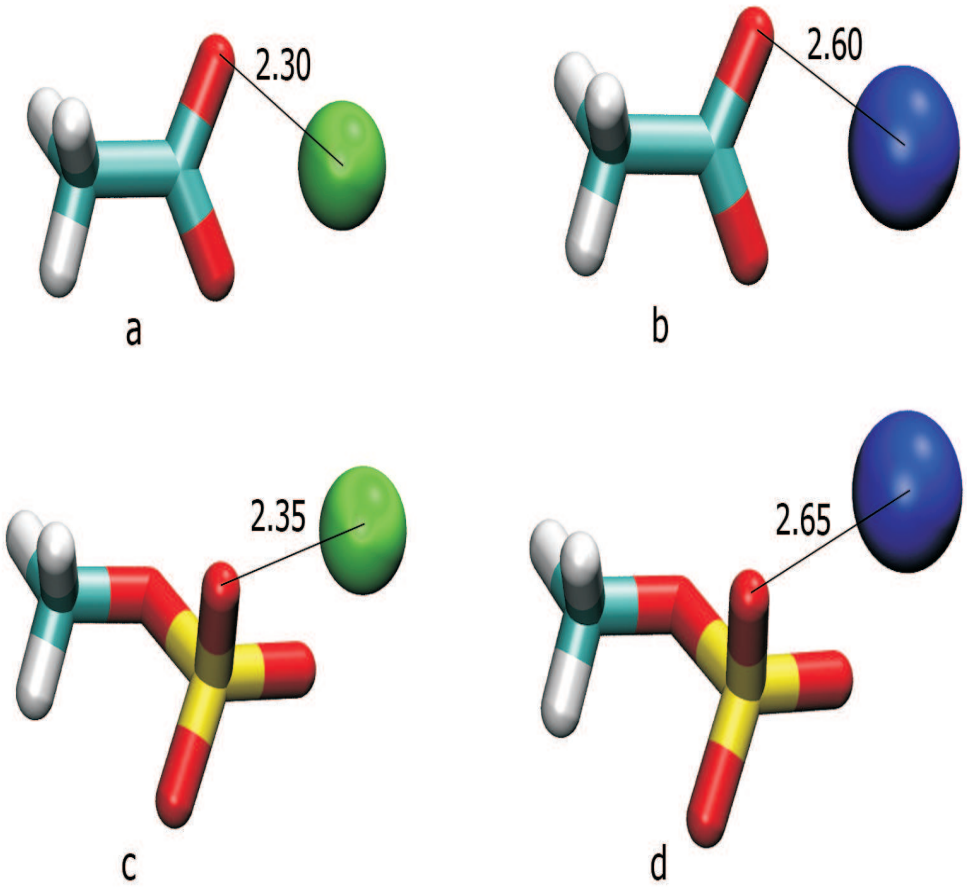

Figure 3.12: Geometries of the contact ion pairs of a) sodium-acetate, b) potassium-acetate, c) sodium-methylsulfate, and d) potassium-methylsulfate. The cations bind bidentally to two anionic oxygens. Reproduced from Vlachy et al.[236].

A combination of *ab initio* calculations with a polarizable continuum solvent model and molecular dynamics simulations were used to quantify the relative cation-anion association free energies, i.e., the values of $\Delta\Delta G$ connected with replacing potassium with sodium in a contact ion pair with acetate or methylsulfate anion[236]. These two free energy differences for CH_3COO^- and $CH_3SO_4^-$ are -2.50 and $+0.37$ kcal/mol, respectively. We see that while acetate strongly prefers sodium over potassium (by about 2.5 kcal/mol), methylsulfate weakly (by roughly 0.4 kcal/mol) prefers potassium over sodium. These findings are consistent with our experimental results

and also with the empirical Law of matching water affinities[101].

3.5.8 Generalization of the Concept: Hofmeister Series of Headgroups

In the preceding paragraphs a comparison of two headgroups is given. However, more headgroups are of interest in colloidal chemistry and biology, especially sulfonates and phosphates. Concerning hydrogen phosphate, both the charge density as well as several experimental results[201,214,237,238] suggest that it can be classified between the carboxylate and the sulfonate headgroup. Following computational as well as experimental results, we propose a way to classify headgroups in a Hofmeister like series, ordering them from cosmotropic to chaotropic headgroups: -carboxylate, -hydrogen phosphate, -sulfonate, -sulfate. (presented in Figure 3.13). With this series many specific-ion phenomena in colloidal systems can now be explained.

3.5.9 The Anionic Effect

The addition of sodium salts proved to have a significant effect on the growth of the micelles (Figure 3.9). This increase of particle size is mainly due to a decrease of the head group repulsions because of electrostatic screening. Since the micelles are very probably negatively charged, the anions will not come into close contact with the micellar surfaces and the onset of vesicle formation occurs at approximately the same concentration for all sodium salts. The small differences in radius size observed are likely to be due to the differences in the hydration of the anions; in the case of strongly hydrated Cl^- larger vesicles were observed than in the presence of other less hydrated ions. A similar effect was previously observed in studies of negatively charged phospholipid vesicles[239].

3.5.10 The Non-Ionic Effect

The fact that the addition of glucose and urea had no effect on the growth of the micelles (no micelle to vesicle transition was observed) suggests that electrostatic interaction is necessary and is the first order effect. Hydration numbers show that

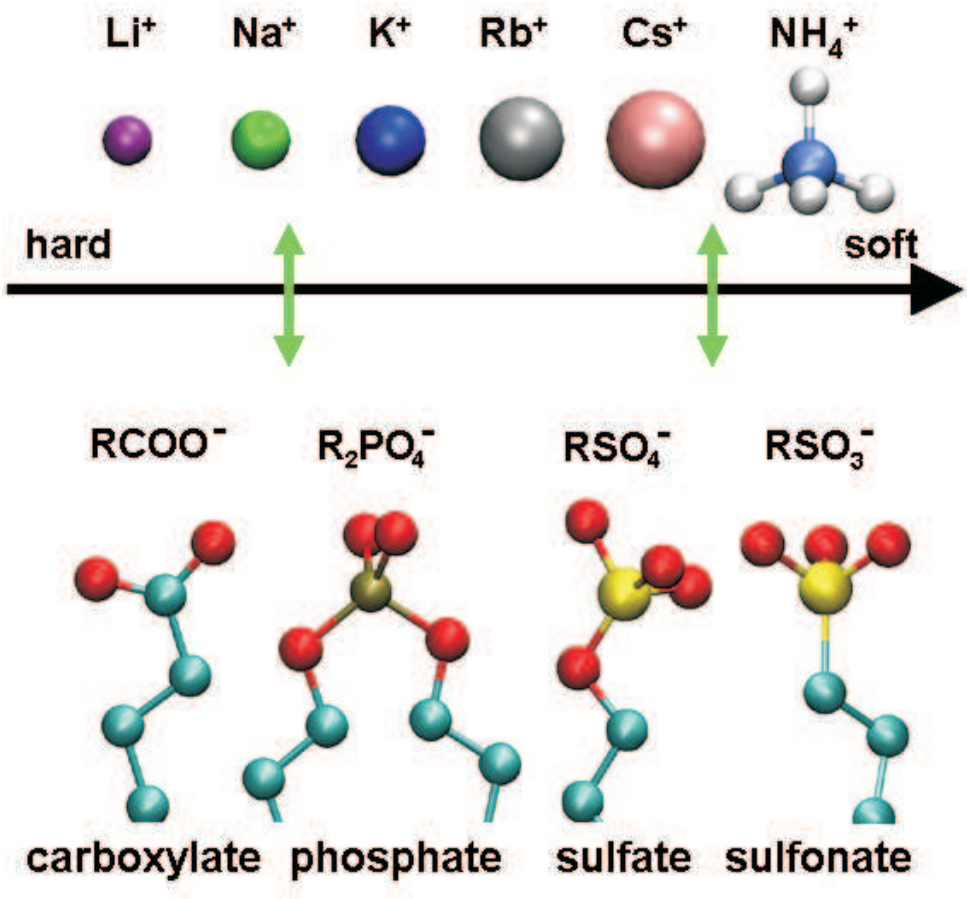

Figure 3.13: Ordering of anionic surfactant headgroups and the respective counterions regarding their capabilities to form close pairs. The green arrows represent strong interactions (close ion pairs).

glucose dehydrates the headgroups as well as the salts (the hydration numbers for Cs^+ and glucose are 4.3[116] and 3.5[240] respectively. Even much higher concentrations of glucose and urea (up to 1M) had no effect on the growth of the surfactant aggregates. This confirms that dehydration of the headgroups alone is not sufficient to trigger the micelle to vesicle transition. The reason must be sought in the electrostatics. Even if these uncharged molecules modified the surrounding water structure, this effect is not strong enough to significantly change the curvature via adsorption to the headgroups. If the micelles were consisted of just one type of surfactant (one charge), then the addition of salt would screen the repulsion between the headgroups, causing the surfactant molecules to arrange in a bilayer. The opposite case would be if the surfactants were mixed in equimolar amounts. Then

the salts would screen the attraction between them, most likely causing the distance between the headgroups to increase. Since our mixed micelles contain an excess of the anionic surfactant, we can assume an asymmetric distribution of charges (as was also proposed in the preceding chapter). Therefore the addition of salt should have a similar effect as in the case of 'single-charged' micelles.

3.5.11 Effects of 'Hydrophobic Ions'

Ammonium cations have a salting-in character and enhance the solubility of otherwise poorly water-soluble compounds. They are well-known as phase transfer catalysts. In water the ionic character of these ions is dominant, whereas in hydrophobic environments the organic character prevails[241]. However, there is a significant difference between the properties of ammonium and tetramethylammonium ions. The ammonium cation behaves much like a big alkali cation; it is weakly hydrated, its hydration sphere being similar to the hydration sphere of the Cs^+ ion.

By contrast, the tetramethylammonium cation is an intermediate case between 'simple' ions and hydrotropes such as xylene sulfate[242]. It seems plausible to assume that this 'hydrophobic' cation can penetrate into the micellar surface much as anions like tosylate and salicylate[243–246] in the case of cationic surfactants. If this is true, the tetramethylammonium ion can act as a co-surfactant, perhaps even partially replacing the cationic surfactant and perturbing lamellar structures - a feature that is well known from hydrotropes[247]. Interestingly, ES-MS suggest that a strong binding of the hydrophobic ions to the mixed micelles is present only in the case of sulfates, but not also when a carboxylate surfactant is present. The initial formation of the vesicles, observed in the SDS / DTAB system at low salt concentrations could be solely due to the increased ionic strength. However, this does not explain the observed changes in membrane flexibility. The destruction of vesicles at higher salt concentrations suggests the incorporation of the hydrophobic ion into the membrane and a change in the packing of the surfactants.

Although the information obtained from electronic microscopy is more or less the same for both systems at high salt concentrations, the reason for the presence of only micelles and small discs are most likely different. In the case of SDS, the

strong binding of the 'hydrophobic ions' should cause a disruption of the membrane, destroying the large vesicular structures. On the other hand, it is likely that the TMA^+ ion does not come into close contact to the SL / DTAB micellar surface. Therefore, it assists aggregate growth only by changing the properties in the bulk. As ammonium ions have salting-in properties, they do not induce the dehydration of the ionic surfactant headgroups and therefore also not assist in vesicle formation. Further discussion on alkyl trimethylammonium groups can be found in Chapter 4.

3.6 Conclusions

Through the addition of salts a transition from rod-like micelles to vesicles was observed in aqueous solutions composed of DTAB and an excess of either SL or SDS. Whereas no anion specificity for the added salts appeared in the formation of vesicles, the nature of the cation was found to influence strongly the critical salt concentrations around which micelles turn to vesicles. In the present case of negatively charged vesicles, ion-specific effects were expected for cations, since they accumulate in high concentration in the vicinity of the vesicle. The observed cation specificity followed the classical Hofmeister series for cation adsorption to sulfate headgroups. When alkylcarboxylates were present in solution, the cations followed a reversed Hofmeister series. The ion specificity could be qualitatively explained according to Collins' concept of matching water affinities. To this purpose, the headgroup of an alkylsulfate had to be regarded as a chaotrope and the alkylcarboxylate as a kosmotrope. The morphologies observed during the micelle-to-vesicle transition are analogous to those presented in the preceding chapter, hinting at a general mechanism common to catanionic systems.

Chapter 4

Anion Specificity Influencing Morphology in Catanionic Surfactant Mixtures with an Excess of Cationic Surfactant

4.1 Abstract

In the previous chapter we reported on an ion specific micelle-to-vesicle transition, when salts were added to a catanionic micellar solution composed of sodium dodecylcarboxylate (sodium laureate, SL) and dodecyltrimethylammonium bromide (DTAB), with an excess of SL. In the present chapter, we illustrate the ion specificity, when DTAB was in excess in the same system. In this case, no transition to vesicles was observed, but an elongation of micelles upon salt addition. The counterion binding and increase in aggregate size was monitored by mass spectrometry, dynamic light scattering measurements, and cryo-transmission microscopy. The mechanism was argued by employing the ability of the counterion to dehydrate the surfactant headgroup. This theory was confirmed in phase with Collins' concept of matching water affinities.

4.2 Introduction

Mixtures of surfactants show enhanced performance in technical processes (e. g. detergency, tertiary oil recovery, drug carrier systems, flotation), when compared to pure surfactant systems. Surfactant mixtures for specific applications are often chosen based on empirical evidence and experience. However, to optimize the applications it is important to have a general understanding of the interplay of interactions between the surfactants in a mixed system and of the factors influencing the phase diagram. Therefore, it is of interest to study the self-aggregation and micellization of such mixtures.

When oppositely charged surfactants are mixed, new properties appear. Aqueous catanionic mixtures exhibit a wide range of unique properties that arise from the strong electrostatic interactions between the oppositely charged heads. They exhibit low critical micelle concentration (CMC) values and a non-monotonic change in the surfactant packing parameter (P) as the mixing ratio is varied[2]. For this reason a large number of aggregate structures such as spherical and rod-like micelles, vesicles, lamellar phases, and precipitate have all been observed depending on the concentration, the size of the chain length or nature of the polar heads, and the ratios of the surfactants in solutions[24,26,48,53–57]. One advantage of catanionic systems as compared with more robust genuinely double chained surfactants are their greater sensitivity to parameters such as temperature[153] or the presence of salts[47].

The effect of salt type on various physico-chemical properties of a system was first observed over one hundred years ago by Franz Hofmeister who discovered the dependence of protein solubility on the type of added inorganic electrolyte[114]. Since then, a wide range of ion-specific phenomena in biology, pharmacy, and chemistry was observed. They have been recently reviewed in a special issue of 'Current Opinion in Colloids and Interface Science'[115]. Extensive studies have shown that the counterion has a strong effect on the thermodynamics and aggregation properties of surfactants[248–250]. Salt effects on the cmc, micellar size, and degree of dissociation for a given surfactant may follow a lyotropic (or Hofmeister) series[251]. An ion's position in the lyotropic series can be correlated with its charge and hydrated

radius. Depending on the charge density of the anion, it can interact more or less strongly with the cationic headgroups of micellar surface. Such a 'binding' decreases the electrostatic repulsion between the surfactant headgroups and hence favors aggregation. This lowers for instance the CMC and the degree of ionization of the micelles. A typical Hofmeister series for anions is as follows: $SO_4^{2-} < C_2H_3O_2^- < Cl^- < NO_3^- < Br^- < ClO_4^- < I^- < CNS^-$ (the positions of the NO_3^- and Br^- ions are often switched in the lytropic series).

Single-tailed surfactants usually form globular micelles in aqueous solution above their CMC[4]. An increase in surfactant concentration may induce the formation of worm-like micelles[252,253]. Similarly, addition of organic and inorganic counterions[206,252–254], uncharged compounds like aromatic hydrocarbons[255], or an oppositely charged surfactant[26,158] can transform spherical micelles into worm-like micelles.

In the previous chapter, we have reported a way to classify headgroups in a Hofmeister like series. We also were able to explain how salt-induced micelle-to-vesicle transitions in the anionic-rich regions of the phase diagrams in catanionic systems depend on both ion and headgroup specificities. In the present chapter, this study is extended to the cationic-rich region. We focus on the influence of the counterion identity on the aggregation behavior of non-equimolar mixed surfactant solutions, composed of sodium dodecanoate (SL) and dodecyltrimethylammonium bromide (DTAB) with an excess of DTAB. The effect of different anions and cations on the micellar solutions will be shown by means of phase diagrams, cryo-TEM, mass spectrometry and dynamic light scattering. Collins' concept of matching water affinities[101] will be shown to be also very valuable for the comprehension of the found series of salt sensitivity. And finally, the aggregation behavior will be compared to the one found in the anionic-rich region of the corresponding phase diagram.

4.3 Experimental Procedures

Materials The surfactants, sodium dodecanoate (SL; Sigma, Germany; grade: 99-100%) and dodecyltrimethylammonium bromide (DTAB; Merck, Germany; assay > 99%) were used as received. All sodium and chloride salts used in the experiments

were supplied by Merck, Germany. They were also used as received without further purification. Millipore water was used as solvent in all cases.

Phase Diagrams Surfactant stock solutions were prepared by dissolving weighed amounts of dried substances in Millipore water. The solutions were then left for 24 hours to equilibrate at 25°C. The catanionic solutions were prepared by mixing the surfactant stock solutions to obtain a fixed anionic / cationic surfactant mass ratio of 30 / 70. The starting ratio was determined from phase diagrams. The total surfactant concentration was kept at 1 wt.% at all times. Salts were added to the micellar solution at increasing concentrations. The solutions were then stirred and left to equilibrate for a day at 25°C before making measurements.

Other Methods Electrospray mass spectrometry, cryo-transmission electron microscopy and dynamic light scattering were performed as described in the previous chapters.

4.4 Results and Discussion

4.4.1 Ion Binding in Catanionic Surfactant Mixtures

In the studied catanionic system, the cationic surfactant DTAB was in excess. Therefore, it was expected that the variation of the anions will produces a larger effect as the variation of the type of cations. Figure 4.1 shows electrospray ionization mass spectra of the SL / DTAB catanionic solutions (mass ratio 30 / 70) upon the addition of different salts. Although in this method the ionization process takes place in the gas phase, the chemical nature of surfactant monomers and of simple ions is the same as in the liquid phase. Therefore, counterion affinities for the surfactant can easily be noted[204,205]. Because our surfactant mixtures already contained counterions, we added the same concentration of salts. In this way, we could observe the competition of the counterions for the surface of the surfactant aggregate.

Figure 4.1 represents the DTA^+ fragmentation patterns upon the addition of

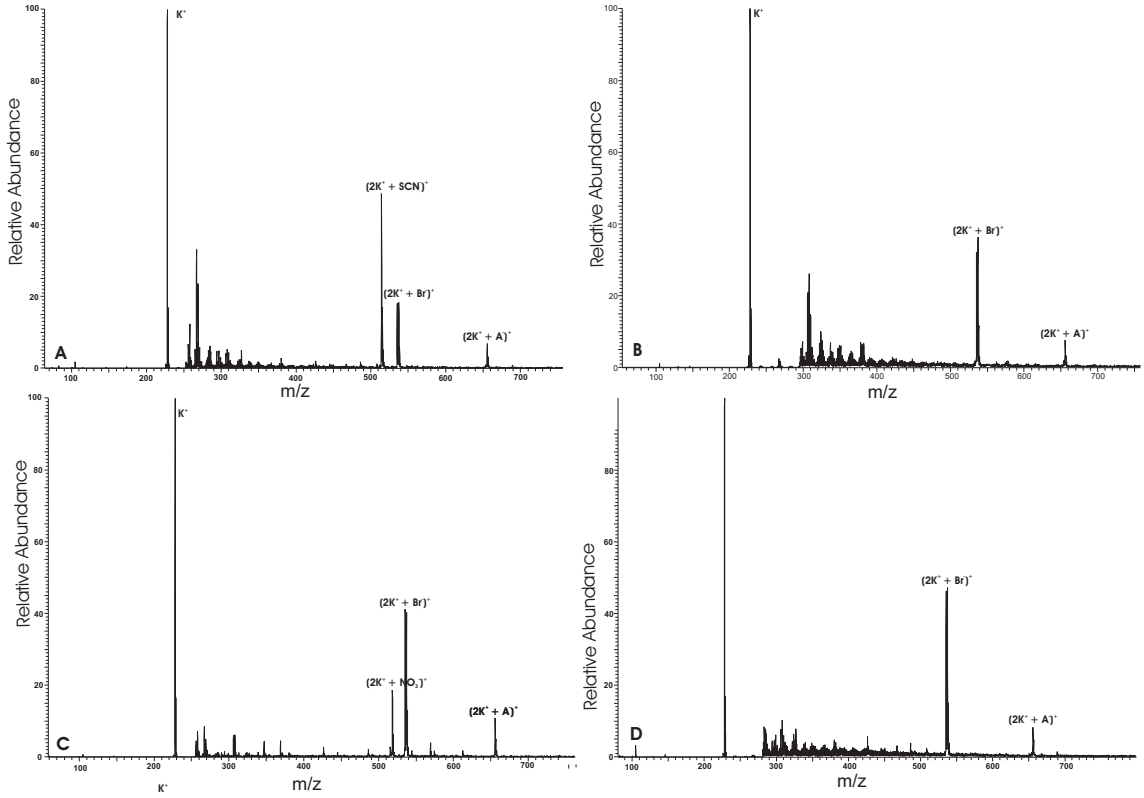

Figure 4.1: Ion binding as determined by ES-MS: addition of 15mM of (A) NaSCN, (B) NaBr, (C) $NaNO_3$ and (D) Na_2SO_4 to a SL / DTAB micellar solution; A^- : dodecylcarboxylate anion (199 Da); K^+ : dodecyltrimethylammonium cation (228 Da); the peaks between 250 and 300 (m/z) are solvent related.

various salts: for better visibility only a part of the m/z region is presented. It turns out that most of the mass signals (peaks) remain unchanged, independently of the nature of the added salts.

A closer look revealed that the position of the peak representing formation of ion pairs between the oppositely charged surfactant ions $(2K^+ + A^-)^+$ remained unchanged. Also the size of the peak was comparable in all spectra. Similarly, the peak corresponding to the binding of bromide ions to the dodecyl trimethylammonium cation $(2K^+ + Br^-)^+$ was present in all spectra, regardless of the nature of the added salt. The height of this peak, however, was less pronounced in spectrum (A). When comparing the binding of anions to the dodecyl trimethylammonium cation, we observed that only the SCN^- exchange the bromide anions at the micellar surface. NO_3^- and Cl^- showed approximately the same affinity for the alkyl trimethylammonium group, whereas in spectrum (D), when Na_2SO_4 was added to

the catanionic mixture, no peak representing the binding of sulfate ions was visible. These results suggest that the strongly hydrated sulfate anion did not come close to the micellar surface, whereas the loosely hydrated thiocyanate anion was able to come closer to the micellar surface, replacing a part of the bromide ions at the interface. A general ordering of the cations could be determined from the ES-MS spectra, with thiocyanate showing the greatest affinity for the anionic group and the other cations following: $SCN^- > Br^- > NO_3^- > Cl^- > CH_3COO^- > SO_4^{2-}$. The variation of the cation of the salt produced no effect on the cation fragmentation patterns, as can be expected in a system with an excess of cationic surfactant. The m/z peaks remained unchanged for all added chloride salts.

4.4.2 Phase Behavior upon Salt Addition

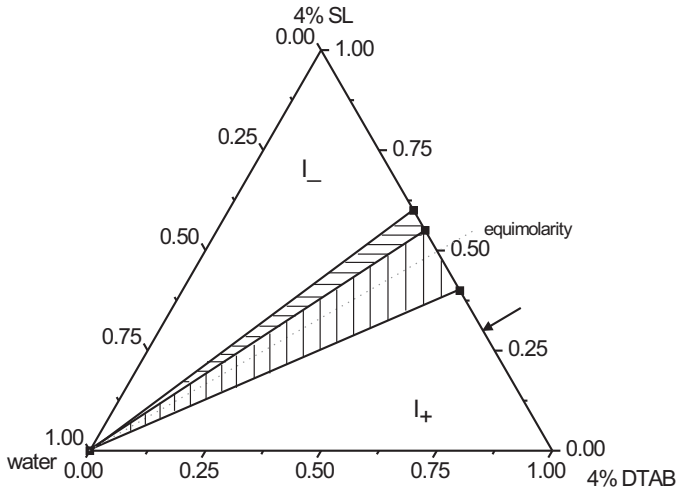

Figure 4.2: Schematic ternary phase diagram of the SL / DTAB system at 25°C (the arrow represents our starting solution (reference sample; mass ratio 30 / 70).

The influence of salts on the SL / DTAB catanionic mixture was further followed by observing the phase behavior; the starting phase point in the phase diagram being a micellar solution, c. f. diagram shown in Figure 4.2. Different salts affected the system in various ways. While the addition of some salts produced no visible effect, others induced an easily observable aggregation (formation of a bluish color

or turbidity). As the salt concentration was increased the aggregation became more pronounced. The effects are reported in Table 4.1.

Salt	25 mM	50 mM
NaSCN	bluish/turbid	turbid
NaBr	bluish/turbid	turbid
$NaNO_3$	bluish	turbid
NaOAc	clear	clear
Na_2SO_4	clear	clear
NaCl	clear	clear/bluish
LiCl	clear	clear/bluish
KCl	clear	clear/bluish
CsCl	clear	clear/bluish
Choline Cl	clear	clear

Table 4.1: Visual observations of the effect of various salts on the SL / DTAB (mass ratio: 30 / 70) catanionic solution. The reference sample was a clear homogeneous solution.

The aggregation was checked by light scattering; however problems were reported by the apparatus due to the high scattering intensity and the high polydispersity of the solutions. Despite that we are able to confirm an increase in the hydrodynamic radius of the particles in accordance with our visual observations (c. f. Figure 4.3). We emphasize that the absolute values of the hydrodynamic radii should be taken with a grain of salt, because the aggregates formed in solutions are rods (as will be shown with cryo-TEM further on), and the CONTIN software used by the Zetasizer 3000 calculates the radius of spherical aggregates. However, the trend in the increase of R_H is important. The degree of micellar growth varied in exactly the inverse order of the hydrated radius of the counterion: $SO_4^{2-} \approx C_2H_3O_2^- < Cl^- < NO_3^- < Br^- < CNS^-$.

Salts containing big anions having a weakly distributed charge (CNS^-) induced more efficiently the micellar growth than the divalent sulphate (SO_4^{2-}). Apparently

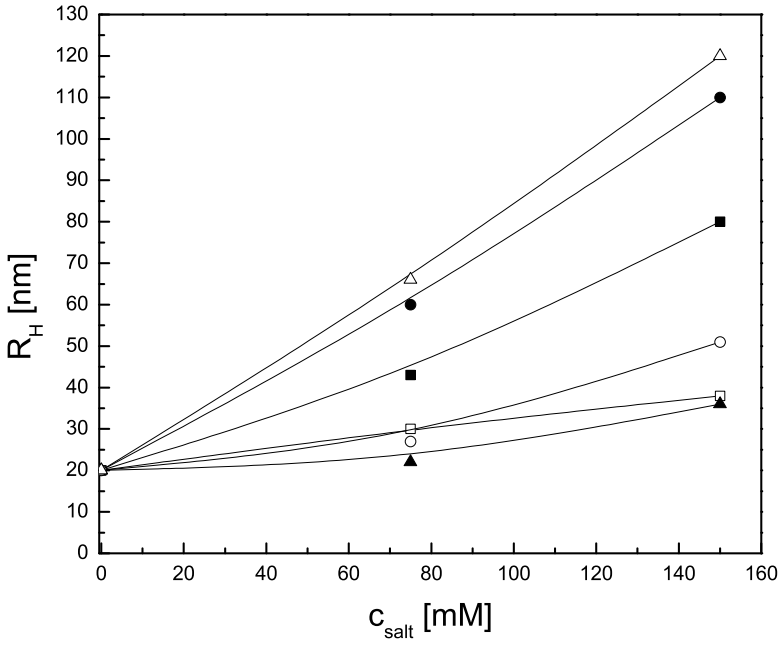

Figure 4.3: The effect of various cations / chloride salts on the growth of the hydrodynamic radii R_H of the catanionic aggregates in SL / DTAB systems: NaOAc (▲), Na_2SO_4 (□), NaCl (○), $NaNO_3$ (■), NaBr (•) and NaSCN (△).

the large hydrated radius of the sulfate ion hinders its ability to bind to the micelle containing an excess of DTAB.

4.4.3 Anion Specificity in Physico-Chemical Properties of Alkyltrimethylammonium Systems

The competition of various anions for the binding sites on the surface of CTAB micelles was checked by Larsen and Magid[256]. They found a strong binding of nitrate to the micelle, displacing bromide. The positions of bromide and nitrate ions are often exchanged in the lyotropic series. As an example, Cohen and Vassiliades[257] found that NO_3^- was less effective than Br^- at lowering the CMC of CTAB. The lyotropic series was observed also when micellization of alkyltrimethylammonium halides, heats of counterion binding, surface tension, and the thermodynamic and

microenvironmental properties of the micelles were compared[256,258–261]. The controlling factor in this ion-specificity seems to be the distance of closest approach of the ion to the micelle.

4.4.4 Influence of Salt on the Aggregation Behavior of Surfactants

The geometry of aggregates in colloidal systems is attributed to the packing of the amphiphilic molecules. The factors governing the shape of the aggregates are expressed in its simplest form by a packing parameter $P = v/(l_{max}a)$, which is dependent on the length (l_{max}) and volume (v) of the hydrophobic tail and the effective size of the hydrophilic headgroup (a). The area per molecule at the interface depends on the hydration of the surfactant headgroup, which in turn depends on the ion charge density and the distance to the small counterions. Furthermore, it can be influenced by the ionic strength of the solution. When ions come close to the headgroups, the charges are more or less neutralized the value a (area per molecule at the interface) decreases, and consequently the structural packing parameter P increases[60]. Therefore, a decrease of the critical micellar concentration and a change in the aggregate morphology can be observed[60,208,209].

As was mentioned above, the system under consideration has an excess of DTAB. Previous studies have shown that the self-aggregation behavior of alkyl tetramethylammonium surfactants is relatively independent of the hydrocarbon chain length[256]. The phase behavior of DTAB (C_{12}) and CTAB (C_{16}) is therefore comparable. The formation of rodlike micelles in CTAB systems at high concentrations is widely known[256,262–266]. Alkylammonium halides have also been reported to exhibit a transition from spherical to rod-like micelle shape with increasing concentration of added salt. At lower ionic strength only spherical micelles are formed, while at salt concentrations higher than a certain threshold, larger rod-like micelles are formed in equilibrium with the spherical micelles. The length of the rod-like micelle increases strongly with increasing ionic strength concentration[253,267–278]. Ozeki, et al.[277] reported that the sphere-rod transitions of micelles took place in aqueous NaBr solu-

tions of DTAB when the salt concentration exceeded 1.8 M, whereas measurements of Sudan red B in the same system indicated that the minimum NaBr concentration required to induce the sphere-rod transition was 1.0-1.5 M. This may be due to a decrease in intramicellar repulsion by electrical shielding due to ionic atmosphere. At higher salt concentrations, there is a dehydration of the spherical micelles due to the salting-out effect of NaBr.

By adding an anionic surfactant, we lower the charge density of the previously

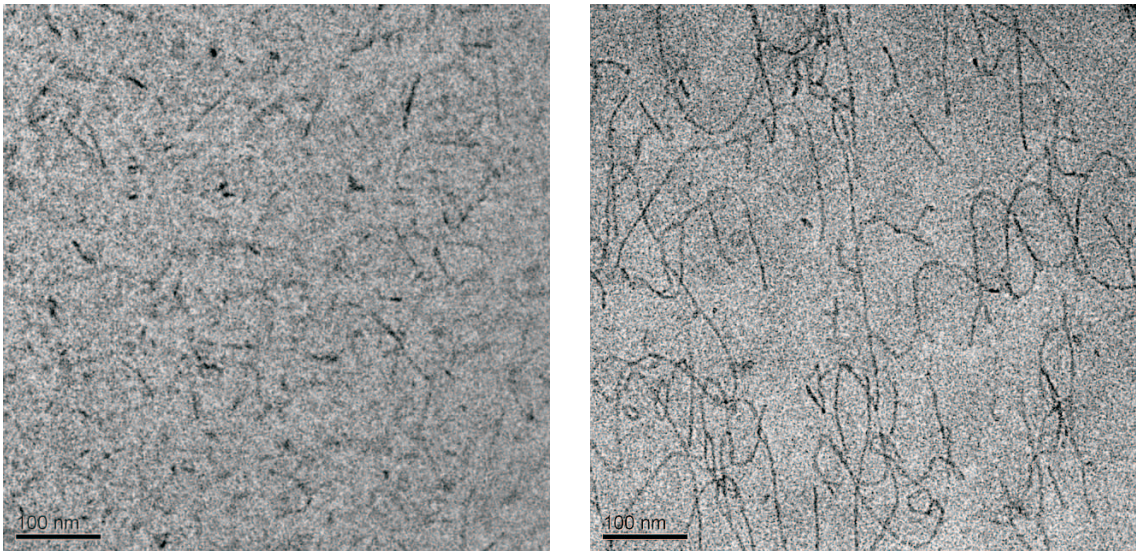

Figure 4.4: Left: spherical and small rod-like micelles in the SL / DTAB reference solution (before the salt was added); right: significant growth and networking of rods upon the addition of salt (25 mM NaBr).

cationic micelles. In this way, we also lower the concentration of salts necessary to produce cylindrical micelles. Similar effects are observed with the addition of anionic hydrotropes to cationic surfactants[279–281]. Hydrotropes bind strongly to oppositely charged surfactant ions and reduce the headgroup area of the surfactant by reducing the headgroup repulsions. Thus, they are effective at promoting the elongated micelle formation.

The elongation of cylindrical micelles was studied by cryo-transmission electron microscopy. Figure 4.4 shows that our initial micellar solution (reference sample) exhibits the presence of spherical micelles, as well as some short rods. An elongation of the cylindrical micelles was observed as salts were added to the solution. These

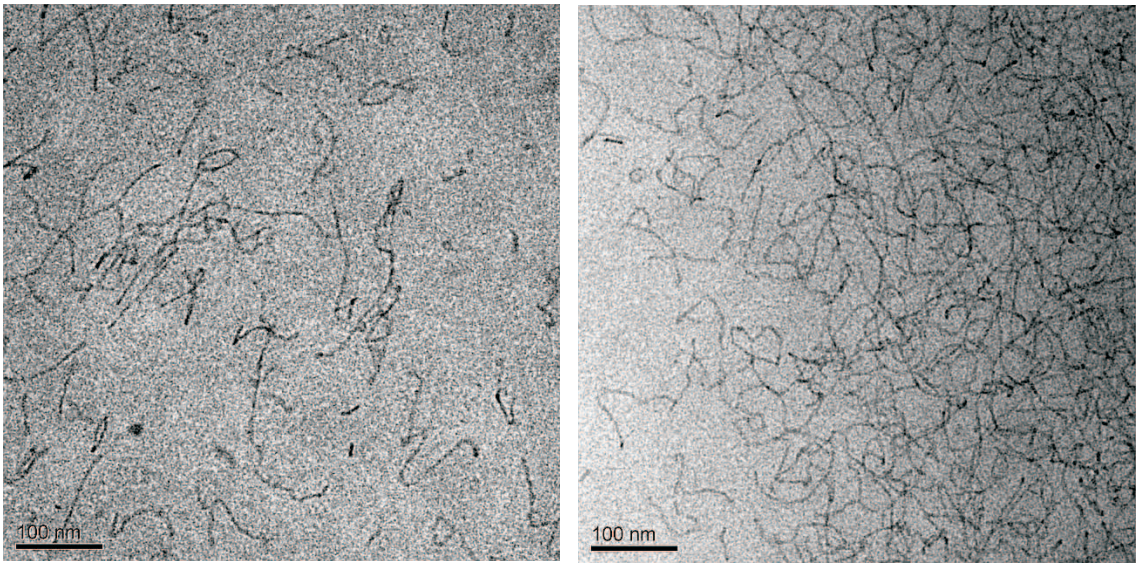

Figure 4.5: Cryo-TEM images representing the cylindrical growth as a function of anion type; the effect of 25 mM $NaNO_3$ (left) and NaBr (right).

micelles were quite flexible; small loops were observed, and the long micelles formed networks. This caused an increase in the viscosity (observed at the preparation of the solutions) and an increase of the turbidity of the solutions. However, the growth and the concentration increase of the rods was salt specific (Figure 4.5). The addition of NaBr produced a higher concentration of longer rods than the addition of $NaNO_3$. These then started networking together and forming a net-like structure. Surprisingly, we could not see any formation of vesicles. Upon the addition of salts, the system transformed from spherical micelles and small rods to long cylindrical micelles, and eventually to precipitation as the salt concentration was increased further. On the other hand, we have observed the transition from rod-like micelles to vesicles in the anionic-rich region of the phase diagram of this sample (when SL was in excess). A similar system to ours was studied by Sierra et al.[282]. They investigated the phase behavior of catanionic mixtures composed of DTAB and sodium undecanoate. They found the presence of spherical micelles on the anionic rich side of the phase diagrams and short rods on the cationic rich side. The rods elongated and aggregated as the composition neared equimolarity. No hexagonal mesophase was detected and the phase separation at equimolarity was preceded by the formation of bundles of rod-like micelles. The entanglement of long thread-like micelles

in CTAB micelles upon salt addition was observed also by Aswal et al.[283].

4.4.5 Explaining Counterion Specificity in Surfactant Systems

Since the cationic surfactant was in excess in the catanionic system, and also in the mixed micelles, it is reasonable to suppose that anions were in average closer to the micellar surface than cations. Consequently, the effect of anion variation was more pronounced than the effect of cation variation. But what makes the difference between anions of the same charge? It is their charge density and polarisability, in line with the ordering from hard (high charge density) ions, such as acetate, to soft (low charge density and often highly polarizable) ions, such as thiocyanate.

Again Collins' concept of so-called 'matching water affinities' will be used to explain counterion specificity. According to Collins' idea, soft ions should come in close contact with soft ions and hard ions in close contact with hard ions[101]. By contrast, when hard and soft ions come together, they do not approach so far that they loose their hydration sphere. Therefore, the interaction between a hard and a soft ion should be weak in water. Numerous phenomena in physical chemistry can be explained by this concept. For quaternary ammonium ions, it is not surprising that they behave like soft, low-density ions. According to Collins' concept it is therefore clear that DTA^+ interact more with softer ions than with harder ones, and this is precisely what was found in the present study. For example, SCN^- ions come in close contact to the cationic headgroup and they share a common hydration shell, whereas acetate anions will stay away from the headgroup and keeps its own hydration shell. Consequently, the packing parameter will increase more, when NaSCN is added to the micellar solution than when NaOAc is added, and therefore the tendency to form rod-like micelles is more pronounced in the case of NaSCN. This effect was already discussed in detail in Chapter 3, where molecular dynamics (MD) simulation was used to classify surfactant headgroups from hard to soft, in the same spirit as the ions[236]. A similar ordering as was done in the previous chapter for anionic headgroups can be done here to represent the counterion binding to the

alkyl ammonium headgroup surfactant (c. f. Figure 4.6).

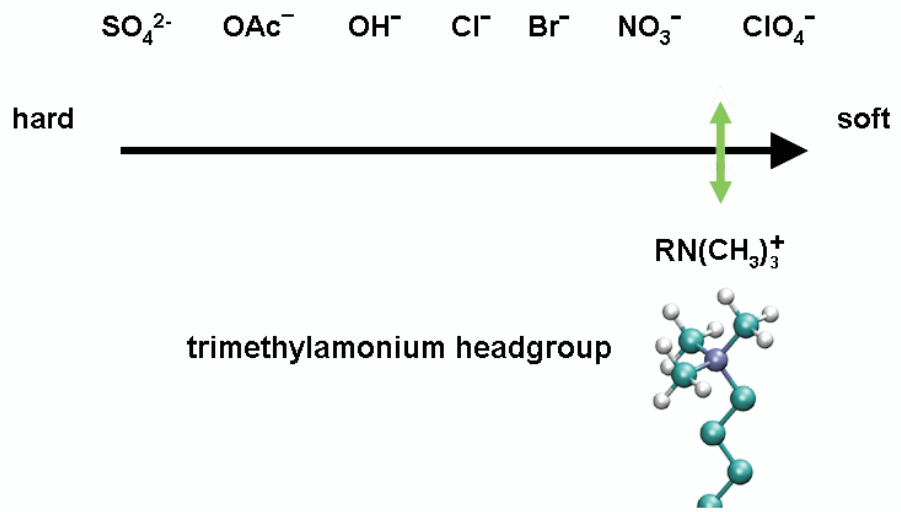

Figure 4.6: Ordering of anionic counterions regarding their affinity for the alkali ammonium headgroup.

4.4.6 Different self-aggregation behavior of catanionic systems in the catanionic- and anionic-rich regions

Why we are able to get vesicles in the anionic-rich region, but only thread-like micelles in the catanionic-rich region is a difficult questions. This phenomenon was already observed by other authors, but never really explained. If the changes in the packing parameter are considered, the values of the hydrophobic part remain the same, only the a value differs. However, a (as reported in literature, e. g. reference Sierra et al.[282]) does not differ enough to explain this significant difference in the end packing. One of the best explanations is the different hydration behavior of the headgroups compared to the hydration of the counterions. With the help of dielectric relaxation spectroscopy Buchner et al.[284] were able to observe that the micelle surface of the SDS surfactant is strongly hydrophilic and the adsorbed counterions are generally separated by a layer of water molecules. On the other hand, is the surface of the alkyltrimethylammonium bromides hydrophobic, with the bound halide ions directly attached[284].

4.5 Conclusions

A study of the influence of added salt on the aggregation behavior of non-equimolar mixed surfactant solutions was conducted. The system was composed of sodium dodecanoate (SL) and dodecyltrimethylammonium bromide (DTAB) with an excess of cationic surfactant. The addition of salts produced a spherocylindrical growth of the micelles, markedly dependent on the anion identity. The efficiency of the anions to elongate the micelles could be explained by Collins' concept of matching water affinities and the classification of the cationic surfactant headgroup as a soft, polarizable entity.

Part II

Increasing the Stability of Catanionic Systems

Chapter 5

Influence of Additives and Cation Chain Length on the Kinetic Stability of Supersaturated Catanionic Systems

5.1 Abstract

The stability of mixed surfactant solutions of sodium dodecylsulfate (SDS) with cetyltrimethylammonium bromide (CTAB) and with dodecyltrimethylammonium bromide (DTAB) was studied as a function of time. These specific mixtures were shown to have a solubility temperature below that of pure surfactant solutions in the anionic-rich region. The stability of such supersaturated solutions was studied with and without different additives. Surfactant mixtures without additives were shown to destabilize with time varying between 3 and 28 days, depending on the surfactant ratio. Generally, the stability of solutions increased by increasing the percentage of the anionic surfactant. The variation of the chain length of the cationic surfactant produced a large effect on the stability of such mixed surfactant systems. The presence of simple electrolytes decreased, while the addition of middle-chain alcohols increased its stability. Bluish solutions corresponding to a vesicular region were

observed at ratios close to equimolarity in samples without salt, and in the anionic-rich region upon the addition of middle-chain alcohols. Fluorescence and dynamic light scattering measurements showed that the destabilization of the solutions is not due to the formation of bigger aggregates, but rather due to a shift of the equilibrium between micelles and monomers, leading to the liberation of monomers, which precipitate. The lifetime of vesicles and micelles could therefore be controlled by varying the composition of the surfactant solutions and by additives. Controlling the precipitation phenomena is of importance for a large number of industrial processes, such as oil / solute recovery processes after extractions or chemical reactions.

5.2 Introduction

Mixtures of cationic and anionic surfactants (catanionics) are constituted of five types of species, including two counterions. In these systems a competition between various molecular interactions due to van der Waals, hydrophobic, electrostatic and / or hydration forces may result in a wide variety of phase behaviors and microstructures[24]. Among others, catanionic micelles, vesicles and bilayer structures, can be more particularly found. In mixtures of anionic and cationic surfactants a precipitation zone is observed around equimolarity[24,134]. The precipitation zone can be controlled by changing the temperature or/and the ionic strength of the solution[47,153]. Increasing temperature results in a general reduction in the tendency of precipitation, whereas the increase of ionic strength generally shows the opposite effect. The formation of finite structures in equimolar catanionic mixtures is thus limited to high temperatures. It is therefore of obvious interest to study the parameters which could extend the temperature range in which catanionic surfactant self-aggregation can take place. Furthermore, controlling the precipitation and micellization phenomena of catanionic mixtures are of practical importance in many industrial processes, such as oil / solute recovery processes after extractions or chemical reactions[47,153,285–287], foaming processes and wetting time of textiles[288,289]. Micelles and surfactant monomers are in dynamic equilibrium and individual surfactant molecules are constantly being exchanged between the bulk and the micelles.

Furthermore, the micelles themselves disintegrate and reassemble continuously[290]. While the process of surfactant micellization is primarily entropically driven, micelle formation depends on the balance of forces between the factors favoring micellization (van der Waals and hydrophobic forces) and those opposing it (electrostatic repulsions and kinetic energy of the molecules)[60,291,292]. The relaxation times of micelles are directly related to the micellar stability and are much longer for nonionic surfactants than for ionic surfactants, because of the absence of ionic repulsions between the headgroups[290]. For the same reason micelle kinetics in catanionic systems were also found to be very slow[293,294]. Thus, mixed surfactant solutions can remain supersaturated for long periods of time before precipitation is complete[295]. As the equilibrium states of such systems are questionable[296], the time dependent stability of common catanionic mixtures was studied in this paper. The effect of ionic strength and the influence of the variation of counterions were investigated, and also the influence of added alcohols as well as the importance of a different chain length.

5.3 Experimental Procedures

Materials The surfactants, sodium dodecyl sulfate (SDS: Merck, Germany, grade: 99%), dodecyltrimethylammonium bromide (DTAB: Merck, Germany; assay > 99%) and cetyltrimethylammonium bromide (CTAB; Sigma, Germany; grade: 99%) were used as received. All sodium and chloride salts used in the experiments were supplied by Merck, Germany. The alcohols: methanol, 1-propanol, 1-butanol, 1-decanol (Merck, Germany, > 99%), ethanol (J. T. Baker, Holland, 99.9%), 1-pentanol (Aldrich, Germany, 99.5%), 1-hexanol (Fluka, Germany, 99%), 1-heptanol (Alfa Aesar, Germany; 99%), 1-octanol (Acros Organics, U.S.A., 98%), and citronellol (Merck, Germany, 98%) were also used as received. Millipore water was used as solvent in all cases.

Determination of the solubility temperature (This measurement was performed by A. Arteaga during his graduate studies. Results are represented with his permission.)The solubility temperature at different time intervals was determined

by visual observation. All systems were observed at 1 wt.% total surfactant concentration. The cationic / anionic mixtures at different mass ratios were prepared from 5 wt.% surfactant stock solutions. The samples were first heated to 39°C, then cooled down and left to equilibrate for 5 hours at 0°C, and then the temperature was increased by approximately 0.5°C per minute. The measured solubility temperatures (between 0°C and 99°C) correspond to the transition from precipitate to isotropic phase; i. e. to a micellar or vesicular solution. The procedure was repeated after a certain time to analyze the kinetics of the system.

Phase Diagrams Phase diagrams of the systems were constructed according to the procedure described above. The samples had to be heated after mixing in order to obtain a homogeneous clear solution. Different surfactant ratios exhibited different initial solubilization temperatures, T_I (more throughly explained in the Results section). The effect of additives was studied by adding an appropriate amount of salt or alcohol to the SDS / CTAB mixture. Again, in some cases the sample had to be heated in order to obtain a clear solution. The maximum temperature to which the samples were heated was 39°C. The samples were then cooled down and kept at 20°C. Phase diagrams were constructed by visual observation and by measuring transmission using a Hitachi U-1000 spectrophotometer. The samples were also observed at 0°C in order to shorten the destabilization times and to check whether the order of destabilization is the same at both temperatures.

Counterion Binding Cation affinities for the surfactant aggregate interface were determined by electrospray mass spectrometry. ES-MS was carried out using a Thermoquest Finnigan TSQ 7000 (San Jose, CA, USA) with a triple stage quadrupole mass spectrometer. The solutions were sprayed through a stainless steel capillary held at 4 kV, generating multiple charged ions. Data were collected using the Xcalibur software. The surfactant concentration was kept 1wt.% and the concentration of the various chloride salts was 0.1 M in all cases.

System Kinetics The evolution of the surfactant aggregates was further followed using fluorescence spectroscopy and dynamic light scattering (DLS) measurements.

Pyrene (Aldrich, optical grade) was used as the external fluorescence probe to monitor the change in surfactant self-assembly. The preparation of water saturated with pyrene was as reported previously[297,298]. The fluorescence emission spectra of pyrene were recorded on a Cary Eclipse fluorescence spectrophotometer (Varian, Inc.) at 20°C. From the spectra, the ratio of intensities of the first and the third vibrational peak of pyrene, I_1/I_3, was calculated. Particle size analysis was performed using a Zetasizer 3000 PCS (Malvern Instruments Ltd., England), equipped with a 5 mW helium neon laser with a wavelength output of 633 nm. The scattering angle was 90° and the intensity auto-correlation functions were analyzed using the Contin software.

Effect of Alcohols on the System Morphology Specimens for cryo-transmission electron microscopy (cryo-TEM) were prepared as described before[169]; frozen samples were examined with a Zeiss EM922 EF Transmission Electron Microscope (Zeiss NTS mbH, Oberkochen, Germany), whereas the replica were examined and photographed with a Philips CM 12 transmission electron microscope.

5.4 Results and Discussion

5.4.1 Shift of Solubility Temperature with Time

The influence of the cationic surfactant chain length on the solubility temperatures of catanionic mixtures was investigated by comparing mixtures of sodium dodecylsulfate (SDS) with cetyltrimethylammonium bromide (CTAB) and with dodecyltrimethylammonium bromide (DTAB). CTAB and DTAB have the same quaternary ammonium polar headgroups, but CTAB has a longer chain (16 carbon atoms) than DTAB (12 carbon atoms). Owing to stronger hydrophobic repulsions of its hydrocarbon chain, CTAB is therefore less soluble in water than DTAB. The Krafft point of pure CTAB in water at 1 wt.% is consequently higher ($\approx$ 25°C)[299] than that of DTAB ($<$ 0°C)[300]. The solubility temperatures (T_S) of the corresponding catanonic mixtures, i. e. DTAB / SDS and CTAB / SDS with a total surfactant concentration of 1 wt.% and different anionic / cationic surfactant (molar) ratios

were followed as a function of time (c. f. Figures 5.1 and 5.2). Both systems displayed the same marked differences in their solubility temperatures over the whole anionic / cationic ratios in the initial days after mixing. The T_S in the cationic-rich regions were generally higher than the T_K of the pure cationic surfactant. The same trend was observed for only a part of the phase diagram in the anionic-rich region. Around equimolarity, a maximum of solubility temperatures (T_S) was reached. This maximum lay within the zone of precipitation usually observed at room temperature. A bluish zone, corresponding to a vesicular region, was located in both sides of the central area of insolubility[301,302]. It was much more extended in the anionic-rich region (approximately between 0.6 - 0.7) than in the cationic-rich region (around 0.35). The vesicular regions could be extended by raising the temperature. Hargreaves and Deamer[61] noted the formation of liposomes in mixtures of CTAB and SDS above $\approx 47°C$. The sequence of different phases resembled those observed in similar catanionic systems[24,49,303]. Obviously, the behaviour of two single-chain surfactants is much different in a catanionic system. The packing between the cationic and anionic surfactants is quite different from the single ionic one and contributes to increase the stability of the catanionic crystal, leading thus to higher solubility (and Krafft) temperatures. Interestingly, however, at a certain ratio of anionic / cationic surfactants a 'solubility temperature depression' exists. This depression was located in a range of a molar fraction of the anionic surfactant between $0.65 - 0.85$ and could be observed immediately after mixing. With time, the mixtures undergo a continuous evolution of T_S toward higher temperatures. Surprisingly, the solubility temperature was almost constant over time in the cationic rich region, whereas a large time dependency could be observed in the anionic rich region, c. f. Figures 5.1 and 5.2. Furthermore, the shift in the solubility temperature was more pronounced in systems containing a longer chain cationic surfactant (Figure 5.2). For this reason we focused our attention on the anionic part of the phase diagram of the CTAB / SDS system.

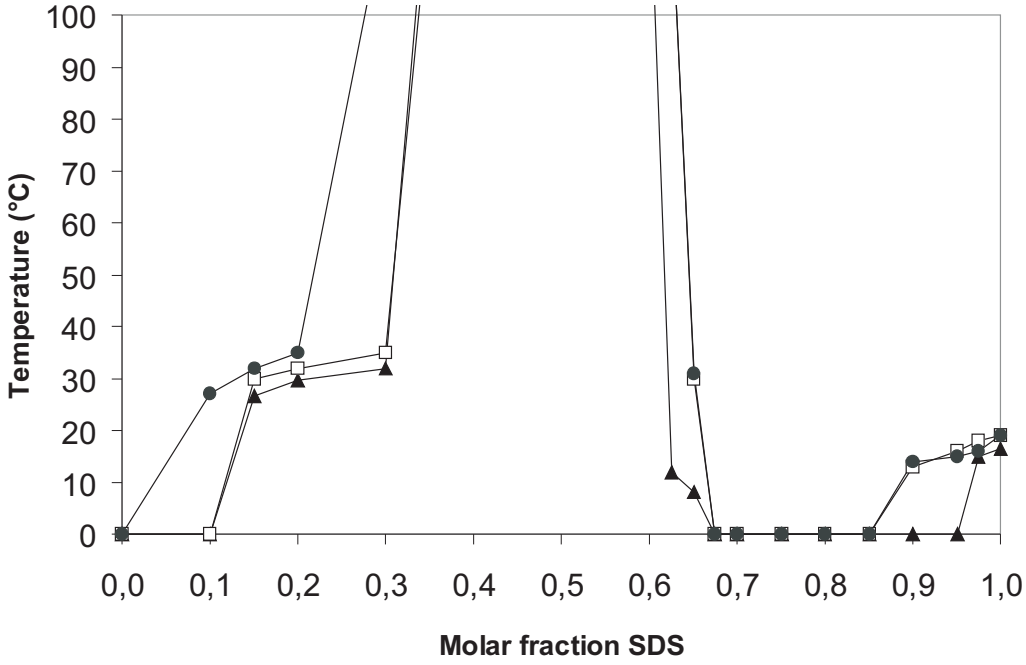

Figure 5.1: Shift of solubility temperature in DTAB / SDS mixtures at different surfactant ratios as a function of time ($c_{tot} = 1wt.\%$): observations after (▲) 1 day, (□) 4 weeks and (•) 6 weeks.

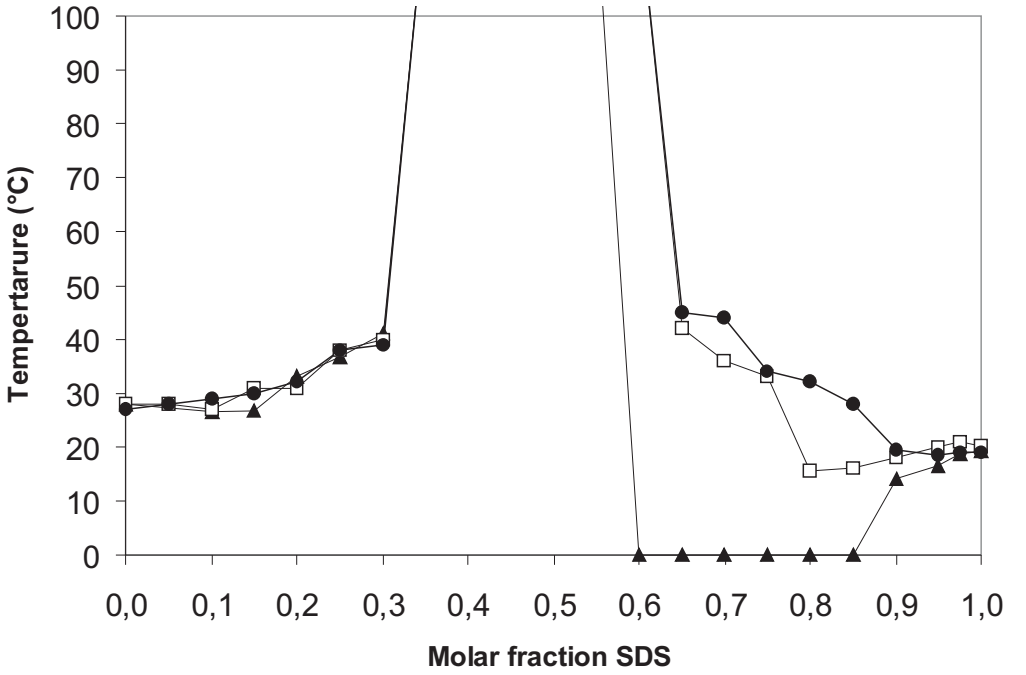

Figure 5.2: Shift of solubility temperature in CTAB / SDS mixtures at different surfactant ratios as a function of time ($c_{tot} = 1wt.\%$): observations after (▲) 1 day, (□) 4 weeks and (•) 6 weeks. Both Figures reproduced with permission from the doctoral dissertation of A. Arteaga.

5.4.2 Behavior of the Anionic-Rich Region of the Phase Diagrams Without Additives

The samples (with an excess of SDS) were prepared as described in the Experimental Section and heated in order to obtain a clear homogeneous solution. The temperature needed can be described by the equation $T_I(°C) = -0.43 \cdot X + 64.9$, where $T_I(°C)$ is the initial solubility temperature expressed in Celsius and X is the percentage of SDS in the solution (c. f. Figure 5.3 (left)). Then the samples were left to cool down and observed at 20°C. The results from spectroscopy measurements of the SDS / CTAB system at 20°C are presented in Figure 5.3 (right).

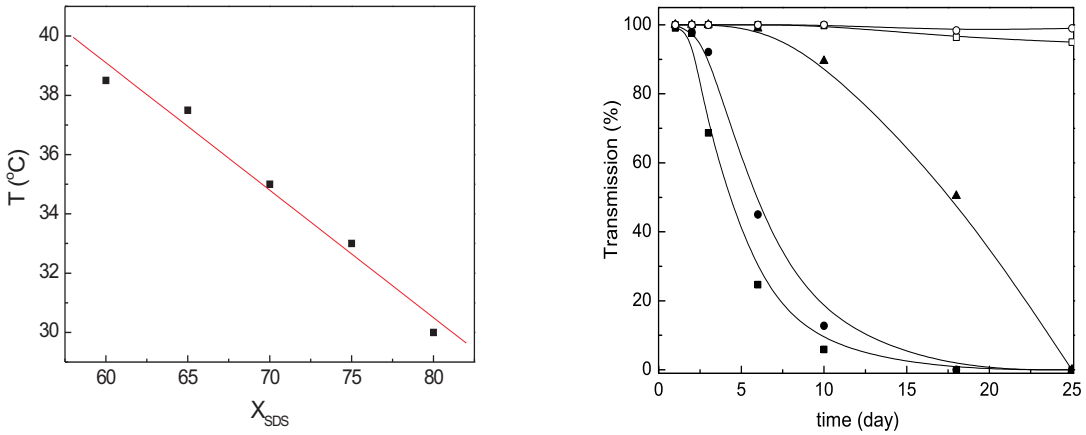

Figure 5.3: Left: The temperature needed to obtain clear homogeneous solutions in the anionic-rich region can be described by a straight line with a slope of $k = -0.43(\pm 0.03)$ and $n = 64.9(\pm 2.6)$; right: Transmission of the SDS / CTAB catanionic system as a function of time for the following ratios: 65/35 (■), 70/30 (●), 75/25 (▲), 80/20 (□), and 85/15 (○)

We see that the higher the ratio of the anionic surfactant, the more stable the system is. Whereas the solution with 65% and 70% of SDS were precipitated after 10 days, solutions with 80% and 85% were still clear after 30 days. The electrostatic interactions and consequent charge neutralization between the SDS molecules and the oppositely charged CTAB promote long relaxation times of catanionic micelles. These, in turn, are accountable for the supersaturation of our system and the temporary solubility temperature depression observed. The anionic and cationic

surfactant molecules can be present in solution either as monomers, incorporated into surfactant aggregates (micelles, vesicles, etc.) or as precipitate (DSCTA(s) - a salt formed from $DS^{-}CTA^{+}$ ions). Thus, there are two equilibria present in such mixtures: monomer-micelle and monomer-precipitate. Two different types of phase separation in such systems can be observed. Phase separation in catanionic surfactant mixtures may occur due to the entanglement of rod-like micelles, the formation of lamellar phase, or the formation of densely packed vesicles. In some cases, however, there seems to be a competition between the kinetics of vesicle formation and the kinetics of precipitation of cationic-anionic pairs[134,304]. Earlier measurements on catanionic systems have shown that precipitation is primarily enthalpically driven, while micellar formation is primarily entropically driven. This is due to the ordering of the surfactant headgroups in the crystalline precipitate as a consequence of charge neutralization[153].

In order to understand whether phase separation is a consequence of precipitation of solid catanionic salt or the consequence of micellar (vesicular) aggregation, dynamic light scattering and fluorescence techniques were employed. Particle size measurements showed a decrease in the size of the particles with time, as can be observed in Figure 5.4. After 3 days the solution was precipitated and the laser beam passing through the upper (clear) part of the solution detected only very small particles ($R_H \approx 2.5nm$).

This behavior is quite different from that observed in a previously studied SDS / DTAB system[169]. There, an increase in turbidity was observed in accordance with the increase of the hydrodynamic radius of the corresponding particles. Although the solutions were turbid, no precipitation took place, even after months of observation. The behavior of the SDS / CTAB was different. A precipitation was observed without any detection of an intermediate turbidity. The reasons for the different behaviors of the two systems are most likely due to the different Krafft temperatures of the two cationic surfactants. Precipitation is a common phenomenon in catanionic surfactant mixtures, which is regulated by two competing forces: the free energy of the solid crystalline state and that of the micellar solution[305]. The strong interactions make packing into a crystalline lattice energetically favorable for surfactant

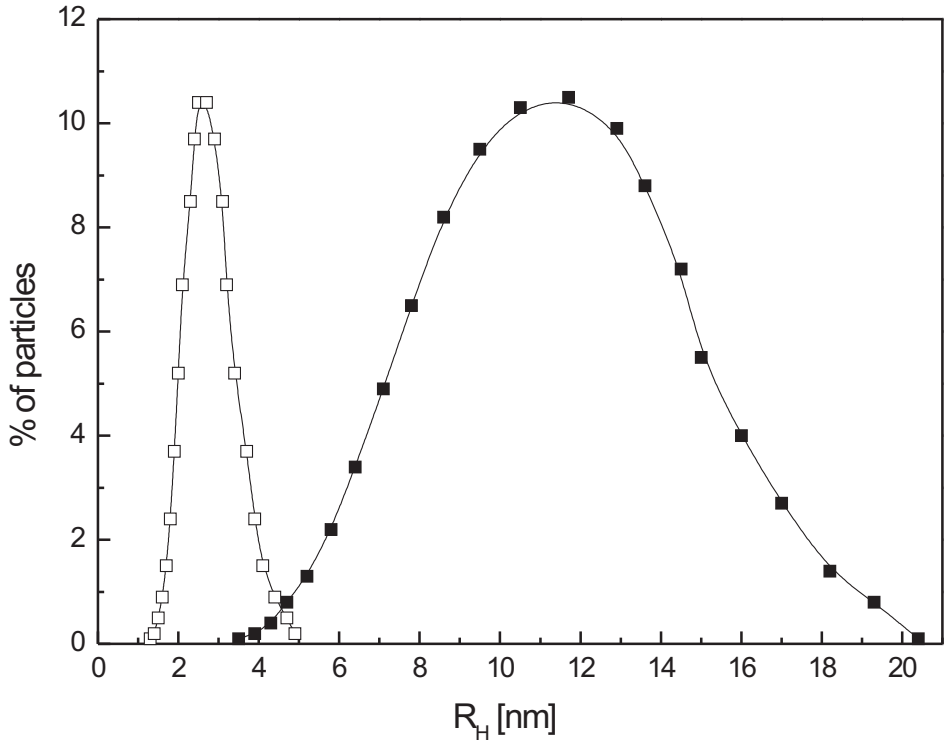

Figure 5.4: Particle size followed by DLS: SDS / CTAB catanionic system with a (molar) ratio 65/35 after 1 day (■) and after 3 days (□).

monomers, particularly when the hydrophobic match is high. It has been shown that by exchanging the counterion, we are able to influence the energetic state of the micellar solution. A much bigger variation between systems is observed in the free energies of the crystalline state. As we can see from the phase diagrams, the solubility of the catanionic salt is directly correlated to the solubility of the surfactant monomers. The solubility (and Krafft point) decreases with increasing chain length, and is therefore lower for the CTAB mixture in comparison to the DTAB surfactant mixture. We can not exclude at this point the possibility that the precipitate was formed from an entanglement of rod-like micelles or similar big particles as was already reported by other authors[282,283]. However, such transitions take a longer time, suggesting the formation of larger particles would be detected before the actual precipitation takes place. For this reason, we believe our system yields

a similarity to the SDS / DPLC (dodecylpyridinium chloride) mixture studied by Stellner et al.[134]. In this case, the destabilization of solutions was not due to particle growth (and formation of big aggregates), rather was the observed precipitation due to the liberation of monomers.

Pyrene fluorescence emission spectroscopy was used to further investigate the changes in phase behavior. The low fluorescence ratio, I_1/I_3, of pyrene on the first day after preparation of the solutions showed the presence of highly hydrophobic particles in the solution ($I_1/I_3 = 1.1$; c. f. Figure 5.5). The I_1/I_3 ratio in 1 week old solutions (macroscopically the solutions were two-phased: the lower part containing the precipitant, whereas the upper part consisted of a clear supernatant) showed an increase from a value of 1.1 to a value around 1.3. This value corresponds to the polarity found for SDS micelles[306]. This suggests that as the catanionic salt precipitated, the remaining pyrene was solubilized inside the micelles formed by the excess anionic surfactant. In this way, a large amount of the surfactant was removed from the solution (as precipitate); only the excess amount remained in solution. Had all of the SDS surfactant precipitated as well, a much higher pyrene ratio would have been observed ($I_1/I_3(water) \approx 1.8$[307,308]), whereas, if bigger aggregates had formed, one would expect the pyrene intensity ratio to remain unchanged. In the latter case, the pyrene probe would be solubilized either inside rod-like micelles or the hydrophobic interior of vesicular membranes, whose environment micro-polarity is the same as that in spherical micelles.

A higher stability of systems when the fraction of one of the components was increased in comparison to the other component was already observed by Stellner et al.[134]. When the SDS concentration is increased (and the CTAB concentration held constant), precipitate can not form due to a change in the micellar (and consequently monomer) composition. The monomer concentration then does not exceed the monomer-precipitate boundary (for a more detailed explanation the reader is referred to Stellner et al.[134]).

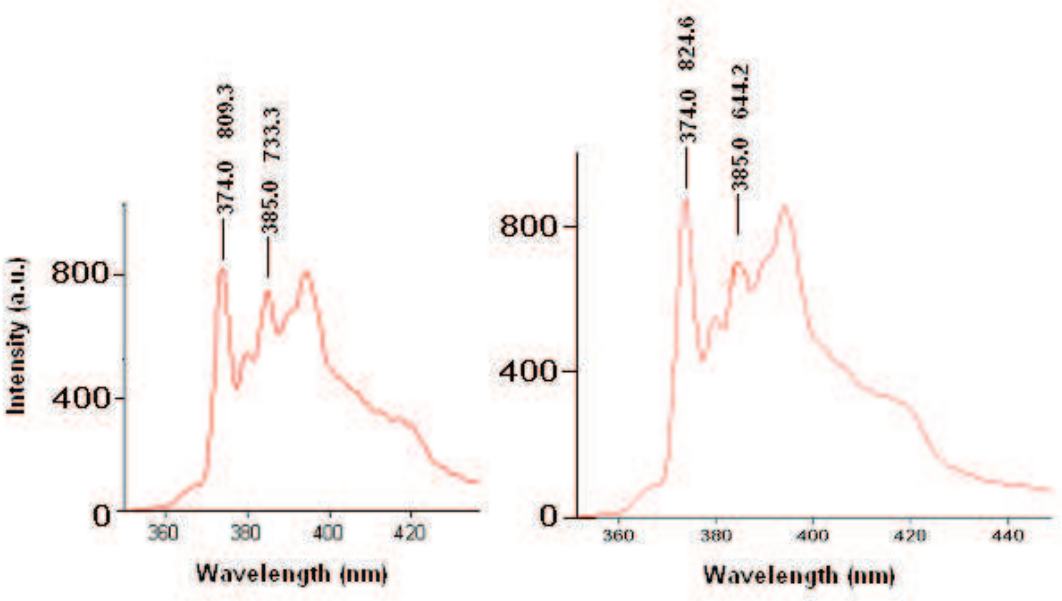

Figure 5.5: Pyrene fluorescence emission spectrum of a SDS / CTAB catanionic system with a (molar) ratio 70/30 after (left) 1 day, (right) 7 days.

5.4.3 Effect of Additives on the Stability and the 'Solubility Temperature Depression'

Effect of Ionic Strength Addition of electrolytes to ionic surfactant solutions may modify both the inter- and intramicellar interactions. Therefore, the phase behavior of surfactant solutions is expected to be affected significantly upon the addition of salts. Sodium bromide was added to the catanionic mixture at different ratios (in the anionic rich region) to study the effect of ionic strength on the phase stability. The observed effect was similar for all ratios. Generally, the increase of ionic strength decreased the destabilization time of the sample (c. f. Figure 5.6). The higher the concentration of the added NaBr was, the shorter were the destabilization times. Whereas the solution with 0.5 M of NaBr was precipitated after only 2 days, the solution with 0.1 M NaBr started showing first signs of turbidity after 10 days. The destabilization times are shortened down to two hours when the solutions are kept in an ice bath. A general increase in the tendency of precipitation of catanionic mixtures upon the increase of ionic strength was already observed previously[47,153]. When surfactant monomers are salted out by the presence of an

electrolyte, micellization is favored[2]. Catanionic systems exhibit different behaviors upon salt addition. This is due to the ability of mixed surfactant systems to adjust the aggregate composition to attain the lowest possible free energy state for given conditions. In catanionic systems two salt-induced phenomena are observed, depending on whether the equimolar[47] ("true") or non-equimolar[169] catanionic systems are studied. To quickly review, if the surfactant micelles consist of just one type of surfactant (one charge) or one of the components is in excess, then the addition of salt screens the repulsion between the headgroups, causing the surfactant molecules to arrange in a bilayer. The opposite case is true, if the surfactants are present in equimolar amounts. The salts then screen the attraction between them, most likely causing the distance between the headgroups to increase. In these cases a vesicle-to-micelle transition was observed. Since we are dealing with non-equimolar catanionic mixtures, where SDS is in excess, the addition of salt to our surfactant mixture is expected to have the same effect as on pure SDS micelles. Addition of NaCl to SDS, for instance, is known to decrease the CMC and increase the micellar size[6]. Furthermore, by raising the ionic strength of the solution, the charges on the surfactant headgroups are screened due to a stronger counterion binding. This, in effect, decreases the solubility of the surfactant monomers and therefore assist in precipitation.

Effect of Cation / Anion Variations A good correlation has been observed between the temperature to which it is required to heat the solution for complete solubilization to occur (T_I) and the stability of the then isotropic solution. For this reason, the heating temperatures of solutions containing various salts and alcohols are reported in Table 5.1. The salt concentration was kept constant in all cases at 0.1 M. The solubility temperatures for all sodium salts are 29($\pm$0.5)°C. The variation of the anion apparently has no effect on the solubility of the catanionic mixture. This was expected as the overall net charge was negative (we had an excess of the anionic surfactant SDS). A big variation of the temperature was observed when different chloride salts were added to the micellar solution. Mass spectroscopy results (Figure 5.7) showed that at this relatively high concentration of added salt (0.05 M 'new'

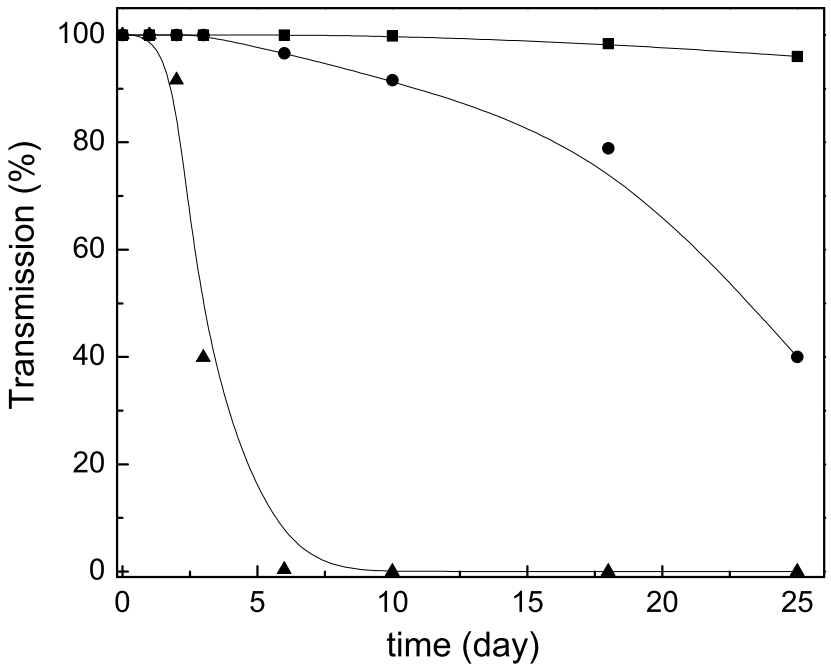

Figure 5.6: Transmission of the SDS / CTAB catanionic system: the effect of ionic strength on the stability of a SDS / CTAB solution (molar ratio 80/20) without salt (■), with 0.1 (●) and 0.5 M (▲) NaBr.

counterions vs. ≈ 0.016 M of 'original' sodium counterions) all counterions were in the close proximity of the mixed micelle surface, regardless of the fact whether they normally exhibit salting-in or salting-out behavior.

Despite this, we saw a large difference in the stability of the solutions when the solutions containing LiCl or NaCl were compared with solutions containing KCl or CsCl. After one week at 20°C, the first two solutions were still clear and isotropic, while the later two were already precipitated (see Figure 5.8). This difference in T_I can be attributed to the stronger binding of less hydrated potassium and cesium ions to the excess dodecyl sulfate ions[309]. The use of KCl precipitation to remove SDS is commonly used in biology[310,311]. The effect of 'hydrophobic' counterions (choline and TMA^+) was found to be in the middle of both.

A stronger binding of organic counterions in comparison to sodium to dodecyl sulfate micelles was already observed using fluorescence techniques[312] showing that

Salt	T_I (0.1 M)	Alcohol	T_I (0.1 M)	T_I (0.2 M)	T_I (0.05 M)
No salt	35.5	Methanol	35.5		
LiCl	29	Ethanol	36	36	
NaCl	29	n-Propanol	36	36	
KCl	37	n-Butanol	35	34.5	
CsCl	31.5	n-Pentanol	30.5	27	
ChCl	37	n-Hexanol	21*		21*
TMACl	37.5	n-Heptanol	21*		21*
NaBr	29.5	n-Octanol	21*		21*
NaSCN	29	n-Decanol	> 39**		> 39**
Na_2SO_4	28.5	Citronellol	> 39**		> 39**

Table 5.1: Effect of additives on the initial solubility temperature (T_I); the initial sample is a 70/30 mixture (with an excess of SDS); * the samples were isotropic and slightly bluish already at room temperature (21°C); **the samples were not clear even at 39°C.

the binding of alkylammonium ions is dominated by their hydrophobicity. As was pointed out previously, we are able to influence the energetic state of the micellar solution by exchanging the counterion. This can explain the small differences in the stability of the systems with different counterions. Mukerjee et al.[313] have investigated the binding of counterions to dodecyl sulphate anions by conductivity. They have reported that the Li^+ ion is less firmly attached to the micelle than the Na^+ ion and this one in turn less than Cs^+. The lower binding therefore promoted the formation of ionized species. The gain in free energy was however not large enough to overcome the free energy of the crystallization, and thus all of the systems eventually precipitated.

The affinity of specific ion-counterion pairing has been previously extensively studied on the vesicular[169] and two-phase regions[31] of a similar system. The ordering of cations was found to follow the Hofmeister series in all cases. The effects of the ions were found to be strongly dependent on the ability of the counterions to form close ion pairs with the surfactant headgroups and the behavior was explained using Collins' Law of Matching Water Affinities[101]. As was shown in Chapters 3 and 4,

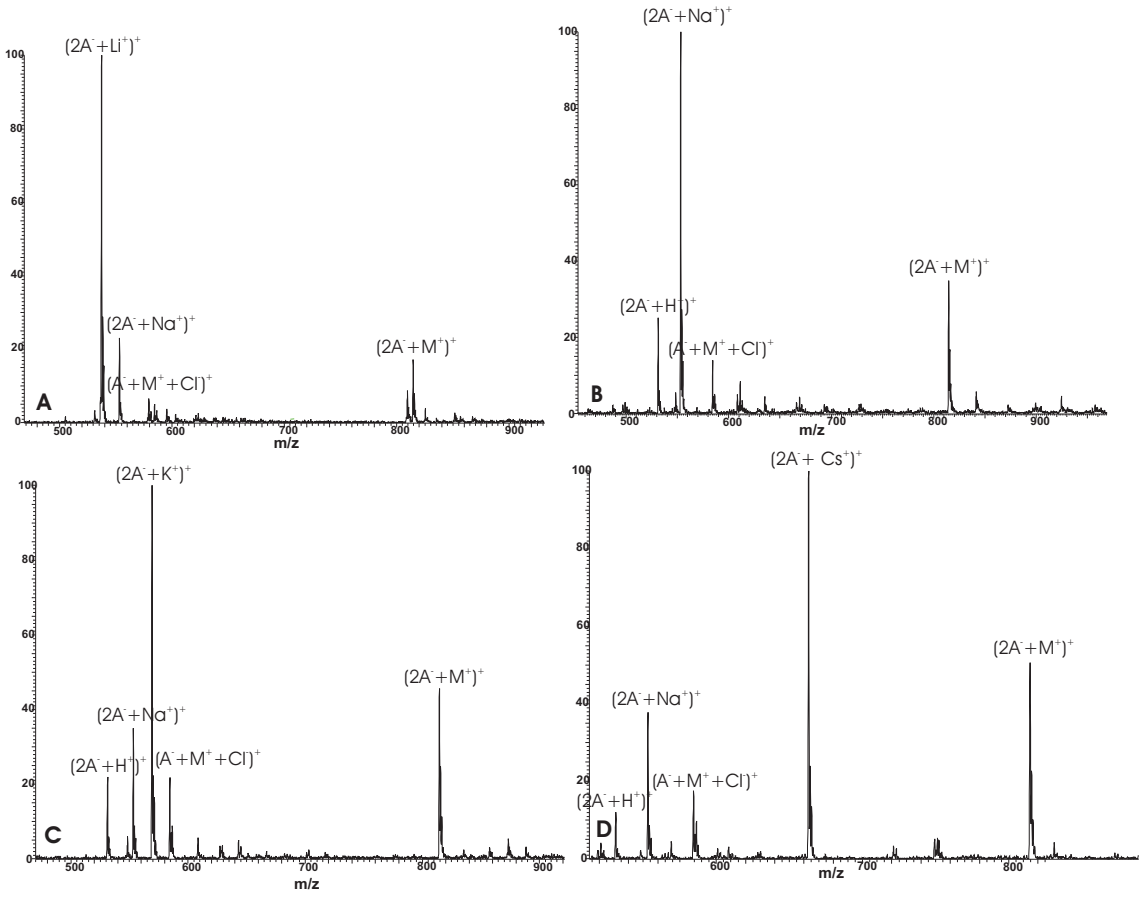

Figure 5.7: Ion binding as determined by ES-MS: addition of 0.1 M of (A) LiCl, (B) NaCl, (C) KCl and (D) CsCl to an SDS / CTAB micellar solution. A^- : dodecylsulphate anion (265 Da); M^+ : cetyltrimethylammonium cation (284 Da).

the alkyl sulfate headgroup behaves like a soft, chaotropic ion.

The anions showed a destabilization time comparable to sodium chloride. The variations of the anion produced no change in the stabilization times and therefore no specificity (c. f. Figure 5.9). This is most likely due to the fact that the anions did not accumulate near the same-charged micellar surface, but assisted purely by increasing the ionic strength of the medium.

Effect of alcohols It is known that alcohol penetrates in the palisade layer of micelles[314] and depresses the surfactant CMC[315–317]. Nakayama et al.[318] and Kaneshina et al.[319] have observed a depression of the CMC and the Krafft point of ionic surfactant in the presence of longer chain alcohols. The Krafft point depression was explained quantitatively by a model in which it is proposed that the melting

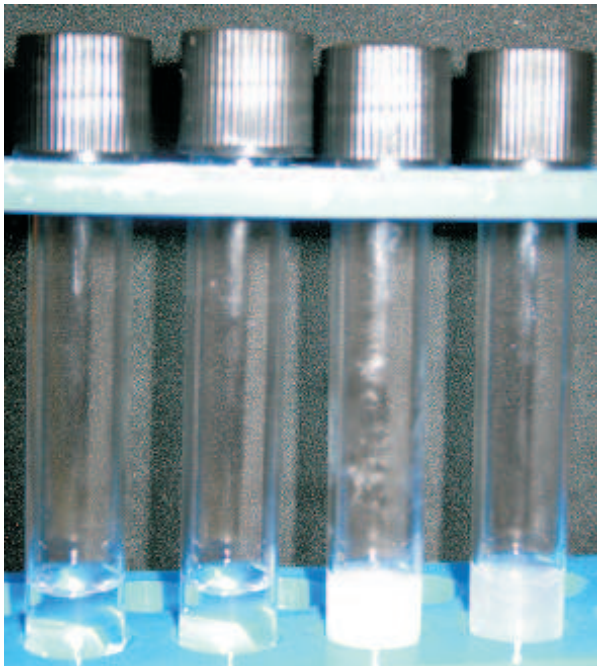

Figure 5.8: Effect of additives on the stability of an SDS / CTAB catanionic system with a (molar) ratio 70/30: (from left to right) LiCl, NaCl, KCl and CsCl (all salts 0.1 M) after 1 week at 20°C

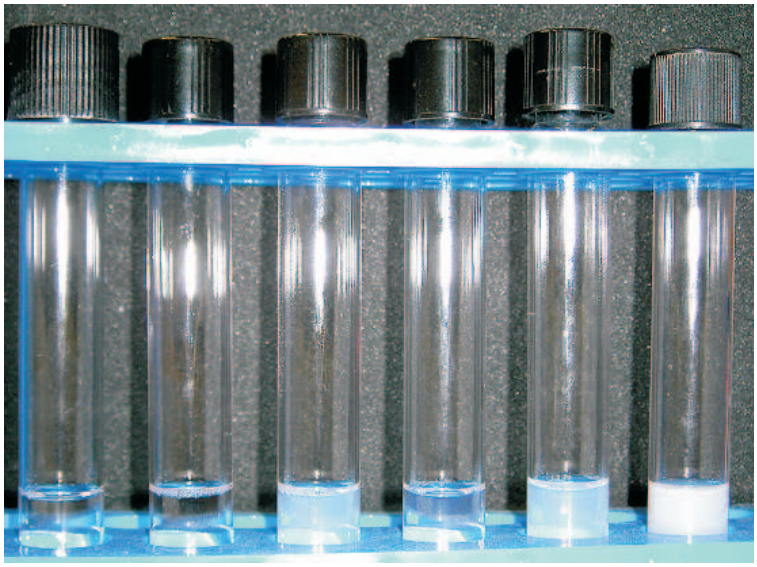

Figure 5.9: Effect of additives on the stability of an SDS / CTAB catanionic system with a (molar) ratio 70/30: (from left to right): without salt, with LiCl, NaCl, ChCl (Choline Chloride), NaSCN, Na_2SO_4 (all 0.1 M) after 3 hours on ice.

point of the hydrated solid agent is depressed owing to the formation of a mixed micelle of surfactant and alcohol[318].

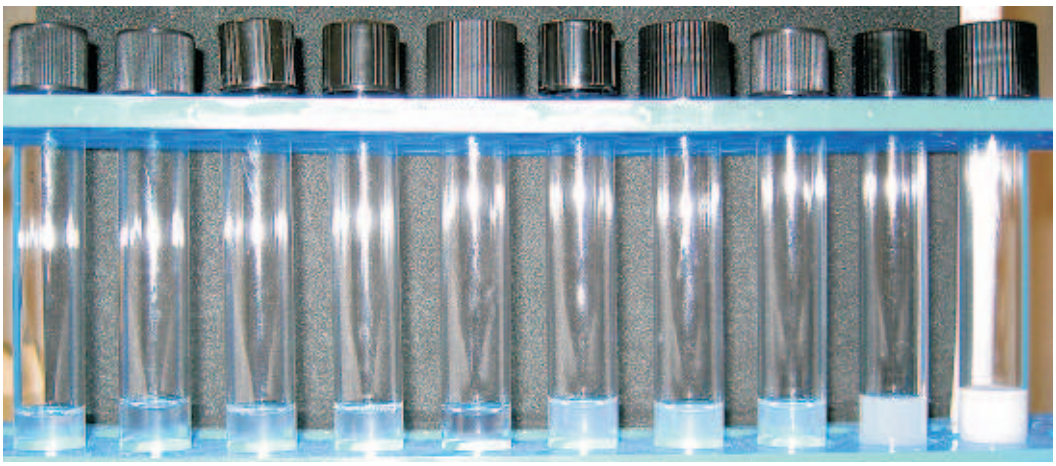

Figure 5.10: Effect of additives on the stability of an SDS / CTAB catanionic system with a (molar) ratio 70/30: (from left to right) methanol, ethanol, n-propanol, n-butanol n-pentanol, n-hexanol, n-heptanol, n-octanol, n-decanol, citronellol (all 0.1 M) after 1 week. Solutions from methanol to butanol are slightly turbid / precipitated, pentanol is clear; hexanol to octanol are bluish and homogeneous, decanol and citronellol are turbid (due to the low alcohol solubility).

The heating temperatures of solutions containing alcohols of various chain length and concentrations are reported Table 5.1. According to the results reported, the alcohols can be classified into four groups: (i) short-chain alcohols ($< C_4$), which have no effect on the T_I or on the stability of the system; (ii) pentanol, which decreases T_I and the solubility somewhat; (iii) middle-chain alcohols (between C_6 and C_8) which lower T_I and increase the stability substantially; and (iv) long-chain alcohols ($> C_{10}$), which are inappropriate for use due to their low solubility (c. f. Figure 5.10). Variation of concentration generally produced little effect. Middle-chain alcohols from hexanol to octanol have provided best results. The initial solubility temperature was reduced to below room temperature ($< 21°C$) and the stability of the solutions was increased drastically. The samples were homogeneous and bluish, hinting at the presence of larger particles. Best effects were observed when the alcohol concentration range was kept between 0.02 and 0.2 M. Lower concentrations produced no effect and larger amounts of alcohol resulted in an alcohol-surfactant gel.

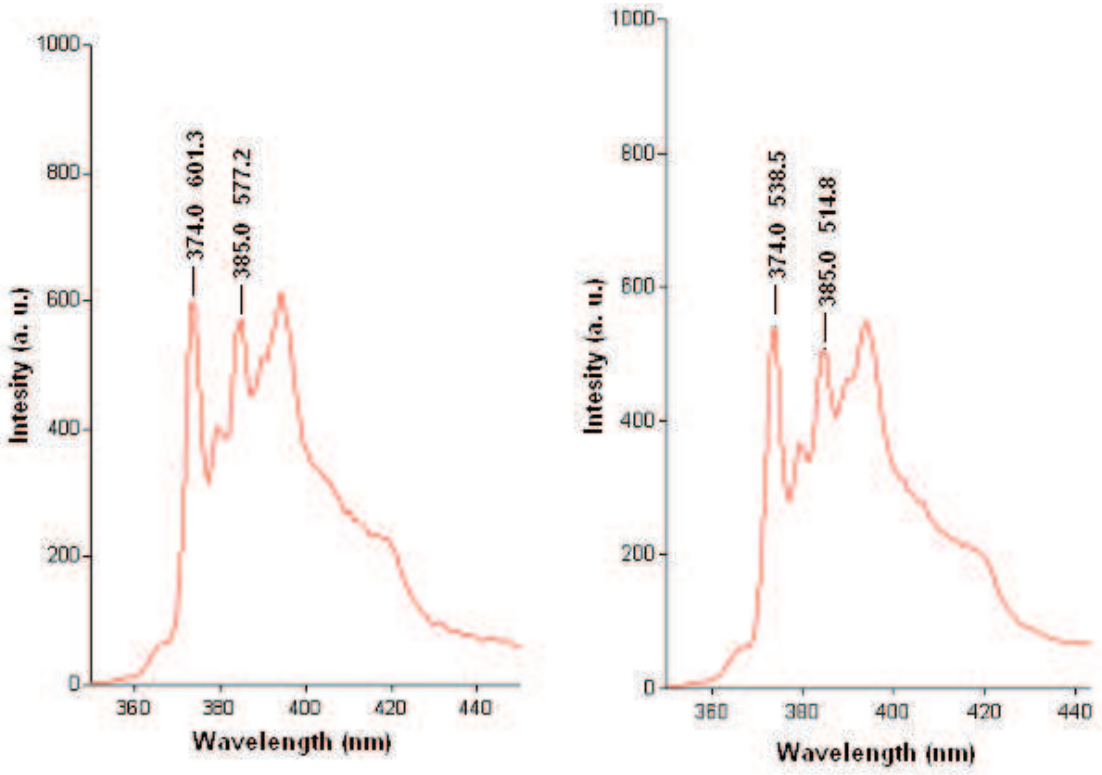

Figure 5.11: Pyrene fluorescence emission spectrum of a SDS / CTAB catanionic system with a (molar) ratio 70/30 upon the addition of 0.05 M hexanol after (left) 1 day, (right) 1 week.

Fluorescence measurements reported a presence of hydrophobic domains in the solution (c. f. Figure 5.11). In fact, the polarity of the aggregates sensed by the pyrene probe was even lower when hexanol was added to the catanionic mixture ($I_1/I_3 = 1.04$); close to that found in toluene ($I_1/I_3 = 1.03$)[307,308] or in 2-propanol ($I_1/I_3 = 1.07$)[307]. This hints at the fact that hexanol forms mixed micelles/aggregates with the two surfactants, thus reducing the concentration of surfactant monomers. Solutions with different amounts of hexanol were observed at room temperature for up to 6 months and still showed no sign of destabilization. Also the I_1/I_3 ratio in such samples remained stable over time.

Furthermore, solutions containing small amounts of hexanol (0.05 M) were kept in an ice bath for a period of up to 2 weeks and again no visible changes appeared. After 2 weeks, the sample was warmed to 20°C and checked by cryo-transmission microscopy. Solutions exhibited a high polydispersity. Spherical and ribbon-like micelles, as well as vesicles were observed (c.f. Figure 5.12). This proves that it

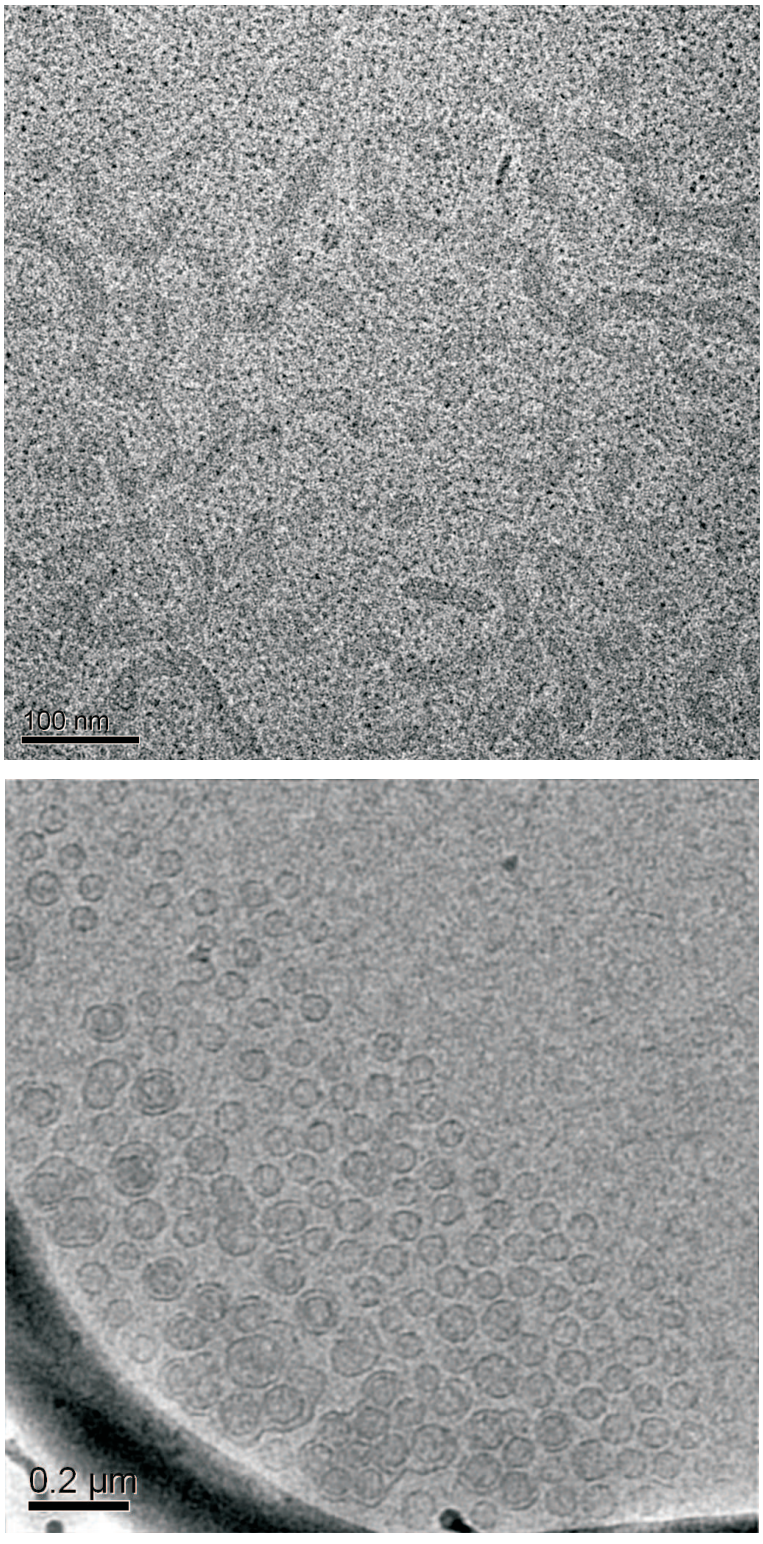

Figure 5.12: Cryo-TEM photographs of a SDS / DTAB aqueous solution at a molar ratio of 70/30 and a total surfactant concentration of 1 wt.% upon the addition of 0.05 M hexanol: spherical (black dots) and ribbon-like micelles (top), as well as vesicles (bottom) are seen.

is possible to obtain vesicles stable for a long time in mixed surfactant systems at temperatures much lower than the Krafft temperatures of the two corresponding surfactants.

5.5 Conclusions

The occurrence of supersaturation has been investigated in mixed surfactant solutions composed of SDS / CTAB and SDS / DTAB. A temporary 'solubility temperature depression' has been observed in the anionic-rich part of the phase diagram. We have shown that the stability of such supersaturated solutions can be tuned by increasing the ionic strength, by variation of counterions, and by the addition of alcohols. The presence of simple electrolytes generally decreased, while the addition of middle-chained alcohols increased its stability.

Destabilization and concurrent precipitation of the systems was shown not to occur due to the formation of bigger aggregates, but rather due to a shift of the equilibrium between micelles and monomers. The addition of low concentrations of middle-chain alcohols resulted in the formation of vesicles in the catanionic systems at temperatures significantly lower than the Krafft temperatures of the ionic surfactants.

The lifetime of vesicles and micelles could therefore be controlled by varying the composition of the surfactant solutions and by additives. Controlling the precipitation phenomena is of importance for a large number of industrial processes, where formulations need to be tuned.

Part III

Toward Application

Chapter 6

Use of Surfactants in Cosmetic Application: Determining the Cytotoxicity of Catanionic Surfactant Mixtures on HeLa Cells

6.1 Abstract

The cytotoxicity of commonly used synthetic surfactants and catanionic mixtures of those was evaluated using MTT on HeLa cells. The 50% inhibition concentration (IC_{50}) for MTT reduction was calculated. The effect on chain length increase and inclusion of polyoxyethylene groups on the toxicity was tested on single surfactant systems. A general trend of increasing toxicity with increasing chain length and the presence of polyoxyethylene groups was observed. The measured IC_{50} values of catanionic systems lie between those of participating surfactants. The increase in toxicity as the cationic surfactant was added to the anionic one was however not linear. A steep decrease of the IC_{50} values (and therefore increase in the toxic properties) was observed immediately already at low concentrations of the cationic surfactants. This behavior is analogous to the enzyme activity in catanonic microemulsions.

6.2 Introduction

Vesicles are commonly used in cosmetics and pharmacy as vehicles for active agents. Active molecules can thus be encapsulated in the bilayer membrane, if they are lipophilic, or in the core of the vesicle, if they are hydrophilic. Encapsulation is useful to protect actives in preventing any undesired reaction. Vesicles can thus be used as vectors to deliver drugs to a specific place, without being destroyed.

Improving the biocompatibility of products used in cosmetic formulation further is sought after. For this reason it is important to identify the irritating properties of commercially used surfactants. Lately, catanionic systems have been investigated as potential delivery systems due to their ability to spontaneously form vesicular phases. Furthermore, new surfactants are being synthesized continuously. For this reason, it is important to establish an easy way to estimate the potential toxicity of such substances.

Performing cytotoxicity tests on established cell lines is a good alternative to expensive and morally questionable animal tests. In the present study, cytotoxicity of commercially used surfactants and common catanionic surfactant mixtures were measured on HeLa cells in order to identify their toxicity for use in pharmaceutical and cosmetic applications. HeLa cells are a well-known cell line that is used to asses the cytotoxicity of chemical compounds[320–323] and reportedly show good reproducibility and a significant correlation with *in vivo* results[324]. Cell viability was evaluated by the tetrazolium MTT reduction assay, based on the uptake and the reduction of the soluble yellow MTT tetrazolium salt by mitochondrial dehydrogenase to a blue insoluble MTT formazan product. The IC_{50} value (concentration of test substance that lowers MTT reduction by 50% compared with the untreated control) was calculated from absorbance data. Previous tests have shown that the mitochondrion-based MTT test is a very sensitive indicator of surfactant cytotoxicity[325]. Intracellular organelles (such as mitochondria) are affected already by low surfactant concentrations due to their high sensitivity to surfactant membrane actions. Furthermore, high correlation between MTT reduction assay tests and cytosolic lactate dehydrogenase leakage (LDH) *in vitro* and the Draize eye irritancy

data *in vivo* were reported[325]. In fact, cytotoxicity *in vitro* proved to be more sensitive and quantitative than the Draize test[326].

A few reports concerning the toxicity of surfactants using different assays should be noted[325,327–332]. The toxicity of SDS is commonly investigated as an example of an ionic surfactant. It has been established that ionic surfactants show higher toxicity values than the non-ionic ones, and that cationic surfactants are more potent than their anionic counterparts[328]. However, reports on the toxic properties of catanionic mixtures are very scarce. The cytotoxicity of a SDS/CTAB/cholesterol mixture was tested on murine macrophage-like cells by Kuo et al.[333]. A dose-dependent apoptosis was observed. The study did however not include the effect caused by the variation of the ratio of the surfactants and their chain lengths.

6.3 Experimental Procedures

6.3.1 Materials

HeLa Cell Line HeLa cells were distributed by the American Type Culture Collection (ATCC). Cells were cultured in Earle's minimum essential medium (MEM) containing 0.85 g/L $NaHCO_3$ supplemented with FCS (fetal calf serum)(10%), L-Glutamin (2 mM), NEA (non-essential amino acids)(1%), Amphotercin B (0.4μg/ml) and Penicilin G / Streptomycin sulfate (100 u/mL).

Surfactant Solutions The surfactants, sodium octanoate (SO; Sigma, Germany; grade: 99%), sodium dodecanoate (SL; Sigma, Germany; grade: 99-100%), sodium dodecyl sulfate (SDS; Merck, Germany; assay $>$ 99%), sodium laurelth sulfate (Texapon 70; $Na^+C_{12}(EO)_{2.2}OSO_3^-$, active assay: 70%, gift from Cognis, Germany) and sodium dodecylethercarboxylate (Akypo Soft 45NV; $Na^+C_{11}(EO)_{4.5}OCH_2COO^-$, active assay: 21%, gift from Kao Chemicals, Germany), octyltrimethylammonium bromide (OTAB; Merck, Germany; assay $>$ 99%), decyltrimethylammonium bromide (DeTAB; Merck, Germany; assay $>$ 99%), dodecyltrimethylammonium bromide (DTAB; Merck, Germany; assay $>$ 99%), cetyltrimethylammonium bromide

(CTAB; Sigma, Germany; grade: 99%) were used as received. Surfactant stock solutions were prepared by dissolving weighed amounts of dried substances in Millipore water. The solutions were then left for 24 hours to equilibrate at 25°C. The catanionic solutions were prepared by mixing the surfactant stock solutions to obtain different anionic / cationic surfactant mass ratios.

6.3.2 Growing HeLa Cell Cultures

Substances: MEM - EARLE Medium, PBS - DUBECCO Buffer, Trypsin / EDTA, Flask containing HeLa cells

1. The old medium was removed from the flask containing HeLa cells that we wished to transplant.
2. The cells were rinsed with approximately 4 ml of PBS buffer solution. With this we have removed all the "free-swimming" cells; only the cells stuck to the bottom of the flask remained.
3. 3 ml of Trypsin / EDTA was added and the cells were incubated at 37°C for 5 minutes. Trypsin disables the cell's ability to bind to surfaces (consequently, the cells are swimming freely in the suspension).
4. The cell suspension was transferred into a new flask, 3 ml of new MEM medium was added to stop the reaction of Trypsin and the cells were centrifuged at 800/min for 5 minutes (20°C).
5. Once centrifuged, the supernatant was carefully removed.
6. 4 ml of new MEM medium was added and the solution was homogenized using a pipette until cell-clusters disappeared.
7. A desired amount of cell suspension (depending on when we needed the cells ready for the next experiments) was transferred into a new flask and MEM medium was added to a collective volume of 20 ml.
8. The cells were left to incubate at 37°C for minimum 3 days.

6.3.3 HeLa Toxicity Test

1. The viability of the cells was checked with Trypanblue (solution: 0.04 g Tryptanblue in 10 ml PBS buffer); 10 μl cell suspension +10 μl Trypanblue => we counted the living cells under the microscope (the defected cells were colored blue, the intact one's white).

2. Number of cells in the 16 squares: f.i. 330

$330 \cdot 2 = 660$ dilution with Trypanblue

$660 \cdot 10 = 6.600$ cells in 1μl

$6.600 \cdot 1.000 = 6.600.000$ cells in 1 ml

3. We need 150.000 cells per experiment:

$6.600.000 : 150.000 = 44$

That means we need to dilute 1 ml of the cell suspension with 44 ml of medium.

For 1 plate (60 wells with 75 μl) 4.5 ml of cell suspension is needed (2 plates = 9 ml); we prepare 0.5 ml cell suspension + 22 ml of medium.

4. Concentration of substances of which we wish to measure toxicity: 1 mg/ml (1 wt.%); 0.1 mg/ml if the substances are very potent (cationic surfactants).

5. Filling the plates:

o The wells at the borders were filled with 150μl of pure medium ($36 \cdot 150$ μl = 5.4 ml)

o The middle 60 wells were filled with 75 μl medium

o 60 μl medium was added to wells 2 / B-G (the columns are described using numbers, and rows using letters)

o Wells 2B/2C were additionally filled with 15 μl of sample 1; 2D/2E with 15 μl of sample 2; 2F/2G with 15 μl of sample 3.

6. With a 6-canal pipette the solutions were thoroughly mixed in wells 2B - 2G and then 75 μl of the solutions was transfered from column 2 to column 3 (wells 3B - 3G). This procedure was repeated until row 10 (10B - 10G). The last 75 μl of solutions from row 10 was discarded. Row 11 was reserved for our "blind" probe.

7. Finally, 75 μl of cell suspension was added to all 60 middle wells with (without mixing)(in the end the whole plate should contain 150 μl / well).

8. The cells were left to incubate for 68 hours ($\pm$1 hour).

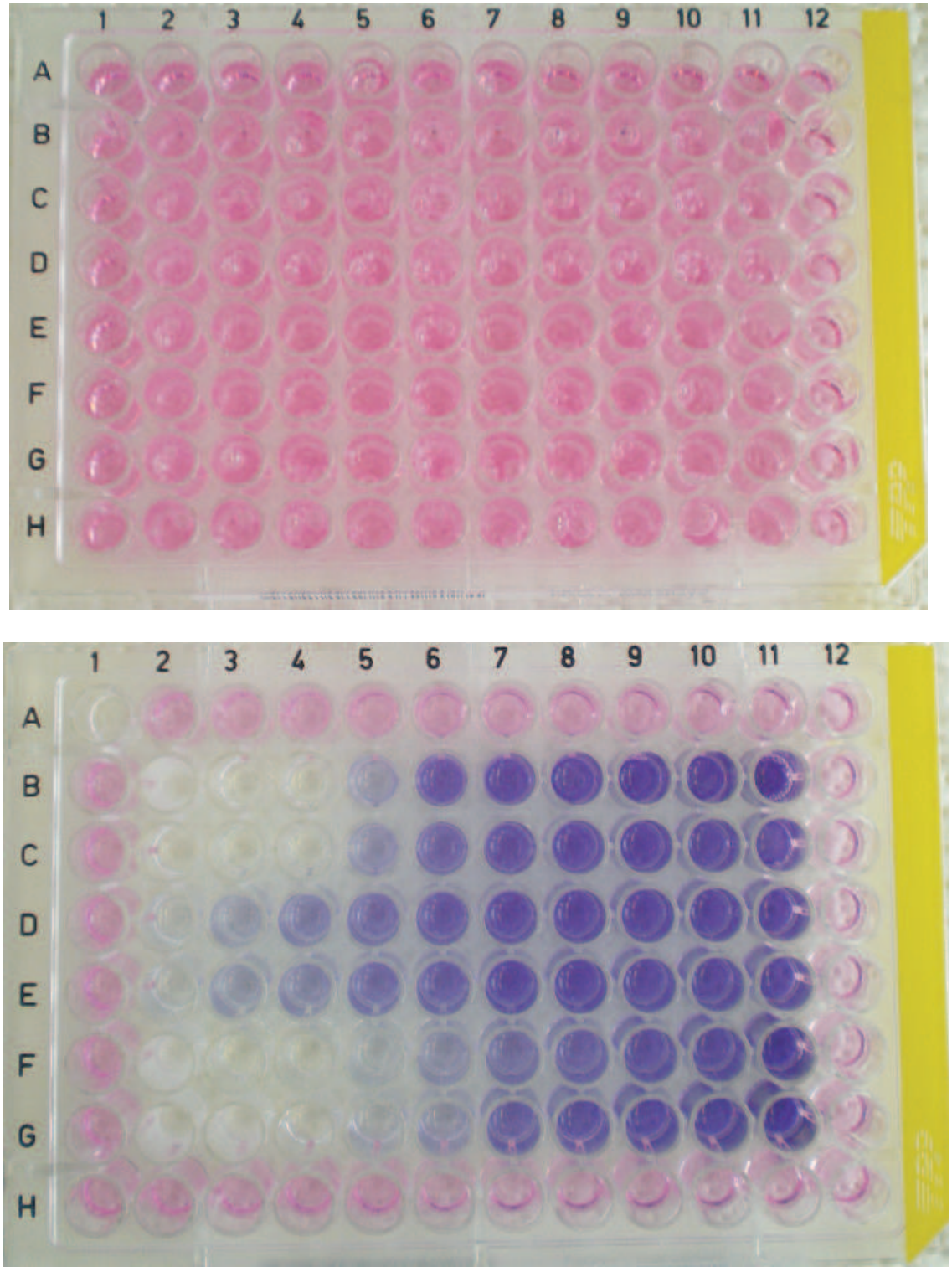

Figure 6.1: 96-well plates used for toxicity studies immediately after preparation (top) and after incubation with MTT (bottom).

6.3.4 Detection

1. 15 μl of MTT solution (4 mg/ml of MTT in PBS buffer) was added to all wells containing cells (0.9 ml MTT solution per plate).
2. The plates were left to incubate for 4 hours.
3. The excess MTT containing medium was carefully remove. Well 1A was emptied as well.
4. The empty wells were filled with 150 μl 10 wt.% SDS solution (in water; 18.3 ml for two plates).
5. The micro-plates were placed in laminar flow overnight, then the optical density of each plate was measured with a microplate reader at 560 nm.

A sample plate immediately after the preparation process and after the MTT incubation is presented in Figure 6.1. The wells at the rims are filled only with medium (pink color), the blue color is a sign of intact cells and the transparent solution of cell apoptosis.

6.3.5 Evaluation of spectroscopical data

The IC_{50} value (in μg /ml), which represents the concentration of test substance that lowers MTT reduction by 50% compared with the untreated control, was calculated for each substance from the concentration-response curve. A sample calculation sheet is presented in Figure 6.2. Experiments were repeated four times (n = 5), and the average IC_{50} is reported. Maximal observed (absolute) standard deviation was about 15%. Positive control measurements were performed with xanthohumol (HeLa cells: $IC_{50} \approx 7$ μg/mL).

6.4 Results and Discussion

6.4.1 Single-Chain Surfactants

Cell viability was determined by the tetrazolium MTT dye reduction in the cell culture system. Evaluation of the results revealed a dose-dependent cytotoxicity after 68 hours of exposure. The IC_{50} values are reported in Table 6.1.

HeLa -Cells							
Testsubstance:SDS/DTAB 90/10							
Konz[µg/ml]	OD			Average	corr. ave.	Restakt. [%]	StAbw [%]
Empty value	0.0428						
				0.043			
Control	0.8590	0.8325	0.8739				
	0.8141	0.9065	0.8372	0.854	0.811		
1000	0.0519	0.0532		0.053	0.0098	1.2	0.1
500	0.0511	0.0472		0.049	0.006	0.8	0.3
250	0.0457	0.0433		0.045	0.002	0.2	0.2
122.5	0.0661	0.0821		0.074	0.031	3.9	1.4
62.5	0.3885	0.3824		0.385	0.343	42.2	0.5
31.25	0.4840	0.5725		0.528	0.485	59.9	7.7
15.63	0.7098	0.7054		0.708	0.665	82.0	0.4
7.8	0.8245	0.8394		0.832	0.789	97.3	1.3
3.9	0.9018	0.9091		0.905	0.863	106.4	0.6
Conc >50%: 31.25Value: 59.9µg/ml							
Conc<50%: 62.5 Value: 42.2µg/ml							
IC_{50} =48.73µg/ml							

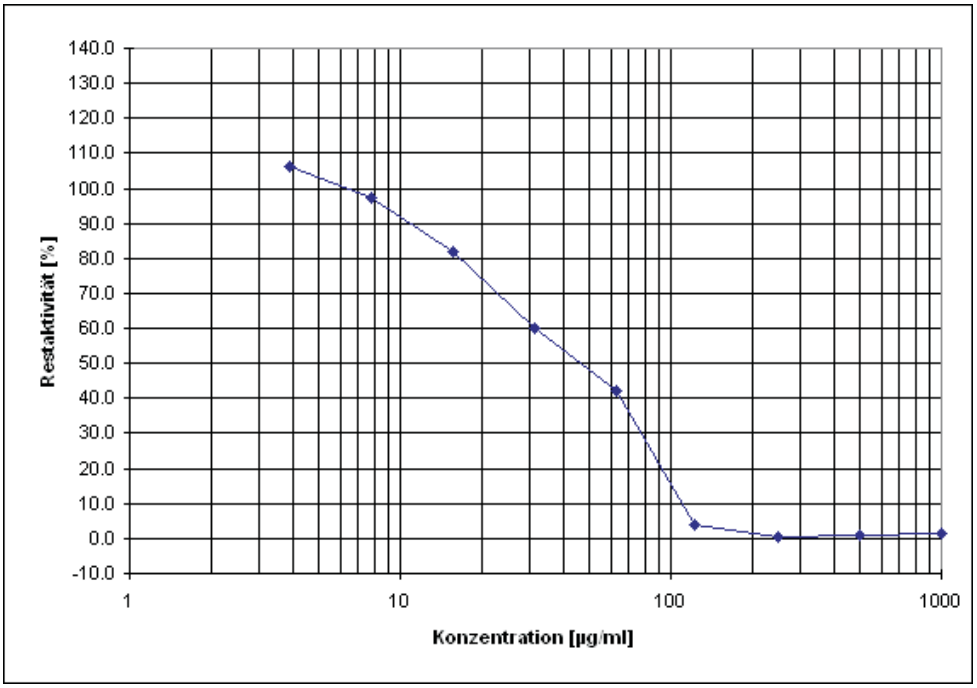

Figure 6.2: Calculation of the IC_{50} value from the spectroscopical data.

Comparison of the IC_{50} values of the surfactants revealed the following cytotoxic properties:

1) Anionic surfactants generally exhibited a lower cytotoxicity than catanionic surfactants.

Anionic surfactants		Cationic surfactants	
name	IC_{50} [μg/mL]	name	IC_{50} [μg/mL]
SO	530.5 ± 41.7	OTAB	23.3 ± 1.8
SL	115.8 ± 8.2	DeTAB	4.8 ± 0.6
SDS	177.1 ± 7.8	DTAB	5.2 ± 0.3
Texapon 70	69.2 ± 1.7	CTAB	1.6 ± 0.2
Akypo Soft 45NV	76.3 ± 4.8		

Table 6.1: The IC_{50} values (concentration of test substance that lowers MTT reduction by 50% compared with the untreated control) of singe-chain ionic surfactants.

2) Surfactants containing sulphate headgroups showed higher IC_{50} values than those bearing a carboxylate (having the same chain-length).
3) An increase of the toxicity of the surfactant was observed as the length of the hydrocarbon chain was increased (c. f. Figure 6.3). An exponential decrease in the IC_{50} values was observed, which leveled off at a certain chain length.
4) The presence of the oxyethylene groups increases the toxic properties of the surfactants. Two surfactants containing 12 carbon atoms, and polyoxyethylene groups, one with a sulphate (Texapon 70) and one with a carboxylate headgroup (Akypo Soft 45 NV) were compared to those without the EO groups. An increase in the toxic properties is observed for both surfactants, however Akypo Soft 45 NV exhibits a higher IC_{50} value, than its sulfate containing counterpart, despite the fact that SDS shows higher IC_{50} values than SL.

6.4.2 Catanionic Surfactant Systems

The toxicity of catanionic surfactant mixtures composed of SDS / DTAB and SL / DTAB were analyzed for different surfactant ratios. The results are presented in Table 6.2 and Figure 6.4.

We can see that the presence of only a small amount of a cationic surfactant increased the toxicity of the mixture significantly. This was somewhat surprising, as a linear increase of the toxicity was expected.

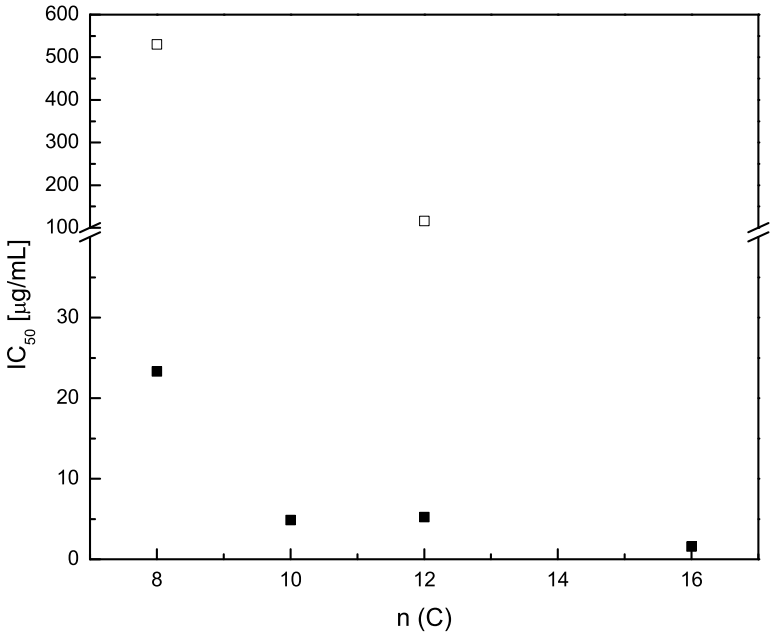

Figure 6.3: Effect of hydrocarbon chain length on the cytotoxicity of ionic surfactants: n(C) represents the number of carbons in cationic CnTAB (■) and anionic SCn (□) surfactants.

SDS / DTAB		SL / DTAB	
x_{SDS}	IC_{50} [μg/mL]	x_{SL}	IC_{50} [μg/mL]
0	4.2 ± 0.2	0	4.2 ± 0.2
0.1	3.5 ± 0.1	0.1	5.1 ± 0.4
0.2	3.8 ± 0.3	0.2	4.6 ± 0.6
0.3	3.7 ± 0.2	0.3	6.3 ± 0.5
0.4	6.7 ± 0.5	0.4	7.1 ± 0.2
0.5	8.2 ± 0.8	0.5	7.2 ± 0.4
0.6	7.9 ± 0.6	0.6	13.0 ± 1.2
0.7	11.6 ± 1.0	0.7	16.4 ± 0.9
0.8	20.1 ± 1.6	0.8	28.6 ± 2.1
0.9	43.1 ± 3.2	0.9	49.7 ± 3.4
1.0	177.1 ± 7.8	1.0	115.8 ± 8.2

Table 6.2: The IC_{50} values of catanionic surfactant mixtures.

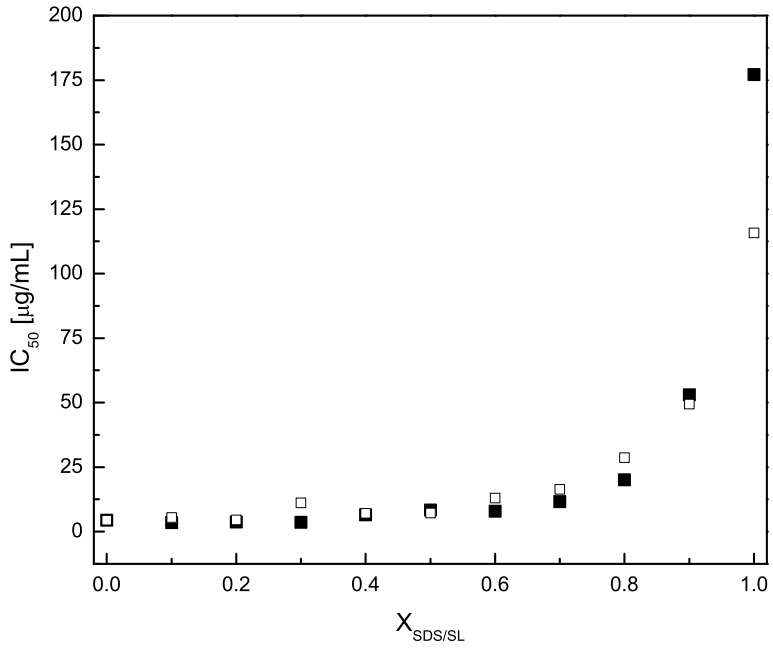

Figure 6.4: The mitochondrial reduction of MTT after a 68-hour incubation of SDS / DTAB (■) and SL / DTAB (□) mixture at different surfactant ratios with HeLa cells.

This behavior is similar to the one found when the enzymatic activity in catanionic emulsions was studied[334]. It was observed that the presence of DTAB exerts an inhibiting effect on the enzyme. At weight fractions higher than 0.22, the enzyme was completely inhibited. This is approximately the weight fraction at which the toxicity of the mixtures equals that of a pure DTAB solution. It is highly probable that at weight fraction lower than 0.22 DTAB is completely incorporated in the catanionic micelles and its toxicity is reduced by the strong electrostatic interactions with the oppositely charged anionic surfactant.

Results suggest that in order to keep the toxicity of potential drug delivery systems low, a high fraction of the anionic component is necessary. So far, vesicles have been shown to exist in the anionic-rich region of the catanionic phase diagrams, however at ratios close to equimolarity. The vesicular region was shifted to higher anionic fractions when salt was added to the system[169,335]. A system of lower toxicity composed of a mixture of anionic surfactants will be reported in the following chapter

(Chapter 7).

6.5 Conclusions

The cytotoxicity of single-chain ionic surfactants and catanionic mixtures was evaluated using MTT on HeLa cells in order to examine their potential use in cosmetic and pharmaceutical formulation. It was confirmed that anionic surfactants generally exhibit higher IC_{50} values than catanionic ones. The toxicity can further be influenced by the hydrocarbon chain length and the presence of polyoxyethylene groups. A general trend of increasing toxicity with increasing chain length and the presence of polyoxyethylene groups was observed. A non-linear increase was observed as cationic surfactants were added to anionic ones. A steep decrease of the IC_{50} values was observed already at low fractions of the cationic surfactants, suggesting that in potential drug delivery systems a high fraction of the anionic component is necessary.

Chapter 7

Spontaneous Formation of Bilayers and Vesicles in Mixtures of Single-Chain Alkyl Carboxylates: Effect of pH and Aging

7.1 Abstract

We report the observation of bilayer fragments, some of which close to form vesicles, over a large range of pH at room temperature from mixtures of single-chain biocompatible commercially available non-toxic alkyl carboxylic surfactants after neutralization with HCl. The pH at which the morphological transitions occur, was varied only by changing the ratio between two surfactants: the alkyl-oligoethyleneoxide-carboxylate and sodium laureate. The effect of aging of the mixed surfactant systems in the pH region desired for dermatologic application ($4.5 < \text{pH} < 7$) was also studied.

7.2 Introduction

There is a growing interest in the field of synthetic surfactants used for dermatologic purposes. These surfactants exhibit a wide range of structures; particularly useful is

the formation of vesicles, which can be used as delivery systems. For cosmetic reasons, the surfactants forming vesicles must be skin compatible (non-irritant), easy to manufacture, and the vesicle region must be stable within the range of physiological pH at room temperature.

A simple geometrical characterization of chain packing can be used to analyze trends in surfactant phase behavior[15,60]. The geometric properties of surfactants depend on the ratio between the cross-sectional area of the hydrocarbon part and that of the headgroup. Low packing parameters (around 1/3) are found for single chain surfactants with a strongly polar headgroup. These systems tend to form spherical micelles, whereas a packing parameter value around one favors the formation of lamellar structures. An increase in the packing parameter can be obtained by adding a second chain, which doubles the hydrocarbon volume. Double-chain surfactants[18,21], two surfactants of opposite charge[23–26], or the association of a surfactant and a co-surfactant[27–33], can be used. In the latter two cases a pseudo-double chain surfactant is obtained by either an ion-pair formation between the anionic and cationic surfactant, or due to association of the two different molecules via hydrogen bonds.

As cationic surfactants and short alcohols are undesirable in cosmetic formulations due to their toxicity, and because long-chain alcohols ($> C_{12}$) exhibit high melting points, monoalkyl carboxylates were chosen for our study. Fatty acids form a range of aggregates depending on the acid concentration and the ionization degree of the terminal carboxylic group[336,337]. The formation of vesicles from monocarboxylic acids has long been known. Gebicki and Hicks[338] first observed the formation of vesicles from unsaturated, long-chain fatty acids. Later, Hargreaves and Deamer showed that also saturated fatty acids can form vesicles[61]. A vesicle phase is spontaneously formed, when short or middle chain ($< C_{12}$) fatty acids are neutralized with HCl[61,81]; two types of amphiphiles are then present in the solution, the protonated and the ionized form. The ratio between the two determines the aggregation morphology.

Despite the simplicity of the mechanism of vesicle formation, possible applications of fatty acid vesicles in cosmetics remain largely unexplored[339,340]. This may be a

consequence of two obstacles: (i) the high solubility temperature of the long-chain carboxylates and, (ii) the generally too basic pH necessary for the solubilization of the carboxylate. The problem of the solubility temperature of the alkyl carboxylates has been discussed by Hargreaves et al.[61] Below 25°C only alkyl carboxylates with short alkyl chains are water-soluble. However, these are inappropriate due to their skin irritating properties. The solubility temperature of sodium laureate is reported to be equal to or above room temperature, depending on the concentration[336]. With longer alkyl chains (n > 12) the solubility temperature becomes even higher.

It has previously been reported that the formation of vesicles occurs at pH values at or near the pKa, where approximately half of the carboxylic groups are ionized[61,336,339]. For this reason, fatty acid vesicles are present only over a narrow pH range. Designing vesicles that become unstable at an easily tuned pH value is of great interest for targeted drug delivery. It is known that, for example, tumors and inflamed tissues exhibit a decreased extracellular pH[63–67]. For this reason a large number of groups have focused their attention on the preparation of pH-sensitive liposomes[68–78] as possible drug carrier systems.

A range of sugar-based gemini surfactants has been recently studied, because they exhibit pH-dependent aggregation behavior. However, these surfactants are cationic and therefore vesicles are observed only at neutral and high pH values[341,342]. The same problem occurs also in solutions of bola-amphiphiles[343]. Systems composed of mixed single- and double-short-tailed PEO ether phosphate esters might be promising for the formation of pH-sensitive vesicles. In that case a vesicle phase was observed at higher concentrations. The pH effect, however, was only studied on vesicular solutions, so one can not confirm a micelle-to-vesicle transition as a consequence of protonation[344].

For carboxylates with longer alkyl chains, desirable for cosmetic formulations (i.e. lauric acid; pKa $\approx 8 - 8.5$[24,61], depending on the concentration), the pH of vesicle formation is also generally too basic. The addition of medium- and long-chain alcohols has been proven to expand the pH region of vesicle formation[61,339], but toward even higher pH values, which is undesirable. One way to lower the pH range of vesicle formation is to introduce another carboxylic group to the fatty acid chain,

thus lowering the pKa of the acid. This has been previously done by de Groot et al. by the formation of 2-(4-butyloctyl) malonic acid[345]. However, to the best of our knowledge, no one has tried to use a mixture of single-chain fatty acid soaps yet. Recently, spontaneous formation of vesicles below room temperature, at acidic pH (between 2 and 4), by neutralization of a particular industrial single-chain alkyl carboxylate surfactant was reported[346]. Our intent was to obtain spontaneously-formed vesicles over a wide range of physiological pH at room temperature, by changing the ratio of two surfactants: Akypo Soft 45NV (an alkyl-oligoethyleneoxide-carboxylate already used in cosmetic formulations; AS) and sodium laureate (SL). The effect of pH and aging on vesicle formation was studied by visual observation, dynamic light scattering and transmission electron microscopy. The biocompatibility of the surfactant mixture was checked by measuring the cell viability. Based on our results, we propose a general method to obtain vesicles on a large range of physiological pH using only non-toxic alkyl carboxylates.

7.3 Experimental Procedures

Chemicals Sodium laureate (SL) was purchased from Sigma-Aldrich at a purity of 99%. Sodium dodecylethercarboxylate (Akypo Soft 45NV; $Na^+C_{12}(EO)_{4.5}OCH_2COO^-$) was a gift from Kao Chemicals (Germany). According to the information given by Kao Chemicals, AKYPO Soft 45NV contains molecules with roughly a Gaussian distribution of the number of EO groups with an average value of 4.5. AKYPO Soft 45NV is supplied as an approximately 21 wt.% aqueous solution. Stock solutions of 1wt.% were prepared by dissolving weighed amounts of sodium laurate in deionized water and by dilution of the original Akypo Soft 45NV solution. Different solutions were then prepared by mixing different ratios of the two stock solutions.

Phase Diagrams The phase behavior as a function of temperature was determined by visual observations. The samples were cooled down and left to equilibrate at 0°C, then the temperature was raised by approximately 0.5°C per minute. The measured solubility temperatures correspond to the transition from precipitate to

isotropic phase, i.e., to a micellar or vesicular solution. The samples were titrated with 0.1 M HCl at 25°C. A Concort, type C831 pH-meter, with a Bioblock Scientific glass electrode (Consort ref. nr. SP02N), was used.

Dynamic Light Scattering Particle size analysis was performed by a Zetasizer 3000 PCS (Malvern Instruments Ltd., England), equipped with a 5 mW helium-neon laser with a wavelength output of 633 nm. The scattering angle was 90° and the intensity autocorrelation functions were analyzed using the CONTIN software. All measurements were performed at 25°C.

Cytotoxicity Tests HeLa cells were provided by the ATCC (American Type Culture Collection). The passage numbers of the HeLa cells used in the project varied from 25 to 30. Cells were cultured in Earle's minimum essential medium (MEM) containing 0.85 g/L $NaHCO_3$ supplemented with FCS (10%), L-Glutamine (2 mM), NEA (1%), Amphotercin B (0.4 μg/ml) and Penicillin G / Streptomycin sulfate (100 u/mL). Keratynocytes (SK-Mel-28) were provided by the ATCC. The passage numbers varied from 15 to 20. Cells were cultured in Dulbecco's MEM containing 3.7 g/L $NaHCO_3$ supplemented with FCS (10%), L-Glutamine (2 mM), NEA (1%), Amphotercin B (0.4 μg/ml) and Penicillin G / Streptomycin sulfate (100 u/mL). MTT (3-(4,5-dimethylthiazol-2-yl)-2,5-diphenyl tetrazolium bromide) assay procedure was prepared according to Mosmann[347] in 96-well micro-plates using the doubling dilution method (as described in the previous chapter). First, the wells of the first column were filled with 135μl of MEM medium. All subsequent columns were filled with 75 μl of medium. Then, 15μl of 1wt.% test solutions was added to each well in the first column and the solutions were thoroughly mixed with a 6-channel pipette. 75μl of the test substance / medium mixture was transferred from the wells in the first column to those in the second. Again the solutions were mixed and the procedure was repeated for the whole plate. Then, 75μl of cells were seeded ($2.5 \cdot 10^3$ cells / well). After a 68-hour incubation at 37°C, 15μl of MTT (5 mg /mL) were added to each well. After a 4-hour incubation, the medium containing MTT was removed and 150μl of 10% SDS solution was added. The

micro-plates were placed in laminar flow overnight, then the optical density of each plate was measured with a microplate reader at 560 nm. The IC_{50} value (μg /ml), which represents the concentration of test substance that lowers MTT reduction by 50% compared with the untreated control, was calculated for each substance from the concentration-response curve. Experiments were repeated four times (n = 5), and the average IC_{50} is reported. Maximal observed (absolute) standard deviation was about 15%. Positive control measurements were performed with xanthohumol (HeLa cells: $IC_{50} \approx 7$ μg/mL).

Cryo-TEM We prepared vitrified cryo-TEM specimens in a controlled environment vitrification system (CEVS), at a controlled temperature of 25°C and fixed 100% relative humidity, followed by quenching into liquid ethane at its freezing point[348]. We examined the specimens, kept below −178°C, by an FEI T12 G2 transmission electron microscope, operated at 120 kV, using a Gatan 626 cryo-holder system. Images were recorded digitally in the minimal electron-dose mode by a Gatan US1000 high-resolution cooled-CCD camera with the DigitalMicrograph software package.

7.4 Results and Discussion

7.4.1 Lowering of the Solubility Temperature of Fatty Acids

To form vesicles at room temperature, the solubility temperature T_{Sol} of the surfactant mixture has to be equal to or below this temperature. The use of sodium laureate is therefore limited, because it is insoluble in water at temperatures below 24°C (for solutions of 1 wt.%). We were able to lower the solubility temperature by mixing sodium laurate with a surfactant that is soluble at lower temperatures. AS was chosen because its $T_{Sol} = 5$°C. Figure 7.1 shows that the solubility temperature decreased linearly with increasing amounts of AS for a fixed total surfactant concentration of 1wt.%, and could be described by the equation: T_{Sol} (°C) = $-19.9 \cdot A + 23.9$, where T_{Sol} represents the solubility temperature of the mixture, and A the amount of AS, expressed in wt.%.

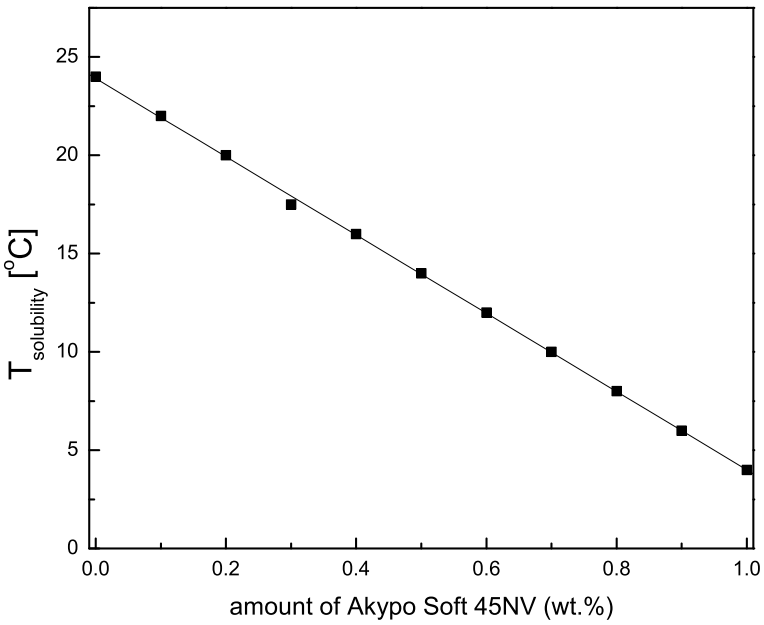

Figure 7.1: Solubility temperature of mixed surfactant solutions (AS and sodium laureate; $c_S^{tot} =$ 1 wt.%) as a function of the amount of AS in the solution. A linear fit describes the dependence with the equation: T_{Sol} (°C) $= (-19.9 \pm 0.1) \cdot A + (23.9 \pm 0.1)$, where T_{Sol} represents the solubility temperature of the mixture and A the amount of Akypo expressed in wt.% (the total surfactant concentration was kept at 1 wt.%)

7.4.2 The Effect of pH on Vesicle Formation

The titration of alkaline soaps with HCl has been described by Rosano et al.[225], when investigating the effects of surface charge on lipid-water interfaces. In these experiments, the appearance of a plateau (buffering capacity) at a precise pH during titration was coincided with the formation of lipid liquid-crystals.We observed this plateau in solutions of dominating quantities of sodium laureate. As more SL was replaced by AS, the plateau region became smaller, disappearing below 0.5 wt.% SL (mass ratio 1 : 1). By reducing the pH of the samples we observed a succession of two (or three) phases, depending on the mass ratio of the two surfactants (Figure 7.2). At high pH, all solutions were isotropic and colorless, corresponding to the micellar region of the phase diagram. By decreasing the pH, a bluish color appeared, attributed to a formation of vesicular structures. In the presence

of pure AS, only two phases appeared consecutively, while in SL / AS mixtures, a second phase transition to precipitation was observed at low pH values. In 1 wt.% SL solutions precipitation began at pH values below 7, whereas the addition of AS lowered the precipitation boundary to pH = 3.5 (in solutions with SL / AS ratio 25/75). Precipitation when the surfactant ratio nears equimolarity, had been observed in previous studies and was attributed to the increased concentration of the conjugated acid[169]. The titrations were performed one week after the preparation of the samples. Macroscopically, the pH values at which the phase transitions took place remained the same with respect to time. This is not true microscopically, as described below.

The formation of fatty acid vesicles is restricted to a narrow pH region close to the pKa of the acidic components[61,336,339]. The apparent shift in the pKa of fatty acid anions (from the pKa = 4.67 of carboxylic group[349] to the pKa = 8 of lauric acid[61]) has been attributed to the local decrease in pH at highly charged surfaces[61]. Since pure fatty acid/soap vesicles (without additional amphiphiles) contain an amphiphile that is not charged (the neutral form of fatty acid), the two bilayer-forming components are associated by hydrogen bonds instead of electrostatic interactions[350]. The formation of vesicles near the pKa of the acid can then be explained by the formation of stable hydrogen bond networks between the ionized and neutral acid forms.

It has been observed that the addition of alcohols to fatty acids causes an increase in the pH of the region of vesicle formation[339]. In that case, vesicles are formed due to stable hydrogen bonds between the alcohol headgroup and the ionized acid headgroup. The addition of the alcohol means larger presence of the non-ionized species in the solution (due to the high pKa of the alcohols); a larger amount of carboxylic acid will be in the ionized form to achieve the same protonated/ionized headgroup ratio needed for vesicle formation (1 : 1). An opposite effect can then be expected in the case when the added component has a much lower pKa than the fatty acid, as is the case of AS. This will be completely ionized at a neutral pH, therefore more protonated acid groups will be required for the formation of vesicles, resulting in a decrease of the pH of vesicle formation. This was confirmed by our titrations, where

the pKa (and corresponding bluish region) decreased with increasing amount of AS in the mixture.

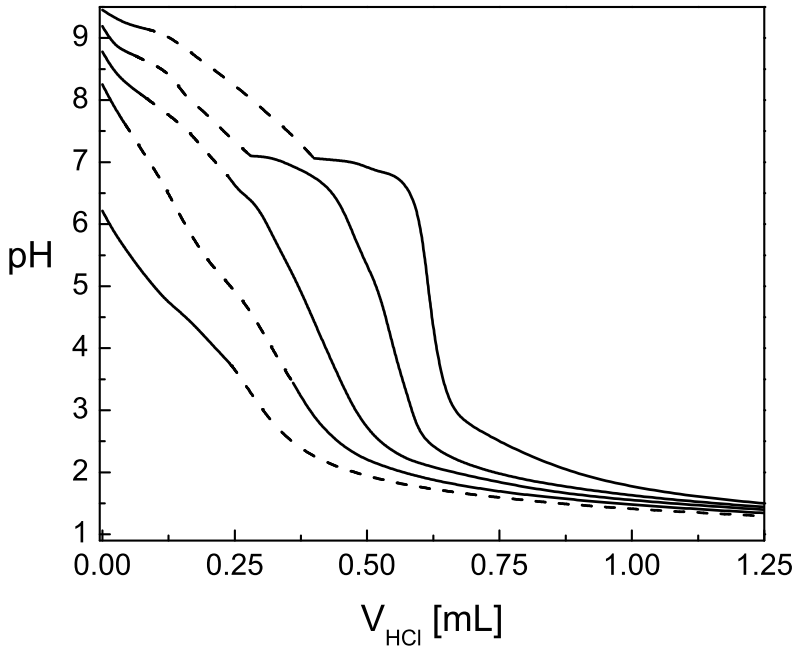

Figure 7.2: Different phase transitions observed by titration of mixed surfactant solutions (sodium dodecanoate and AS; c_S^{tot} = 1 wt.%; V_o = 15 mL) containing (from bottom to top) $1; 0.75; 0.5; 0.25$; and 0 wt.% of AS. The dashed lines represent a bluish solution (possibly vesicles); the solid lines represent the clear (micellar) solution (to the left) and the turbid phase (to the right of the vesicular phase).

The hydrodynamic radius of particles in solutions at different surfactant ratios was measured by dynamic light scattering. The results confirmed the presence of large aggregates (possibly vesicles) over a large pH region (Figure 7.3) in mixed surfactant solutions. Because solutions of industrial surfactants are highly polydisperse (the polydispersity of AS has been previously reported[169]), only the average radius could be measured. The regions where R_H was found to be $80 - 120$ nm (the average radius of vesicles) is plotted in Figure 7.3 for different surfactant ratios. Increasing the amount of AS lead to a decrease of the pH, at which vesicles were formed. The width of the pH range depended strongly on the surfactant ratio. This range is the largest for the ratio AS / SL : 0.75 / 0.25, where it extends from pH 3.5

to 7.5. At this ratio the complete range of skin pH or physiological pH is covered. A reduction of this range was observed when the amount of Akypo Soft 45NV was either increased or decreased.

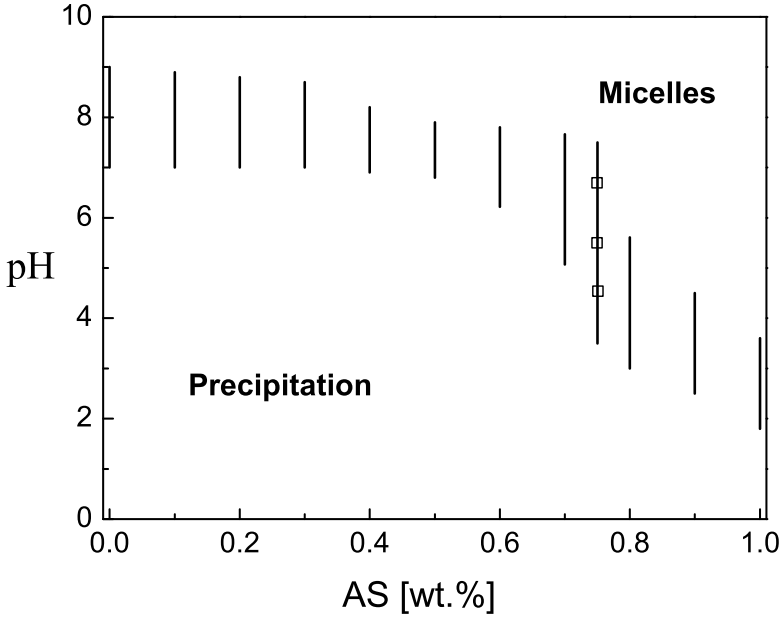

Figure 7.3: pH range where (after 3 weeks) the average hydrodynamic radius R_H was approximately 100 nm (possible region of vesicle formation) in mixed surfactant solutions (SL and AS) as a function of AS concentration (c_S^{tot} = 1 wt.%); the open squares (□) represent the solutions examined by cryo-TEM.

The (average) hydrodynamic radius (R_H) of the objects present in the vesicle containing solutions is shown in Figure 7.4 for different surfactant ratios as a function of the pH. The obtained values suggest the presence of vesicles, but large variations exist. In presence of 0.75 wt.% of AS only small vesicles are measured with a small polydispersity index (around 0.2). At smaller ratios of AS, or in presence of pure sodium laurate, bigger objects of higher polydispersity are observed. Because light scattering is insufficient to characterize systems of high polydispersity, cryo-TEM was used to analyze the system further.

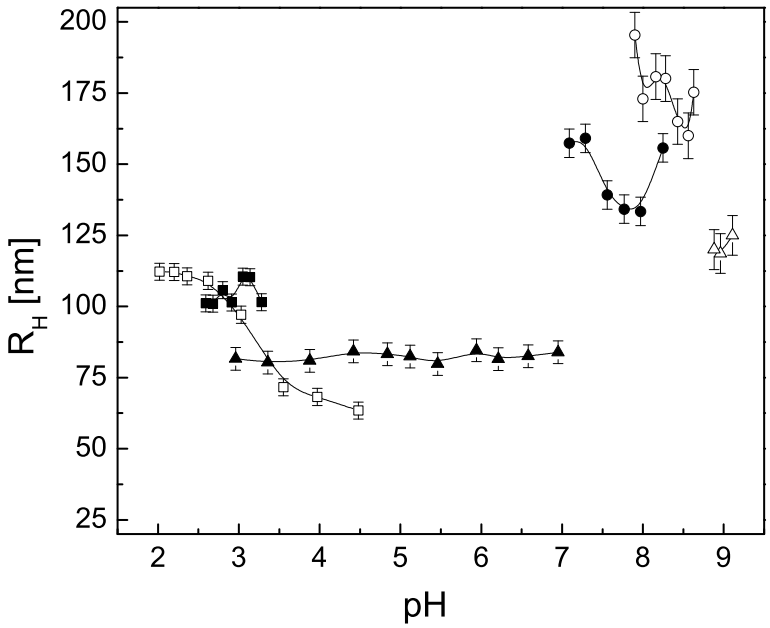

Figure 7.4: Average hydrodynamic radius, R_H, of the aggregates present in bluish solutions as a function of pH for different surfactant ratios: (△) 0; (○) 0.25; (●) 0.5; (▲) 0.75; (□) 0.85; (■) 1 (all expressed in wt.% of AS; $c_S^{tot} = 1$ wt.%).

7.4.3 Cryo-TEM Study of Time-Dependent Vesicle Formation

The AS / SL ratio (75/25), at which the largest pH interval of vesicle formation was measured, was further investigated by cryo-transmission electron microscopy. The evolution of self-assembly aggregates was followed over a period of two months at three different pH values. The sequence of observed morphologies is summarized in Table 7.1.

We see from Table 7.1 that in the first weeks after preparation micelles and discs are the observed structures; these are presented in Figure 7.5. With time, membranes started forming and eventually vesicles appeared (Figure 7.6). The higher the pH of the solution, the faster this transition took place; in samples with pH = 6.7 vesicles were observed already after 2 weeks, whereas in solution with pH = 5.5, these were visible just after 4 weeks. After 2 months vesicles were still

pH	No. of days after preparation				
	5	10	17	28	60
4.5		D, MP	M	D	MP
5.5	M, D		M, D	M, V	M, MP
6.7			MP, V	M, D, V (C)	M, MP, V (I)

Table 7.1: Development of various surfactant self-assembled aggregates with time; M - micelles, D - discs, MP - membrane pieces, V - vesicles, V (C/I) - vesicles with either cusps, or incomplete vesicles.

not observed in solution with the lowest pH (c. f. Figure 7.7 a). However, the two samples at higher pH values already showed incomplete vesicles and membrane pieces (c. f. Figure 7.7 b). It seems that after a certain time, the vesicles in these systems begin to destabilize. We noted that despite the rich morphological development that could be observed by microscopy, macroscopically the solutions appeared about the same during the period of observation. Furthermore, we can see that not all regions where big objects were detected by DLS contain vesicles. These were only found at higher pH values (above 5.5), whereas at low pH, discs and membrane pieces were the dominating form.

The results suggest it is possible to obtain vesicles in the region defined by the two pKa; at certain surfactant ratios an even broader pH range was observed. This is in accordance with results obtained by de Groot et al.[345] for a branched monoalkyl surfactant with a malonate headgroup. A bluish zone was observed between the two pKa values (the pKas of the two carboxylate groups on malonic acid are 2.85 and 5.70, respectively)[345]. In that region co-existence of small unilamellar (SUV) and multilamellar (MLV) vesicles was found. Above pH = 5.8 the solutions were clear and only SUVs were observed by TEM[345].

Such a high polydispersity of morphologies, where flat discs coexist in equilibrium with spherical open and complete unilamellar vesicles, was previously observed in catanionic systems. A possible explanation for the coexistence of these structures was proposed by Jung et al. by evaluating the parameters contributing to the spontaneous curvature[351]. In some systems however (namely mixtures of anionic

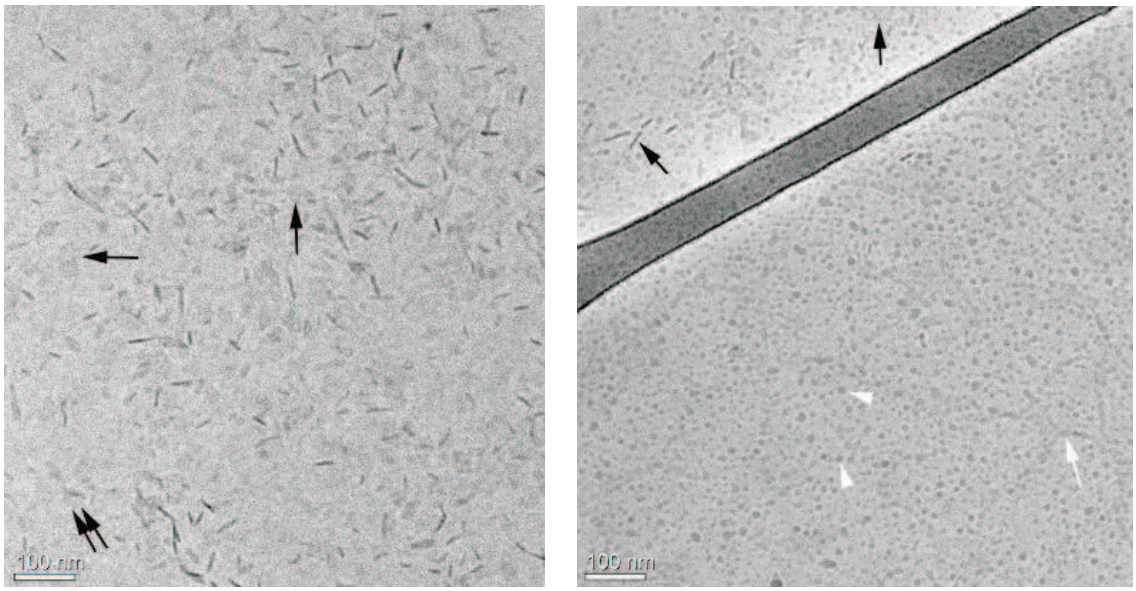

Figure 7.5: Cryo-TEM images of a SL / AS mixed surfactant solution at (left) pH = 4.5, 10 days after mixing, and (right) pH = 5.5, 5 days after mixing. The black arrows point to discs, the double arrows to a partially folded disc, whereas the white arrowheads to globular structures (possibly micelles). The white arrow points to an elongated structure.

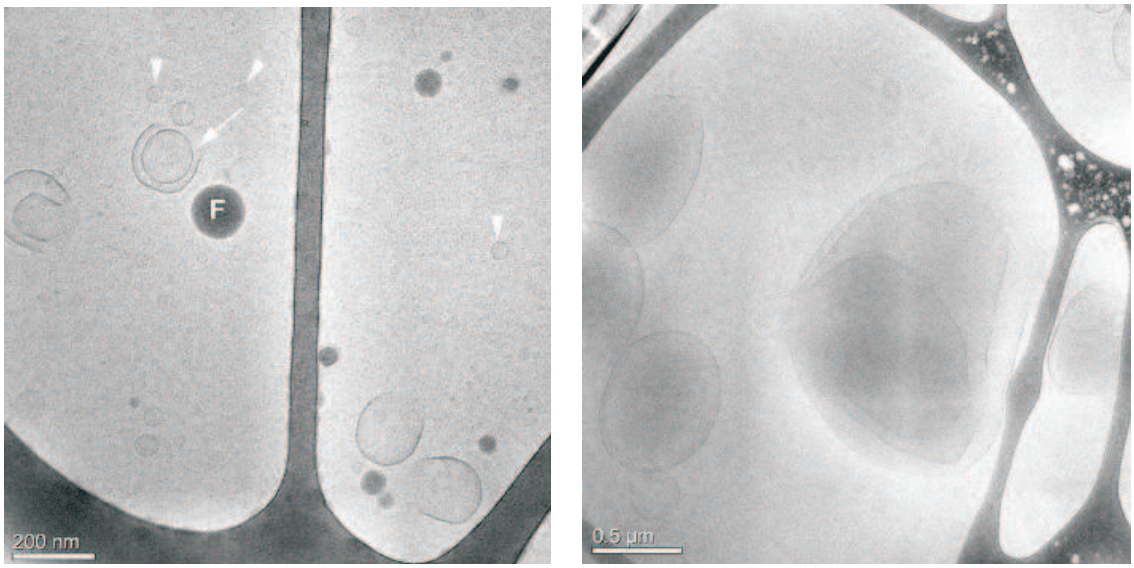

Figure 7.6: The formation of small vesicles after 2 weeks in samples with pH = 6.7 and large multilamellar vesicles after 4 weeks (pH = 5.5); arrowheads point to very small perfect vesicles, while the arrow points to an incomplete two-lamellar vesicle ('F' indicates a frost particle).

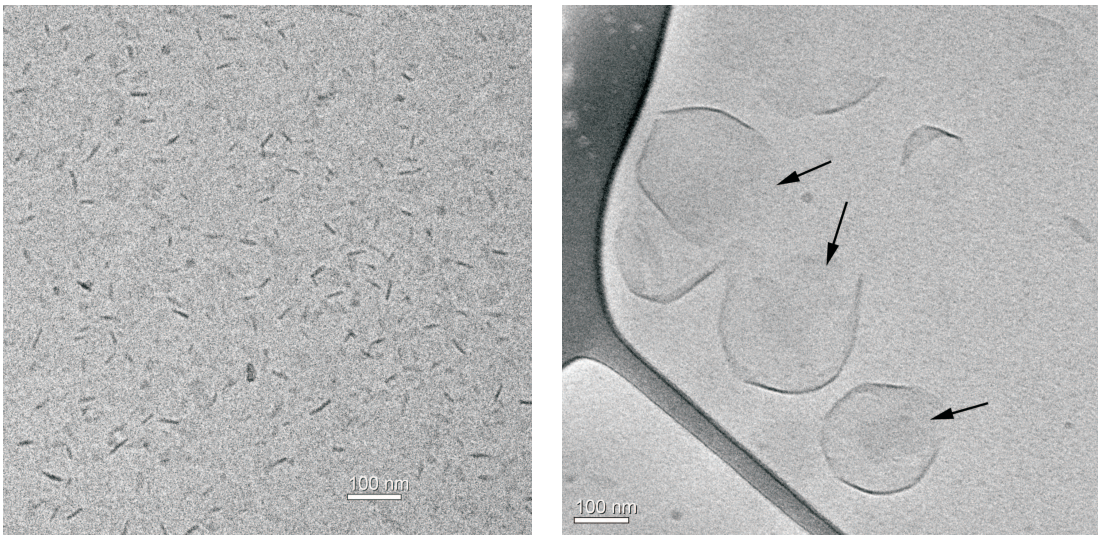

Figure 7.7: Phase behavior after 2 months: (a) small membrane fragments at low pH (= 4.5); (b) destabilization of vesicles at high pH (= 6.7).

and zwitterionic surfactants), discoidal structures are only short-lived intermediates in the micelle-to-vesicle transitions[352]. The vesiculation depends on the balance between the unfavorable edge energy of the disks and the bending energy required to form spherical structures. In the case of catanionic surfactant mixtures, the edges of the discs are stabilized by the excess cationic surfactant. It is possible that the relatively bulky EO groups stabilize the discs observed in our system.

7.4.4 Cytotoxicity Potential of Surfactant Mixtures

Akypo Soft 45 NV is commonly used in cosmetic formulations, such as hair conditioners and hair dyes[353–357]. Improving the biocompatibility of products used in cosmetic formulation even further is always sought after. Cytotoxicity of our mixtures on HeLa cells and Keratynocytes was measured in order to identify the toxic properties of the two surfactants for use in pharmaceutical and cosmetical applications. Cell viability was evaluated by the tetrazolium MTT reduction assay, based on the uptake and the reduction of the soluble yellow MTT tetrazolium salt by mitochondrial dehydrogenase to a blue insoluble MTT formazan product. The IC_{50} value was calculated from absorbance data. HeLa cells were used, because they reportedly show good reproducibility and a significant correlation with *in vivo* re-

sults[324], whereas Keratynocytes were chosen to check the skin compatibility of such surfactant mixtures.

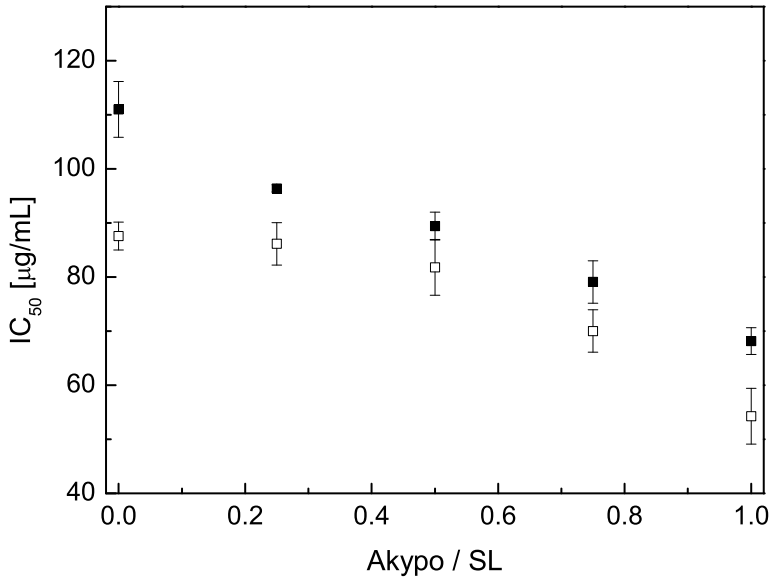

Figure 7.8: The mitochondrial reduction of MTT after a 3-day incubation of SL / AS mixture at different surfactant ratios with HeLa cells (■) and Keratynocytes (□).

IC_{50} values reported in Figure 7.8 show a dose-dependent decrease in toxicity when AS is exchanged for SL. Therefore any surfactant mixture formed with SL is beneficial. The order of the IC_{50} values was the same for both cell lines; however the absolute values were slightly lower in the case of the Keratynocytes. The lowering of the pH of the surfactant test solutions showed no pronounced effect. The volume of the added surfactant solution was probably too small to change the pH value of the cell medium significantly and the buffering capacity of the medium too large for any effects to be observed.

7.5 Conclusions

Two obstacles mentioned in the introduction, namely, the high solubility temperature of alkyl carboxylates and limited pH region of vesicle formation have been

overcome by using a mixture of two alkyl carboxylates with two very different pKa values. The presented results show that it is then possible to spontaneously form bilayer structures, such as vesicles, in a pH range between the two considered pKa. Sodium laureate (with a pKa around 8.5) and Akypo Soft 45 NV (with a pKa = 4.67) could be thus used at different mixing ratios to obtain vesicular solutions over the entire range of pH comparable to skin or physiological pH. Furthermore, we have used commercially available and biocompatible surfactants that are already used for cosmetic purposes and are inexpensive, which is of significant importance for application purposes[358]. However, more research is required to improve their application potential by increasing the colloidal stability of fatty acid vesicles and assure the vesicles are completely closed. Both are common problems in such systems[81,359].

Conclusion

In this thesis the formation and stabilization of catanionic vesicles was studied. Catanionic surfactant mixtures were chosen, because they were shown to form vesicle spontaneously under certain conditions and exhibit an enhanced sensitivity to outside parameters, such as temperature or the presence of salts. Due to this sensitivity, catanionic mixtures are a good system to study specific-ion effects. The interest in vesicles was further motivated by their potential as models for biological membranes and as encapsulation systems. To optimize the applications it is important to have a general understanding of the interplay of interactions between the surfactants and of the factors influencing the phase diagram of a mixed system.

First, the morphological transitions occurring in mixed surfactant systems upon the increase of the ionic strength were explored. The transition of mixed ionic micelles to vesicles in a catanionic surfactant solution, comprised of sodium dodecylsulfate and dodecyltrimethylammonium bromide, with an excess of the anionic component, upon the addition of salt is described in Chapter 2. A new type of intermediate structure was found: a symmetrically shaped spherical super-structure, which we named blastulae vesicle. A mechanism of formation for this type of super-structures was proposed, suggesting the importance of charge fluctuation in the vesicle membrane.

The specific-ion effects on this system was further studied and compared to one where the sulphate surfactant was replaced by a carboxylate surfactant (sodium dodecanoate). No anion specificity was found in the anionic-rich region of the phase diagram for the added salts, whereas the nature of the cation was found to strongly influence the critical salt concentrations around which micelles turn to vesicles. This was explained by taking into account that in the present case of negatively charged

vesicles, the cations accumulate in high concentration in the vicinity of the vesicle. The observed cation specificity followed the classical Hofmeister series for cation adsorption to sulfate headgroups. When alkylcarboxylates were present in solution, the cations followed a reversed Hofmeister series. The ion specificity was qualitatively explained according to Collins' concept of matching water affinities. To this purpose, the headgroup of an alkylsulfate had to be regarded as a chaotrope and the alkylcarboxylate as a kosmotrope. Based on MD simulations performed on the aforementioned headgroups, a general 'Hofmeister series of surfactant headgroups' is established in Chapter 3.

In Chapter 4, the study of ion-specificity was extended to the cationic-rich region of the phase diagram of the catanionic system. No vesicles were found, however, the addition of salts produced a spherocylindrical growth of the micelles, markedly dependent on the anion identity. The efficiency of the anions to elongate the micelles could again be explained by the Collins' concept and the classification of the trimethylammonium surfactant headgroup as a soft, polarizable entity.

The effect of various additives on the stability of mixed surfactant solutions of sodium dodecylsulfate with cetyltrimethylammonium bromide and with dodecyltrimethylammonium bromide was studied as a function of time and is reported in Chapter 5. The lifetime of vesicles and micelles in these systems could be controlled by varying the composition of the surfactant solutions and by additives. Controlling the precipitation phenomena is of importance for a large number of industrial processes, where formulations need to be tuned. These specific mixtures were shown to have a solubility temperature below that of pure surfactant solutions in the anionic-rich region. The stability of such supersaturated solutions was increased by increasing the percentage of the anionic surfactant and shortening the chain of the cationic surfactant. The presence of simple electrolytes decreased, while the addition of middle-chain alcohols increased their stability. Experimental results suggested that the destabilization and concurrent precipitation of the systems was not due to the formation of bigger aggregates, but rather to a shift of the equilibrium between micelles and monomers. The addition of low concentrations of middle-chain alcohols resulted in the formation of vesicles in the catanionic systems at temperatures sig-

nificantly lower than the Krafft temperatures of the participating ionic surfactants. In Chapter 6 we evaluated the cytotoxicity of single-chain ionic surfactants and catanionic mixtures using MTT on HeLa cells. It is important to consider the toxicity of participating surfactants when formulating new encapsulating systems for either cosmetic or medical use. It was confirmed that anionic surfactants generally exhibit higher IC_{50} values (lower toxicity) than catanionic ones. The toxicity could further be influenced by the hydrocarbon chain length and the presence of polyoxyethylene groups. A general trend of increasing toxicity with increasing chain length and inclusion of polyoxyethylene groups was observed. A non-linear increase was observed as cationic surfactants are added to anionic ones. A steep decrease of the IC_{50} values is observed already at low fractions of the cationic surfactants, suggesting that in potential drug delivery systems a high fraction of the anionic component is necessary.

Seeing that the presence of only a small amount of a cationic surfactant in the mixture resulted in a large increase in its toxicity, we focused on a mixture of two anionic and in cosmetic formulation already commonly used surfactants. In chapter 7 we present a way to form vesicles in a mixture of two alkyl carboxylates with two very different pKa values. We have shown that it is then possible to spontaneously form vesicles in a pH range between the two considered pKa. Sodium laureate and Akypo Soft 45 NV could be thus used at different mixing ratios to obtain vesicular solutions over the entire range of pH comparable to skin or physiological pH.

Bibliography

[1] K. Holmberg, B. Joensson, B. Kronberg, and B. Lindman. *Surfactants and Polymers in aqueous solutions, 2nd ed.* John Wiley & Sons, 2003.

[2] M. J. Rosen. *Surfactants and Interfacial Phenomena (2nd ed.).* John Wiley & Sons, 1989.

[3] D. F. Evans and H. Wennerström. *The Colloidal Domain.* Wiley-VCH, 1999.

[4] B. Lindman and H. Wennerström. *Topics in Current Chemistry, Vol. 87.* Springer-Verlag, Germany, 1980.

[5] K. Meguro, M. Ueno, and K. Esumi. *Nonionic Surfactants, Physical Chemistry.* Marcel Dekker, New York, 1987.

[6] K. Shinoda, T. Nakagawa, B. I. Tamamush, and T. Isemura. *Colloidal surfactants, Some physico-chemical properties.* Academic Press, London, 1963.

[7] G. Gunnarsson and H. Jönsson, B.and Wennerström. *J. Phys. Chem.*, 84:3114, 1980.

[8] J. Goodwin. *Colloids and Interfaces with Surfactants and Polymers.* John Wiley & Sons, 2004.

[9] J. H. Fendler. *Membrane Mimetic Chemistry.* Wiley, New York, 1982.

[10] W. Helfrich. *Z. Naturforsch.*, 28:693, 1973.

[11] M. Kléman. *Proc. R. Soc. London, Ser. A*, 347:387, 1976.

[12] W. Helfrich. *J. Phys.*, 47:321, 1986.

[13] S. A. Safran, P. Pincus, and D. Andelman. *Science*, 248:354, 1990.

[14] J. N. Israelachvili, D. J. Mitchell, and B. W. Ninham. *Biochem. Biophys. Acta*, 470:185, 1977.

[15] J. N. Israelachvili, D. J. Mitchell, and B. W. Ninham. *J. Chem. Soc., Faraday Trans. 2*, 72:1525, 1976.

[16] D. J. Mitchell and B. W. Ninham. *J. Chem. Soc., Faraday Trans. 2*, 77:601, 1981.

[17] M. Dubois and T. Zemb. *Langmuir*, 7:1352, 1991.

[18] E. F. Marques, O. Regev, A. Khan, and B. Lindman. *Adv. Coll. Interf. Sci.*, 100:83, and refs. therein, 2003.

[19] D.D. Miller, J.R. Bellare, T. Kaniko, and D.F. Evans. *Langmuir*, 4:1363, 1988.

[20] B.W. Ninham, D.F. Evans, and G.J. Wei. *J. Phys. Chem.*, 87:5020, 1983.

[21] Y. Talmon, D. F. Evans, and B. W. Ninham. *Science*, 221:1047, 1983.

[22] M.I. Viseu, M.M. Velazquez, C.S. Campos, I. Garcia-Mateos, and S.M.B. Costa. *Langmuir*, 16:4882, 2000.

[23] B. A. Coldren, H. Warriner, R. van Zanten, and J. A. Zasadzinski. *Langmuir*, 22:2465, 2006.

[24] E. W. Kaler, A. K. Murthy, B. E. Rodriguez, and J. A. Zasadzinski. *Science*, 245:1371, 1989.

[25] A. Kihisa and T. A. Hatton. *Langmuir*, 18:7341, 2002.

[26] M. T. Yatcilla, K. L. Herrington, L. L. Brasher, E. W. Kaler, S. Chiruvolu, and J. A. Zasadzinski. *J. Phys. Chem.*, 100:5874, 1996.

[27] M. Bergmeier, H. Hoffmann, and C. Thunig. *J. Phys. Chem. B*, 101:5767, 1997.

[28] M. Bergmeier, H. Hoffmann, F. Witte, and S. Zouraub. *J. Colloid Interface Sci.*, 203:1, 1998.

[29] M. Gradzielski, M. Bergmeier, M. Mueller, and H. Hoffmann. *J. Phys. Chem. B*, 101:1719, 1997.

[30] M. Gradzielski, M. Mueller, M. Bergmeier, H. Hoffmann, and E. Hoinkis. *J. Phys. Chem. B*, 103:1416, 1999.

[31] J. Hao, H. Hoffmann, and K. Horbaschek. *Langmuir*, 17:290, 2001.

[32] J. Huang, Y. Zhu, B. Zhu, R. Li, and H. Fu. *J. Colloid Interface Sci.*, 236:201, 2001.

[33] R. Oda and L. Bourdieu. *J. Phys. Chem. B*, 101:5913, 1997.

[34] M. Andersson, L. Hammarström, and K. Edwards. *J. Phys. Chem.*, 99:14531, 1995.

[35] A. M. Carmona-Ribeiro. *Chem. Soc. Rev.*, 21:207, 1992.

[36] J.B.F.N. Engberts and D. Hoeskstra. *Biochim. Biopphys. Acta*, 1241:323, 1995.

[37] E. Feitosa and G. Barreleiro, P.C.A and; Olofsson. *Chem. Phys. Lipids*, 105:201, 2000.

[38] E. Feitosa and W. Brown. *Langmuir*, 13:4810, 1997.

[39] P. Saveyn, J. Cocquyt, P. Bomans, P. Frederik, M. De Cuyper, and P. Van der Meeren. *Langmuir*, 23:4775, 2007.

[40] H. Hauser. *Chem. Phys. Lipid*, 43:283, 1987.

[41] N. E. Gabriel and M. F. Roberts. *Biochemistry*, 23:4011, 1984.

[42] A. K. Murthy, E. W. Kaler, and J. A. Zasadzinski. *J. Colloid Interf. Sci.*, 145:598, 1991.

[43] J. E. Brady, D. F. Evans, B. Kachar, and B. W. Ninham. *J. Am. Chem. Soc.*, 106:4279, 1984.

[44] S. Hashimoto, J. K. Thomas, D. F. Evans, S. Mukherjee, and B. W. Ninham. *J. Colloid Interface Sci.*, 95:594, 1983.

[45] B. W. Ninham and D. F. Evans. *Faraday Discuss. Chem. Soc.*, 81:1, 1986.

[46] Z. Lin, M. He, L. E. Scriven, and H. T. Davis. *J. Phys. Chem.*, 97:3571, 1993.

[47] L. L. Brasher, K. L. Herrington, and E. Kaler. *Langmuir*, 11:4267, 1995.

[48] K. L. Herrington, E. W. Kaler, D. D. Miller, J. A. Zasadzinski, and S. Chiruvolu. *J. Phys. Chem.*, 97:13792, 1993.

[49] E. W. Kaler, K. L. Herrington, A. K. Murthy, and J. A. N. Zasadzinski. *J. Phys. Chem.*, 96:6698, 1992.

[50] Y. Kondo, H. Uchiyama, N. Yoshino, K. Nishiyama, and M. Abe. *Langmuir*, 11:2380, 1995.

[51] G. Gregoriadis. *Liposome Technology. Volume II: Entrapment of Drugs and Other Materials, 2nd ed.* CRC Press: Boca Raton, FL, 1988.

[52] D. D. Lasic. *Liposomes: From Physics to Applications.* Elsevier Publishing Co., Amsterdam, 1993.

[53] M. Dubois and T. Zemb. *Curr. Opin. Colloid Interface Sci.*, 5:27, 2000.

[54] R.D. Koehler, S.R. Raghavan, and E.W. Kaler. *J. Phys. Chem. B*, 104:11035, 2000.

[55] X. Li and H. Kunieda. *Curr. Opin. Colloid Interface Sci.*, 8:327, 2003.

[56] E. Marques, A. Khan, M. Miguel, and B. Lindman. *J. Phys. Chem.*, 97:4729, 1993.

[57] S.R. Raghavan, G. Fritz, and E.W. Kaler. *Langmuir*, 18:3797, 2002.

[58] A. Khan. *Curr. Opin. Colloid Interface Sci.*, 1:614, 1996.

[59] P. K. Yuet and D. Blankschtein. *Langmuir*, 12:3802, 1996.

[60] C. Tanford. *The Hydrophobic Effect: Formation of Micelles and Biological Membranes (2nd ed.)*. John Wiley & Sons, New York, 1980.

[61] W. R. Hargreaves and D. W. Deamer. *Biochemistry*, 17:3759, 1978.

[62] C. Tondre and C. Caillet. *Adv. Colloid Interface Sci.*, 93:115, 2001.

[63] P. M. Gullino, F. H. F. H. Grantham, S. H. Smith, and M. Haggerty. *J. Natl. Cancer Inst.*, 34:857, 1965.

[64] H. Kahler and W. V. B. Robertson. *J. Natl. Cancer Inst.*, 3:495, 1943.

[65] K. A. Meyer, E. M. Kummerling, L. Altman, M. Koller, and S. J. Hoffman. *Cancer Res.*, 8:513, 1948.

[66] J. Naeslund and K. E. Swenson. *Acta Obstet. Gynecol. Scand.*, 32:359, 1953.

[67] M. Stubbs, P. M. J. McSheehy, J. R. Griffiths, and C. L. Bashford. *Mol. Med. Today*, 6:15, 2000.

[68] M. C. De Oliveira, E. Fattal, C. Ropert, C. Malvy, and P. Couvreur. *Journal of Controlled Release*, 48:179, 1997.

[69] I. M. Hafez, S. Absell, and P. R. Cullis. *Biophys. J.*, 79:1438, 2000.

[70] L. Huang and C. Y. Wang. *Biochemistry*, 28:9508, 1989.

[71] X. Li and M. Schick. *Biophys. J.*, 80:1703, 2001.

[72] C. Ropert, M. Lavignon, C. Dubernet, P. Couvreur, and C. Malvy. *Biochem. Biophys. Res. Commun.*, 183:879, 1992.

[73] S. Simões, J. Nuno Moreira, C.; Fonseca, N. Duzgunes, and M. C. Pedroso de Lima. *Adv. Drug Deliv. Rev.*, 56:947, 2004.

[74] S. Simões, V. Slepushkin, N. Duzgunes, and M. C. Pedroso de Lima. *Biochim. Biophys. Acta*, 1515:23, 2004.

[75] J.J. Sudimack, W. Guo, W. Tjarks, and R.J. Lee. *Biochim. Biophys. Acta*, 1564:31, 2002.

[76] V.P. Torchilin, F. Zhou, and L. Huang. *J. Liposome Res.*, 3:201, 1993.

[77] P. Venugopalan, S. Jain, S. Sankar, P. Singh, A. Rawat, and S. P. Vyas. *Pharmazie*, 57:659, 2002.

[78] M. B. Yatvin, W. Kreutz, B. A. Horwitz, and M. Shinitzky. *Science*, 210:1253, 1980.

[79] I. A. Chen and J. W. Szostak. *Proc. Natl. Acad. Sci.*, 101:7965, 2004.

[80] I. Chen and J. W. Szostak. *Biophys. J.*, 82:988, 2004.

[81] K. Morigaki, S. Dallavalle, P. Walde, S. Colonna, and P. L. Luisi. *J. Am. Chem. Soc.*, 119:292, 1997.

[82] C.G. Goltner and M. Antonietti. *Adv. Mat.*, 9:431, 1997.

[83] R. Hoss and F. Voegtle. *Angew. Chem.*, 106:389, 1994.

[84] S. Mann, S.L. Burkett, S. A. Davis, C.E. Fowler, N.H. Mendelson, S.D. Sims, D. Walsh, and N.T. Whilton. *Chemistry of Materials*, 9:2300, 1997.

[85] C.A. McKelvey, E.W. Kaler, J.A. Zasadzinski, B. Coldren, and H.-T. Jung. *Langmuir*, 16:8285, 2000.

[86] Z. Yuan, Z. Yin, S. Sun, and J. Hao. *J. Phys. Chem. B*, 112:1414 – 1419, 2008.

[87] A. Bonincontro, M. Falivene, C. La Mesa, G. Risuleo, and M. R. Pena. *Langmuir*, 24:1973, 2008.

[88] J. D. Bernal and R. H. Fowler. *J. Chem. Phys.*, 1:515, 1933.

[89] R. W. Gurney. *Ionic Processes in Solution.* McGraw-Hill Book Co., 1953.

[90] G. A. Krestov. *Thermodynamics of Solvation.* Ellis Horwood: New York, 1990.

[91] R. A. Robinson and R. H. Stokes. *Electrolyte Solutions.* Butterworth Scientific Publications: London, 1959.

[92] O. Y. Samoilov. *Water and Aqueous Solution: Structure, Thermodynamics, and Transport Processes*, pages 597–612. Wiley-Interscience: New York, 1972.

[93] O. Y. Samoilov. *Discuss. Faraday Soc*, 24:141, 1957.

[94] G. Galli and M. Parrinello. *Computer Simulations in Materials Science.* Kluwer: Dordrecht, 1991.

[95] K. Heinzinger and P. C. Vogel. *Z. Naturforsch.*, 29:1164, 1974.

[96] G. Hummer, L. R. Pratt, and A. E. Garcia. *J. Phys. Chem. A*, 102:7885, 1998.

[97] D. Marx, M. Sprik, M. Sprik, and M. Parinello. *Chem. Phys. Lett.*, 273:360 and refs therein, 1997.

[98] M. C. Payne, M. P. Teter, D. C. Allan, T. A. Arias, and J. D. Joannopoulos. *Rev. Mod. Phys.*, 64:1045, 1992.

[99] W. Kauzmann. *Adv. Protein Chem.*, 14:1, 1959.

[100] M. Kaminsky. *Discuss. Faraday Soc.*, 24:171, 1957.

[101] K. D. Collins. *Methods*, 34:300, 2004.

[102] N. T. Skipper and G. W. Neilson. *J. Phys.: Condens. Matter*, 1:4141, 1989.

[103] K. D. Collins. *Biophys. J.*, 72:65, 1997.

[104] P. Debye and B. Hückel. *Phys. Z.*, 24:185, 1923.

[105] K.D. Collins. *Proc.Natl.Acad. Sci.*, 92:5553, 1995.

[106] K. D. Collins and M. W. Washabaugh. *J. Biol. Chem.*, 261:12477, 1986.

[107] K. D. Collins and M. W. Washabaugh. *Q. Rev. Biophys.*, 18:323, 1985.

[108] S. Gopalakrishnan, D. Liu, H.C. Allen, M. Kuo, and M. J. Shultz. *Chem. Rev.*, 106:1155, 2006.

[109] P.B. Petersen and R.J. Saykally. *Annu. Rev. Phys. Chem.*, 57:333, 2006.

[110] J. Cheng, C.D. Vecitis, M.R. Hoffmann, and A. J. Colussi. *J. Phys. Chem. B*, 110:25598, 2006.

[111] P. Jungwirth and D. J. Tobias. *Chem. Rev.*, 106:1259, 2006.

[112] L. Vrbka, M. Mucha, B. Minofar, P. Jungwirth, E. C. Brown, and D. J. Tobias. *Curr. Opin. Colloid Interface Sci.*, 9:67, 2004.

[113] M. Bostrom, F.W. Tavares, B.W. Ninham, and J.M. Prausnitz. *J. Phys. Chem. B*, 110:24757, 2006.

[114] F. Hofmeister. *Arch. Exp. Pathol. Pharmakol.*, 24:247, 1888.

[115] W. Kunz, P. Lo Nostro, and B. W. Ninham. *Curr. Opin. Colloid Interface Sci.*, 9:1, 2004.

[116] Y. Marcus. *Ion Solvation.* Wiley: Chichester, U.K., 1985.

[117] Y. Marcus and G. Hefter. *Chem. Rev.*, 106:4585, 2006.

[118] Y. V. Kalyuzhnyi, V. Vlachy, and K. Dill. *Acta Chim. Slov.*, 48:309, 2001.

[119] T. V. Chalikian, J. Volker, E. Plum, and K. Breslauer. *Proc. Natl. Acad. Sci.*, 96:7853, 1999.

[120] J. Darnell, H. Lodish, and D. Baltimore. *Molecular Cell Biology.* Scientific American Books, New York, 1990.

[121] K. A. Dill. *Biochemistry*, 29:7133, 1990.

[122] N. Korolev, A. P. Lyubartsev, A. Rupprecht, and L. Nordenskiold. *Biophys. J.*, 77:837, 1999.

[123] J. Rupley and G. Careri. *Adv. Protein Chem.*, 41:37, 1991.

[124] T. P. Lybrand, A. McCammon, and G. Wiff. *Proc. Natl. Acad. Sci.*, 83:833, 1986.

[125] F. Sussman and H. Weinstein. *Proc. Natl. Acad. Sci.*, 86:7880, 1989.

[126] P. C. Jordan. *Biophys. J.*, 58:1133, 1990.

[127] B. Katz. *Nerve, Muscle, and Synapse*. McGraw-Hill: London, 1966.

[128] M. G. Cacace, E. M. Landau, and J. J. Ramsden. *Q. ReV. Biophys.*, 30:241, 1997.

[129] M. F. Kropman and H. J. Bakker. *Science*, 291:2118, 2001.

[130] M. Maroncelli, J. MacInnins, and G. R. Fleming. *Science*, 243:1674, 1989.

[131] V. L. Larwood, B. J. Howlin, and G. A. Webb. *J. Mol. Model.*, 2:175, 1996.

[132] S. Habuchi, H. B. Kim, and N. Kitamura. *Anal. Chem.*, 73:366, 2001.

[133] M. Chavez-Paez, K. Van Workum, L. de Pablo, and L. L. de Pablo. *J. Chem. Phys.*, 114:1405, 2001.

[134] K. L. Stellner, J. C. Amante, J. F. Scamehorn, and J. H. Harwell. *J. Colloid Interface Sci.*, 123:186, 1988.

[135] L. S. Romsted. *Langmuir*, 23:414, 2007.

[136] H. Fukuda, K. Kawata, and H. Okuda. *J. Am. Chem. Soc.*, 112:1635, 1990.

[137] Th. Zemb, M. Dubois, B. Demé, and T. Gulik-Krzywicki. *Science*, 283:816, 1999.

[138] M. Dubois, B. Demé, T. Gulik-Krzywicki, J.-C. Dedieu, C. Vautrin, S. Désert, E. Perez, and Th. Zemb. *Nature*, 411:672, 2001.

[139] A. Song, S. Dong, X. Jia, J. Hao, W Liu, and T. Liu. *Angew. Chem. Int. Ed.*, 44:4018, 2005.

[140] P. André, A. Filankembo, I. Lisiecki, C. Petit, T. Gulik-Krzywicki, B.W. Ninham, and M. P. Pileni. *Adv. Mat.*, 12:119, 2000.

[141] S. T. Hyde, S. Andersson, K. Larsson, Z. Blum, T. Landh, S. Lidin, and B. W. Ninham. *The Language of Shape*. Elsevier, Amsterdam, 1997.

[142] P. André, B. W. Ninham, and M. P. Pileni. *New J. Chem.*, 25:563, 2001.

[143] P. André, B. W. Ninham, and M. P. Pileni. *Adv. Coll. Interf. Sci.*, 89:155, 2001.

[144] D. Miller, J. Bellare, D. F. Evans, Y. Talmon, and B. W. Ninham. *J. Phys. Chem.*, 91:674, 1987.

[145] B. W. Ninham, S. Hashimoto, and J. K. Thomas. *J. Colloid Interface Sci.*, 95:594, 1983.

[146] B. W. Ninham, Y. Talmon, and D.F. Evans. *Science*, 221:1047, 1983.

[147] J. L. Parker, H. K. Christenson, and B. W. Ninham. *J. Phys. Chem.*, 92:4155, 1988.

[148] E. Z. Radlinska, B. W. Ninham, J. P. Dalbiez, and T. N. Zemb. *J. Coll. Surf.*, 46:213, 1990.

[149] E. Z. Radlinska, T. N. Zemb, J. P. Dalbiez, and B. W. Ninham. *Lamgmuir*, 9:2844, 1993.

[150] T. Bramer, M. Paulsson, K. Edwards, and K. Edsman. *Pharm. Res.*, 20:1661, 2003.

[151] H. P. Hentze, S. R. Raghavan, C. A. McKelvey, and E. W. Kaler. *Langmuir*, 19:1069, 2003.

[152] M. Kepczynski, F. Ganachaud, and P. Hemery. *Adv. Mat.*, 16:1861, 2004.

[153] J. C. Amante, J. F. Scamehorn, and J. H. Harwell. *J. Colloid Interface Sci.*, 144:243, 1991.

[154] N. Kamenka, M. El Amrani, J. Appell, and M. Lindheimer. *J. Colloid Interface Sci.*, 143:463, 1991.

[155] A. Renoncourt, P. Bauduin, D. Touraud, W. Kunz, N. Azemar, and C. Solans. *Comunicaciones presentadas a las Jornadas del Comite Espanol de la Detergencia*, 34:273, 2004.

[156] N. Filipovic-Vincekovic, M. Bujan, I. Smit, Lj. Tusek-Bozic, and I. Stefanic. *J. Colloid Interface Sci.*, 201:59, 1998.

[157] A. J. O'Connor, T. A. Hatton, and A. Bose. *Langmuir*, 13:6931, 1997.

[158] O. Soederman, K. L. Herrington, E. W. Kaler, and D. D. Miller. *Langmuir*, 13:5531, 1997.

[159] H. Yin, Z. Zhou, J. Huang, R. Zheng, and Y. Zhang. *Angew. Chem.*, 42:2188, 2003.

[160] H. Yin, S. Lei, S. Zhu, J. Huang, and J. Ye. *Chem. Eur. J.*, 12:2825, 2006.

[161] L. Hao, Y. Nan, H. Liu, and Y. Hu. *J. Dispersion Sci. and Technology*, 27:271, 2006.

[162] L. Zhai, G. Li, and Z. Sun. *Colloids Surf., A*, 190:275, 2001.

[163] L. Zhai, M. Zhao, D. Sun, J. Hao, and L. Zhang. *J. Phys. Chem. B*, 109:5627, 2005.

[164] A. Renoncourt. PhD thesis, University of Regensburg, 2005.

[165] M. Bergström and J. S. Pedersen. *Langmuir*, 15:2250, 1999.

[166] E. F. Marques, A. Khan, and B. Lindman. *Thermochimica Acta*, 394:31, 2002.

[167] K. Tsuchiya, H. Nakanishi, H. Sakai, and M. Abe. *Langmuir*, 20:2117, 2004.

[168] C. Vautrin, M Dubois, Th. Zemb, St. Schmölzer, H. Hoffman, M. Colloids Gradzielski, and 165. Surfaces A: Physicochem. Eng. Aspects 2003, 217. *Colloids Surf., A*, 217:165, 2003.

[169] A. Renoncourt, N. Vlachy, P. Bauduin, M. Drechsler, D. Touraud, J.-M. Verbavatz, M. Dubois, W. Kunz, and B. W. Ninham Langmuir 23 (2007) 2376. *Langmuir*, 23:2376, 2007.

[170] K. Edwards, J. Gustafsson, M. Almgren, and G. Karlsson. *J. Colloid Interface Sci.*, 161:161, 1993.

[171] J. Gustafsson, G. Orädd, G. Lindblom, U. Olsson, and M. Almgren. *Langmuir*, 13:852, 1997.

[172] J. Gustafsson, G. Orädd, M. Nydén, P. Hansson, and M. Almgren. *Langmuir*, 14:4987, 1998.

[173] H. Hoffmann, C. H. Thunig, U. Munkert, H. W. Meyer, and W. Richter. *Langmuir*, 8:2629, 1992.

[174] M. Silvander, G. Karlsson, and K. Edwards. *J. Colloid Interface Sci.*, 179:104, 1996.

[175] A.-L. Bernard, M.-A. Guedeau-Boudeville, L. Jullien, and J.-M. di Meglio. *Biochim. Biophys. Acta*, 1567:1, 2002.

[176] C. Ménager and V. Cabuil. *J. Phys. Chem. B*, 106:7913, 2002.

[177] J. B. F. N. Sein, A.and Engberts. *Langmuir*, 11:455, 1995.

[178] S. Chiruvolu, S. A. Walker, J. Israelachvili, F. J. Schmitt, D. Leckband, and J. A. Zasadzinski. *Science*, 264:1753, 1994.

[179] S. A. Walker, M. T. Kennedy, and J. A. Zasadzinski. *Nature*, 387:61, 1997.

[180] S. A. Walker and J. A. Zasadzinski. *Langmuir*, 13:5076, 1997.

[181] H. Aranda-Espinoza, Y. Chem, N. Dan, T. C. Lubensky, P. Nelson, L. Ramos, and D. A. Weitz. *Science*, 1999:285, 394.

[182] A. A. Gurtovenko. *J. Chem. Phys.*, 122:244902, 2005.

[183] B. Hribar and V. Vlachy. *J. Phys. Chem. B*, 101:3457, 1997.

[184] A. Walter, P. K. Vinson, A. Kaplun, and Y. Talmon. *Biophys. J.*, 60:1315, 1991.

[185] B. Demé, M. Dubois, T. Gulik-Krzywicki, and Th. Zemb. *Langmuir*, 18:997, 2002.

[186] M. Dubois, V. Lizunov, T A. Meister, Gulik-Krzywicki, J.-M. Verbavatz, E. Perez, J. Zimmerberg, and Th. Zemb. *Proc. Natl. Acad. Sci.*, 101:15082, 2004.

[187] H. W. Meyer, W. Richter, and J. Gumpert. *Biochim. Biophys. Acta*, 1026:171, 1990.

[188] B. Sternberg, J. Gumpert, G. Reinhardt, and K. Gawrisch. *Biochim. Biophys. Acta*, 898:223, 1987.

[189] H. W. Meyer, H. Bunjes, and A. S. Ulrich. *Chem. Phys. Lipids*, 99:111, 1999.

[190] E.; Sackmann and T. Feder. *Mol. Membr. Biol.*, 12:21, 1995.

[191] V. S. Kulkarni, W. H. Anderson, and R. E. Brown. *Biophys. J.*, 69:1976, 1995.

[192] M. Antonietti, A. Wenzel, and A. Thünemann. *Langmuir*, 12:2111, 1996.

[193] H. W. Meyer, K. Semmler, W. Rettig, W. Pohle, A. S. Ulrich, S. Grage, C. Selle, and P. Quinn. *J. Chem. Phys. Lipids*, 105:149, 2000.

[194] C. Gebhardt, H. Gruler, and E. Sackmann. *Zeitschrift für Naturforschung*, 32:581, 1977.

[195] W. Helfrich. *Liquid Crystals*, 5:1647, 1989.

[196] P. G. Dommersnes and J. B. Fournier. *Biophys. J.*, 83:2898, 2002.

[197] J. B. Fournier. *Phys. Rev. Lett.*, 76:4436, 1996.

[198] R. Goetz and W. Helfrich. *J. Phys. II*, 6:215, 1996.

[199] K. D. Collins. *Biophysical Chemistry*, 119:271, 2006.

[200] K. D. Collins, G. W. Neilson, and J. E. Enderby. *Biophysical Chemistry*, 128:95, 2007.

[201] B. Jagoda-Cwiklik, R. Vácha, M. Lund, M. Srebro, and P. Jungwirth. *J. Phys. Chem. B (2007), doi: 10.1021/jp709634t*, doi: 10.1021/jp709634t, 2007.

[202] I. Boime, E. E. Smith, and F. E. Hunter. *Arch. Biochem. Biophys.*, 139:425, 1970.

[203] G. J. van de Vusse, R. S. Reneman, and M. van Bilsen. *Prostaglandins, Leukotrienes Essent. Fatty Acids*, 57:85, 1997.

[204] A. Jakubowska. *ChemPhysChem*, 6:1600, 2005.

[205] M. Yamashita and J. B. Fenn. *J. Phys. Chem.*, 88:4671, 1984.

[206] C. Gamboa and L. Sepulveda. *J. Colloid Interface Sci.*, 113:566, 1986.

[207] S. Ikeda, S. Hayashi, and T. Imae. *J. Phys. Chem.*, 85:106, 1981.

[208] M. L. Corrin and W. D. Harkins. *J. Am. Chem. Soc.*, 69:683, 1947.

[209] N. A. Mazer, G. B. Benedek, and M. C. Carey. *J. Phys. Chem.*, 80:107, 1976.

[210] L. Vrbka, P. Jungwirth, P. Bauduin, D. Touraud, and W. Kunz. *J. Phys. Chem. B*, 110:7036, 2006.

[211] E. Leontidis. *Curr. Opin. Colloid Interface Sci.*, 7:81 and refs. therein, 2002.

[212] H. Gustavsson and B. Lindman. *J. Am. Chem. Soc.*, 100:4647, 1978.

[213] N. Hedin, I. Furo, and P. O. Eriksson. *J. Phys. Chem. B*, 140:8544, 2000.

[214] V. E. Haverd and G. G. Warr. *Langmuir*, 16:157 and refs. therein, 2000.

[215] H. P. Gregor and M. J. Frederick. *Polymer Sci.*, 23:451, 1957.

[216] K. Hutschneker and H. Deuel. *Helv. Chim. Acta*, 39:1038, 1956.

[217] U. P. Strauss. *Polyelectrolytes*, page 79. D. Reidel Publishing Company, Dordrecht-Holland, 1974.

[218] U. P. Strauss and Y. P. Leung. *J. Am. Chem. Soc.*, 87:1476, 1965.

[219] H. P. Gregor, M. J. Hamilton, R. J. Oza, and F. Bernstein. *J. Phys. Chem.*, 60:263, 1956.

[220] F. Helfferich. *Ion Exchange*. McGraw-Hill Book Co., Inc., New York, N.Y., 1962.

[221] H. G. Bungenberg de Jong. *Colloid Science, Vol. II*, chapter 9. Elsevier Publishing Co., Inc., New York, N. Y., 1949.

[222] G. Eisenman. *Symposium on Membrane Transport and Metabolism*, page 163. Academic Press, New York, N. Y., 1961.

[223] M. E. Feinstein and H. L. Rosano. *J. Colloid Interface Sci.*, 24:73, 1967.

[224] I. Weil. *J. Phys. Chem.*, 70:133, 1966.

[225] H. L. Rosano, A. P. Christodoulou, and M. E. Feinstein. *J. Colloid Interface Sci.*, 29:335, 1969.

[226] R. M. Fuoss, A. Katchalsky, and S. Lifson. *Proc. Natl. Acad. Sci. U. S.*, 37:579, 1951.

[227] G. S. Manning. *J. Chem. Phys.*, 51:924, 1969.

[228] H. Daoust and M.-A. Chabot. *Macromolecules*, 13:616, 1980.

[229] D. Dolar. *Polyelectrolytes*, page 97. Reidel Publishing Company, Dordrecht-Holland, 1974.

[230] I. Lipar, P. Zalar, C. Pohar, and V. Vlachy. *J. Phys. Chem. B*, 111:10130, 2007.

[231] G. E. Boyd and B. A. Soldano. *Z. Elektrochem.*, 57:162, 1953.

[232] L. Xu, X. Li, M. Zhai, L. Huang, J. Peng, J. Li, and G. Wei. *J. Phys. Chem. B*, 111:3391, 2007.

[233] H. P. Gregor, L. B. Luttinger, and E. M. Loebl. *J. Am. Chem. Soc.*, 76:5879, 1954.

[234] H. Gustavsson and B. Lindman. *J. Am. Chem. Soc.*, 97:3923, 1975.

[235] J. M. Chialvo, A. A.; Simonson. *J. Phys. Chem. B*, 109:23031, 2005.

[236] N. Vlachy, B. Jagoda-Cwiklik, R. Vácha, D. Tourauda, P. Jungwirth, and W. Kunz. 2008, submitted.

[237] M. M. A. E. Claessens. *Size regulation and stability of charged lipid vesicles, Doctoral dissertation.* PhD thesis, 2003.

[238] H. Ti Tien. *J. Phys. Chem.*, 68:1021, 1964.

[239] M. M. A. E. Claessens, B. F. van Oort, F. A. M. Leermakers, F. A. Hoekstra, and M. A. Cohen Stuart. *Biophys. J.*, 87:3882, 2004.

[240] J. A. W. M. Beenackers, B. F. M. Kuster, and H. S. . van der Baan. *Carbohydr. Res.*, 140:169, 1985.

[241] W. Kunz, P. Calmettes, T. Cartailler, and P. Turq. *J. Chem. Phys.*, 99:2074, 1993.

[242] P. Bauduin, A. Renoncourt, A. Kopf, D. Touraud, and W. Kunz. *Langmuir*, 21:6769, 2005.

[243] J Narayanan, C. Manohar, D. Langevin, and W. Urbach. *Langmuir*, 13:398, 1997.

[244] S. R. Raghavan, H. Edlund, and E. W. Kaler. *Langmuir*, 18:1056, 2002.

[245] J. F. A. Soltero, J. E. Puig, O. Manero, and P. C. Schulz. *Langmuir*, 11:3337, 1995.

[246] H. Wu, S. Kawaguchi, and I. Koichi. *Colloid Polym. Sci.*, 283:636, 2005.

[247] S. Friberg and I. Blute. *Hydrotropy, Surfactant Science Series, Liquid Detergents 2nd ed.* Dekker, New York, 2006.

[248] S. Berr, R. R. M. Jones, and J. S. Johnson Jr. *J. Phys. Chem.*, 96:5611, 1992.

[249] G. Biresaw, D. C. McKenzie, C. A. Bunton, and D. F. Nicoli. *J. Phys. Chem.*, 89:5144, 1985.

[250] M. S. Vethamuthu, M. Almgren, E. Mukhtar, and P. Bahadur. *Langmuir*, 8:2396, 1992.

[251] P. H. von Hippel and T. Schleich. *Biological Macromolecules, Vol. 3.* Marcel Dekker, New York, N. Y., 1969.

[252] S. Gravsholt. *J. Colloid Interface Sci.*, 57:575, 1976.

[253] T. Imae, R. Kamiya, and S. Ikeda. *J. Colloid Interface Sci.*, 108:215, 1985.

[254] C. Gamboa, H. Ríos, and S. J. Sepúlveda. *J. Chem. Phys.*, 93:5540, 1989.

[255] A. J. Hyde and D. W. M. Johnstone. *J. Colloid Interface Sci.*, 53:349, 1975.

[256] J. W. Larsen and L. J. Magid. *J. Am. Chem. Soc.*, 96:5774, 1974.

[257] I. Cohen and T. Vassiliades. *J. Phys. Chem.*, 65:1774, 1961.

[258] H. Fabre, N. Kamenka, A. Khan, G. Lindblom, B. Lindman, and G. J. T. Tiddy. *J.Phys.Chem.*, 84:3428, 1980.

[259] N. Jiang, P. Li, Y. Wang, J. Wang, H. Yan, R. K. Thomas, I. Chakraborty, and S. P. Moulik. *J. Phys. Chem. B*, 111:3658, 2007.

[260] G. Para, E. Jarek, and P. Warszynski. *Adv. Colloid Interface Sci.*, 122:39, 2006.

[261] G. Para, E. Jarek, and P. Warszynski. *Colloids Surf., A*, 261:65, 2005.

[262] U. Henriksson, L. Ödberg, J. C. Eriksson, and L. Westman. *J. Phys. Chem.*, 81:76, 1977.

[263] G. Lindblom, B. Lindman, and L. Mandell. *J. Colloid Interface Sci.*, 42:400, 1973.

[264] F. Reiss-Husson and V. Luzzati. *J. Phys. Chem.*, 68:3504, 1964.

[265] J. Ulmius, B. Lindman, G. Lindblom, and T. Drakenberg. *J. Colloid Interface Sci.*, 65:88, 1978.

[266] J. Ulmius and H. Wennerström. *J. Magn. Reson.*, 28:309, 1977.

[267] A. Abe, T. Imae, and S. Ikeda. *Colloid Polym. Sci.*, 265:637, 1987.

[268] J. K. Backus and H. A. Scheraga. *J. Colloid Interface Sci.*, 6:508, 1951.

[269] S. J. Candau, E. Hirsch, and R. Zana. *J. Colloid Interf. Sci.*, 105:521, 1985.

[270] S. J. Candau, E. Hirsch, and R. Zana. *J. Physique*, 45:1263, 1984.

[271] P. Debye and E. W. Anacker. *J. Phys. Colloid Chem.*, 55:644, 1951.

[272] R. Dorshow, J. Briggs, C. A. Bunton, and D. F. Nicoli. *J. Phys. Chem.*, 86:2388, 1982.

[273] R. B. Dorshow, C. A. Bunton, and D. F. Nicoli. *J. Phys. Chem.*, 87:1409, 1983.

[274] S. Ikeda. *Surfactants in Solution, Vol. 2*, page 825. Plenum, New York, 1984.

[275] T. Imae, A. Abe, Y. Taguchi, and S. Ikeda. *J. Colloid Interface Sci.*, 109:567, 1986.

[276] T. Imae and S. Ikeda. *J. Phys. Chem.*, 90:5216, 1986.

[277] S. Ozeki and S. Ikeda. *J. Colloid Interface Sci.*, 87:424, 1982.

[278] H. A. Scheraga and J. K. Backus. *J. Am. Chem. Soc.*, 73:5108, 1951.

[279] N. A. Riegelman, M. K. Allawa, M. K. Hrenoff, and L. A. Strait. *J. Colloid Sci.*, 12:208, 1958.

[280] L. Sepulveda. *J. Colloid Interface Sci.*, 46:372, 1974.

[281] B. C. Smith, L. C. Chou, and J. L. Zakin. *J. Rheol.*, 38:73, 1994.

[282] M. B. Sierra, P. V. Messina, M. A. Morini, J. M. Russo, G. Prieto, P. C. Schulz, and F. Sarmiento. *Colloids Surf., A*, 277:75, 2006.

[283] V. K. Aswal, P. S. Goyal, and P. Thiyagarajan. *J. Phys. Chem.*, 109:2469, 1998.

[284] R. Buchner, C. Baar, P. Fernandez, S. Schrödle, and W. Kunz. *J. Mol. Liq.*, 118:179, 2005.

[285] M. C. Brum and J. F. Oliveira. *Minerals Engineering*, 20:945, 2007.

[286] M. Nyman, J. M. Bieker, S. G. Thoma, and D. E. Trudell. *J. Colloid Interface Sci.*, 316:968, 2007.

[287] B. Wu, S. D. Christian, and J. F. Scamehorn. *Prog. Colloid Polym. Sci.*, 109:60, 1998.

[288] A. Patist, S. G. Oh, R. Leung, and D. O. Shah. *Colloids Surf., A*, 176:3, 2000.

[289] D. O. Shah. *Micelles, Microemulsions and Monolayers.* Dekker, New York, 1998.

[290] A. Patist, J. R. Kanicky, P. K. Shukla, and D. O. Shah. *J. Colloid Interface Sci.*, 245:1 and refs. therein, 2002.

[291] P. C. Hiemenz and R. Rajagopalan. *Principles of Colloid and Surface Chemistry, 3rd ed.* Dekker, New York, 1997.

[292] R. J. Hunter. *Foundations of Colloid Science.* Oxford Univ. Press, New York, 1987.

[293] H. Chakraborty and M. Sakar. *Langmuir*, 20:3551, 2004.

[294] E. F. Marques. *Langmuir*, 16:4798, 2000.

[295] J. M. Peacock and J. E. Matijevic. *J. Colloid Interface Sci.*, 77:548, 1980.

[296] R. G. Laughlin. *Colloids Surf., A*, 128:27, 1997.

[297] D. Chu and J. K. Thomas. *J. Am. Chem. Soc.*, 108:6270, 1986.

[298] K. Kogej and J. Skerjanc. *Langmuir*, 15:4251, 1999.

[299] C. Vautier-Giongo and B. L. Bales. *J. Phys. Chem. B*, 107 (2003) 5398:5398, 2003.

[300] A. R. Tehrani-Bagha, H. Bahrami, B. Movassagh, M. Arami, S. H. Amirshahi, and F. M. Menger. *Colloids Surf., A*, 307:121, 2007.

[301] M.-P. Nieh, T. A. Harroun, V. A. Raghunathan, C. J. Glinka, and J. Katsaras. *Biophys. J.*, 86:2615, 2004.

[302] B. Sohrabi, H. Gharibi, S. Javadian, and M. Hashemianzadeh. *J. Phys. Chem. B*, 111:10069, 2007.

[303] M. Bergström, J. S. Pedersen, P. Schurtenberger, and S. U. Egelhaaf. *J. Phys. Chem. B*, 103:9888, 1999.

[304] I. Yaacob and A. Bose. *J. Colloid Interface Sci.*, 178:638, 1996.

[305] B. Lindman. *Handbook of Applied Surface and Colloid Chemistry*. John Wiley & Sons Ltd, England, 2002.

[306] N. Vlachy, K. Kogej, D. Touraud, and W. Kunz. *J. Colloid Interface Sci.*, 315:445, 2007.

[307] E. B. Abuin and J. C. Scaiano. *J. Am. Chem. Soc.*, 106:6274, 1984.

[308] D. S. Karpovich and G. J. Blanchard. *J. Phys. Chem.*, 99:3951, 1995.

[309] D. H. Kim, S. G. Oh, and C. G. Cho. *Colloid Polym. Sci.*, 279:39, 2001.

[310] R. J. Anderson, C. Delgado, D. Fisher, J. M. Cunningham, and G. E. Francis. *Analytical Biochemistry*, 193:101, 1991.

[311] S. Askolin, T. Nakari-Setälä, and M. Tenkanen. *Appl. Microbiol. Biotechnol.*, 57:124, 2001.

[312] J. B. S. Bonilha, R. M. Z. Georgetto, E. Abuin, E. Lissi, and F. Quina. *J. Colloid Interface Sci.*, 135:238, 1990.

[313] P. Mukerjee, K. Mysels, and P. Kapauan. *J. Phys. Chem.*, 71:4166, 1967.

[314] W. D. Harkins, R. W. Mattoon, and R. Mittelman. *J. Chem. Phys.*, 15:763, 1947.

[315] A. E. Alexander. *Trans. Faraday Soc.*, 38:54, 1942.

[316] P. F. Grieger and C. A. Krauss. *J. Am. Chem. Soc.*, 70:3803, 1948.

[317] K. Shinoda. *J. Phys. Chem.*, 58:1136, 1954.

[318] H. Nakayama, K. Shinoda, and E. Hutchinson. *J. Phys. Chem.*, 70:3502, 1966.

[319] S. Kaneshina, H. Kamaya, and I. Ueda. *J. Colloid Interface Sci.*, 83:589, 1981.

[320] T. Okubo, K. Hiraiwa, S. Kinoshita, and M. Watanabe. *Alternatives to Animal Testing and Experimentation*, 1:2, 1990.

[321] M. C. Scaife. *International Journal of Cosmetic Science*, 4:179, 1982.

[322] J. Selling and B. Ekwall. *Xenobiotica*, 15:713, 1985.

[323] A. Trivedi, N. Kitabake, and E. Doi. *Agricultural and Biological Chemistry*, 54:2961, 1990.

[324] K. Chiba, I. Makino, J. Ohuchi, Y. Kasai, H. Kakishima, K. Tsukumo, T. Uchiyama, E. Miyai, J. Akiyama, Y. Okamoto, H. Kojima, H. Okumura, Y. Tsurumi, M. Usami, K. Katoh, S. Sugiura, A. Kurishita, M. Sunouchi, A. Miyajima, M. Hayashi, and Y. Ohno. *Toxicology in Vitro*, 13:189, 1999.

[325] W. Yang and D. Acosta. *Toxicol. Lett.*, 70:309, 1994.

[326] O. P. Flint. *Altern. Test. Lab. Anim.*, 18:11, 1990.

[327] M. Cornelis, Ch. Dupont, and J. Wepierre. *Toxic. in Vitro*, 6:119, 1992.

[328] R. L. Grant, C. Yao, D. Gabaldon, and D. Acosta. *Toxicology*, 76:153, 1992.

[329] H. Kojima, J. Ohuchi, Y. Kasai, J. Okada, K. Tsukumo, H. Kakishima, E. Miyai, J. Akiyama, Y. Okamoto, M. Kotani, K. Inoue, M. Hibata, H. Okumura, M. Arashima, T. Atsumi, I. Makino, K. Chiba, Y. Ohno, and A. Takanaka. *Alternatives to Animal Testing and Experimentation*, 3:191, 1995.

[330] T. Ohno, Y.and Kaneko, T. Kobayashi, T. Inoue, Y. Kuroiwa, T. Yoshida, J. Momma, M. Hayashi, J. Akiyama, T. Atsumi, K. Chiba, T. Endo, A. Fujii, H. Kakishima, H. Kojima, Y. Masamoto, M. Masuda, K. Matsukawa, K. Ohkoshi, J. Okada, K. Sakamoto, K. Takano, T. Suzuki, and A. Takanaka. *Alternatives to Animal Testing and Experimentation*, 3:123, 1995.

[331] E. Owen, J. Clifford, and A. Marson. *J. Cell Sci.*, 32:363, 1978.

[332] J. F. Sina, G. J. Ward, M. A. Laszek, and P. D. Gautheron. *Fundam. Appl. Toxicol.*, 18:515, 1992.

[333] J.-H. S. Kuo, M.-S. Jan, C.-H. Chang, H.-W. Chiu, and C.-T. Li. *Colloids Surf., B*, 41:189, 2005.

[334] S. Mahiuddin, A. Renoncourt, P. Bauduin, D. Touraud, and W. Kunz. *Langmuir*, 21:5259, 2005.

[335] N. Vlachy, M. Drechsler, J.-M. Verbavatz, D. Touraud, and W. Kunz. *J. Colloid Interface Sci.*, 319:542, 2008.

[336] D. P. Cistola, J. A. Hamilton, D. Jackson, and D. M. Small. *Biochemistry*, 27:1881, 1988.

[337] K. Fontell and L. Mandell. *Colloid Polym. Sci.*, 271:974, 1993.

[338] M. Gebicki, J. M.and Hicks. *Nature*, 243:232, 1973.

[339] C. L. Apel, D. W. Deamer, and M. N. Mautner. *Biochimica et Biophysica Acta*, 1559:1, 2002.

[340] K. Morigaki and P. Walde. *Curr. Opin. Colloid Interface Sci.*, 12:75, 2007.

[341] M. Bergsma, M. L. Fielden, and J. B. F. N. Engberts. *J. Colloid Interface Sci.*, 243:491, 2001.

[342] M. Johnsson, A. Wagenaar, M. C. A. Stuart, and J. B. F. N. Engberts. *Langmuir*, 19:4609, 2003.

[343] S. Franceschi, V. Andreu, N. de Viguerie, M. Riviere, A. Lattes, and A. Moisand. *New J. Chem.*, 22:225, 1998.

[344] Z. Yuan, J. Hao, and H. Hoffmann. *J. Colloid Interface Sci.*, 302:673, 2006.

[345] A. de Groot, R. W. and; Wagenaar, A. Sein, and J. B. F. N. Engberts. *Recl. Trav. Chim. Pays-Bas*, 114:371, 1995.

[346] A. Renoncourt, P. Bauduin, E. Nicholl, D. Touraud, J.M. Verbavatz, M. Dubois, M. Drechsler, and W. Kunz. *ChemPhysChem*, 7:1892, 2006.

[347] T. Mosmann. *J. Immunol. Methods*, 65:55, 1983.

[348] Y. Talmon. *Modern Characterization Methods of Surfactant Systems*, page 147. Marcel Dekker: New York, 1999.

[349] R. Smith and C. Tanford. *Proc. Natl. Acad. Sci.*, 70:289, 1973.

[350] T. H. Haines. *Proc. Natl. Acad. Sci.*, 80:160, 1983.

[351] H.-T. Jung, S. Y. Lee, E. W. Kaler, and J. A. Zasadzinski. *Proc. Natl. Acad. Sci.*, 99:15318., 2002.

[352] T. M. Weiss, T. Narayanan, C. Wolf, M. Gradzielski, P. Panine, S. Finet, and W. I. Helsby. *Phys. Rev. Lett.*, 94:38303, 2005.

[353] H. Hoeffkes, K. Nelles, and B. Bergmann, 2000. DE 19835327 A1 200002210.

[354] H. Hoeffkes, M. Seiler, W. Gross, G. Knuebel, D. Oberkobusch, S. Kainz, and A. Reichert, 2007. DE 102005055340 A1 20070524.

[355] S. Kainz, H. Hoeffkes, M. Krippahl, and C. Kolonko, 2006. WO 2006097167 A1 20060921.

[356] A. Kleen, M. Akram, S. Hoepfner, and H. Manneck, 2005. WO 2005058260 A1 20050630.

[357] A. Kleen and B. Frauendorf, 2007. EP 1762220 A2 20070314.

[358] Y. Barenholz. *Curr. Opin. Colloid Interface Sci.*, 6:66, 2001.

[359] J. Dong, D. R. Whitcomb, A. V. McCormick, and H. T. Davis. *Langmuir*, 23:7963, 2007.

Acknowledgements

From experience I can tell you that these last pages of a PhD thesis are the most widely read pages of the entire publication. It is here where you supposedly find out to what extent you have influenced the life and work of the author. While this may be true to some extent, you have to weigh my verdict with the disturbingly low level of sanity left in this PhD candidate after several years of studying toxic molecules, redefining the color blue and searching for 'berries' in aqueous surfactant solutions.

The work described in this thesis has been carried out under the guidance of Prof. Dr. Werner Kunz at the Institute for Physical and Theoretical Chemistry, University of Regensburg. I would like to thank him for the trust he showed by letting me work independently and the opportunity to collaborate with a number of other groups around the world. Furthermore, thanks to all of his various personalities (the arabic one I am especially fond of) for keeping us amused during lunches and long conference rides.

Part of the experimental work was performed at the Department of Pharmaceutical Biology, University of Regensburg. Thank you to Prof. Dr. Jörg Heilmann, Dr. Birgit Kraus, and Gabi Brunner for their patience and trust they showed by letting this near-theoretician work in their sterile environment.

Special thanks to Dr. Didier Touraud for decorating our lab in pink color and making ammoniac the commonly used air freshener. Furthermore, Didier, thank you for your encouragement through the years; for knowing when to push me further and when to back off and, especially, for always taking the time to discuss new (mostly crazy) ideas.

The good basics were developed already during my undergraduate studies. For that, I am thankful to Prof. Dr. Ksenija Kogej, for teaching me to pay attention

to detail and work in an organized fashion. An indispensable skill that was proven necessary to survive in the sometimes hectic half-French institute.

No scientific work is done in solitude. Three microscopists are responsible for my newly found appreciation for (abstract) art: Dr. Jean-Marc Verbavatz (CEA, Saclay), Dr. Marcus Drechsler (University of Bayreuth), and Prof. Dr. Ishi Talmon (Technion-Israel Institute of Technology). Thank you for your wonderful pictures and informative discussions.

I thank my coworkers that transformed the 'supposed-to-be' serious work environment into a fun place (although it sometimes resembled more a loony-bin): Alina for showing me the ropes from the first day on, Chloé for her ability to turn back time and make me feel like a kid whenever I'm in her company, Geli for the smile I was greeted with every morning, Jeremy for his conversations on and off the OrbiTrek.

To my traveling companions: Mojca & Neza. After the adventures we had, coming back to work seemed like vacation. I am looking forward to all the cities that still await us.

Thank you to Jorge Cham, the creator of PhD comics, for helping me fight insanity with irony.

To Daniel: Thank you for reading my thesis, listening to my endless complaining, helping me pick out my interview suit, wiping the tears away when the reviewers (wrongfully, of course!) rejected my manuscripts and nursing me after my eye operation. You are my endless source of motivation and I am lucky to have you to open my eyes (despite my newly-found 150% vision) when needed.

To my father: thank you for encouraging me on all my paths. I am still waiting for that Vlachy & Vlachy article however ...

List of Publications

Published:

1-N. Vlachy, J. Dolenc, B. Jerman, K. Kogej, Influence of Stereoregularity of the Polymer Chain on Interactions with Surfactants: Binding of Cetylpyridinium Chloride by Isotactic and Atactic Poly(methacrylic acid). *J. Phys. Chem. B* **2006** 110, 9061-9071.

2-A. Renoncourt, N. Vlachy, P. Bauduin, M. Drechsler, D. Touraud, J.-M. Verbavatz, M. Dubois, W. Kunz, B. W. Ninham, Specific alkali cation effects in the transition from micelles to vesicles through salt addition. *Langmuir* **2007** 23, 2376-2381.

3-N. Vlachy, D. Touraud, K. Kogej, W. Kunz, Solubilization of methacrylic acid based polymers by surfactants in acidic solutions. *J. Colloid Interf. Sci.* **2007** 315, 445-455.

4-N. Vlachy, M. Drechsler, J.-M. Verbavatz, D. Touraud, W. Kunz, Role of the surfactant headgroup on the counterion specificity in the micelle-to-vesicle transition through salt addition. *J. Colloid Interf. Sci.* **2008** 319, 542-548.

5-N. Vlachy, A. Renoncourt, M. Drechsler, J.-M. Verbavatz, D. Touraud, W. Kunz, Blastulae aggregates: New intermediate structures in the micelle-to-vesicle transition of catanionic systems. *J. Colloid Interf. Sci.* **2008** 320, 360-363.

Accepted:

6-N. Vlachy, A. F. Arteaga, A. Klaus, D. Touraud, M. Drechsler, W. Kunz, Influence of additives and cation chain length on the kinetic stability of supersaturated catanionic systems. *Colloids Surf., A* **2008**.

7-N. Vlachy, C. Merle, D. Touraud, J. Schmidt, Y. Talmon, J. Heilmann, W. Kunz,

Determining the delayed cytotoxicity of catanionic surfactant mixtures on HeLa cells. *Langmuir* **2008**.

Submitted:

8-N. Vlachy, M. Drechsler, D. Touraud, W. Kunz, Anion specificity influencing morphology in catanionic surfactant mixtures with an excess of cationic surfactant. *Comptes rendus Chimie Académie des sciences* **2008**.

9-N. Vlachy, B. Jagoda-Cwiklik, R. Vácha, D. Touraud, P. Jungwirth, and W. Kunz, Hofmeister series of headgroups and specific interaction of charged headgroups with ions. *J. Phys. Chem. B* **2008**.

10-N. Vlachy, D. Touraud, J. Heilmann, W. Kunz, Determining the delayed cytotoxicity of catanionic surfactant mixtures on HeLa cells. *Colloids Surf., B* **2008**.

List of Oral and Poster Presentations

Oral Presentations:

09/2007 **21th Conference of the European Colloid and Interface Society**, Genève, Switzerland. Blastula vesicles: Formation of regular patterns through secondary self-assembly of catanionic vesicles.

Poster Presentations:

08/2005 **29. International Conference of Solution Chemistry**, Portoroz, Slovenia.
Mixed Solutions of Isotactic Poly(methacrylic acid) and Cetylpyridinium Chloride in water.

08/2006 **1st European Chemistry Congress**, Budapest, Hungary.
Solubilization of Hydrophobic Polymers with Surfactants.

09/2007 **21th Conference of the European Colloid and Interface Society**, Genève, Switzerland.
Effect of "hydrophobic" cations on vesicular self-assembly.

11/2007 **Formula V**, Potsdam, Germany.
Influence of additives on the stability of (eutectic) supersaturated catanionic systems.

Herewith I declare that I have made this existing work single-handed. I have only used the stated utilities.

Regensburg, June 2008

Nina Vlachy